

LUDWIG-MAXIMILIANS-UNIVERSITÄT MÜNCHEN
FACULTY OF PHYSICS

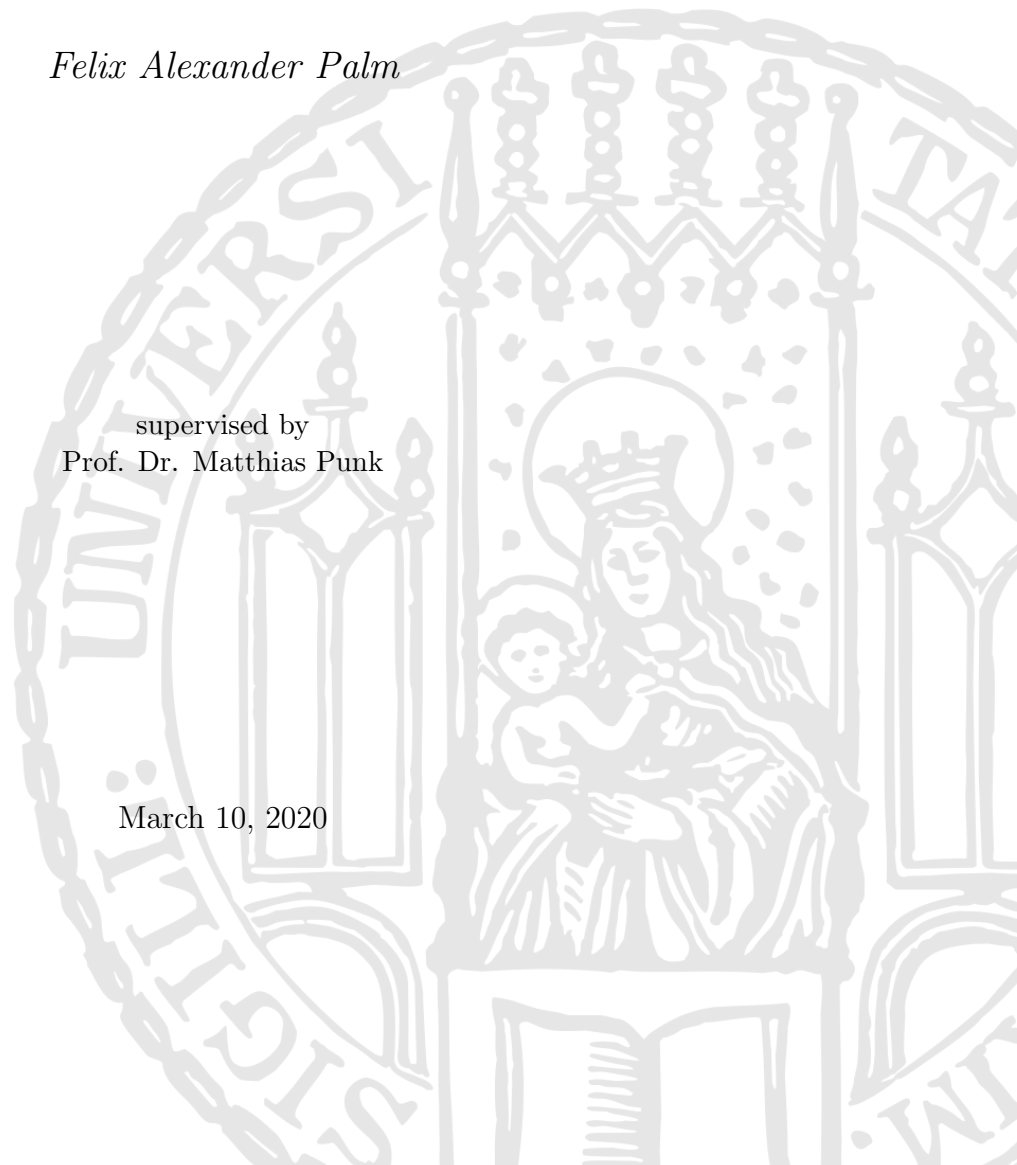
MASTER THESIS

**Renormalization Group Studies of
Quantum Phase Transitions in the
Heisenberg-Kitaev Model on the
Triangular Lattice**

Felix Alexander Palm

supervised by
Prof. Dr. Matthias Punk

March 10, 2020



LUDWIG-MAXIMILIANS-UNIVERSITÄT MÜNCHEN
FAKULTÄT FÜR PHYSIK

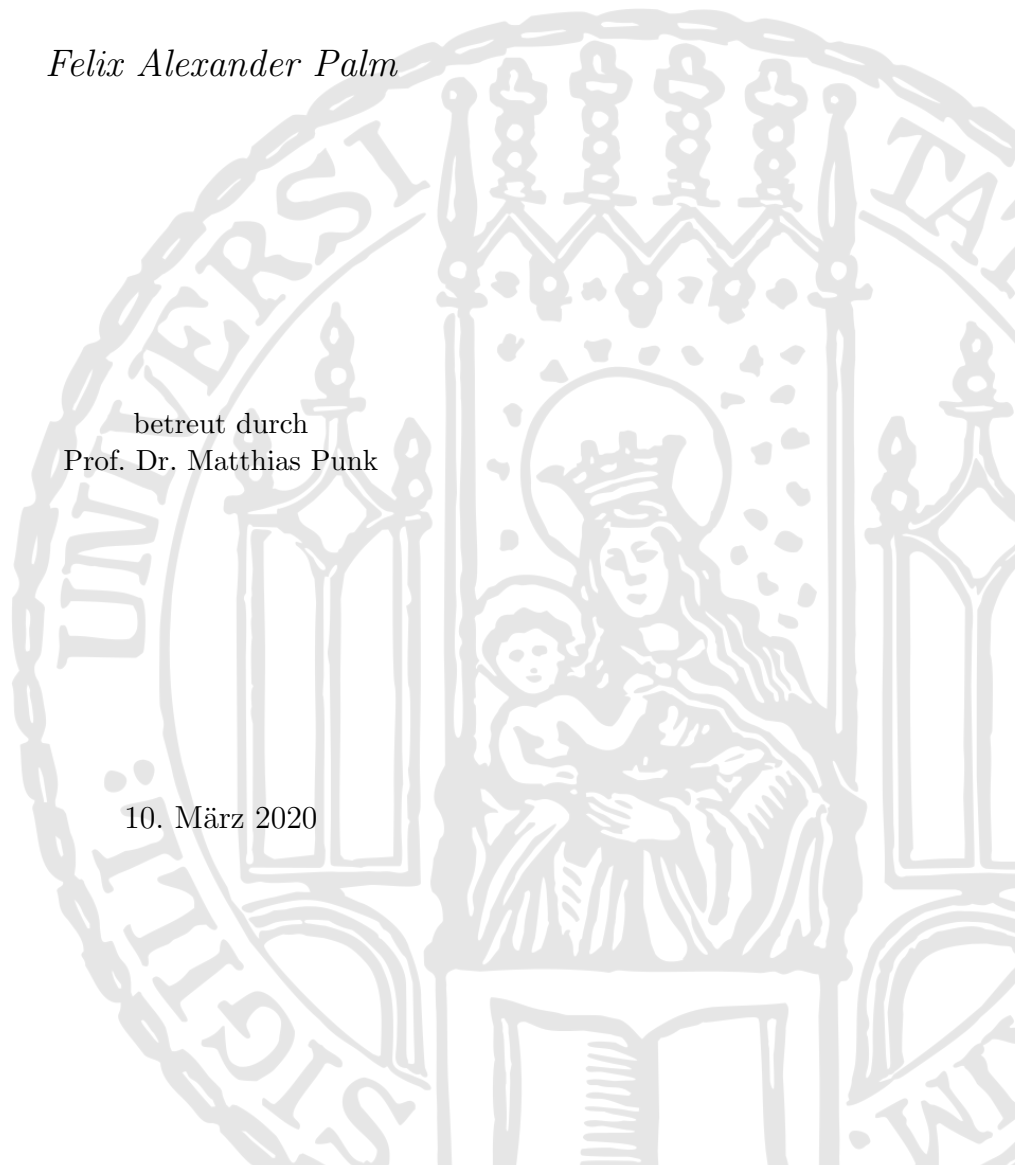
MASTERARBEIT

**Renormierungsgruppen-Studien von
Quantenphasenübergängen im
Heisenberg-Kitaev-Modell auf dem
Dreiecksgitter**

Felix Alexander Palm

betreut durch
Prof. Dr. Matthias Punk

10. März 2020



Abstract

Recently, quantum spin liquids (QSL), as an example of topologically ordered phases, have attracted much attention [1]. A prominent model potentially hosting QSL states is the Heisenberg-Kitaev model on the triangular lattice. Earlier analyses using Schwinger boson mean-field theory (SBMFT) predicted three QSL phases in this model [2]. In this thesis, we use an effective action approach to study the system analytically in order to gain insight into the nature of one of the corresponding quantum phase transitions. Starting from a Schwinger boson representation of the model, we perform a Hubbard-Stratonovich decoupling in the pairing channel using singlet and triplet fields. Integrating out the Schwinger bosons, we derive a critical theory for the phase transition. This results in a theory of three interacting bosonic fields, dispersing along one of the lattice directions each. We study the critical phenomena of this theory using mean-field theory and the functional renormalization group (fRG), and find the phase transition to be of second order in agreement with the predictions of SBMFT. This shows that the combination of an effective action and fRG can give insights into phase transitions between different QSLs. Furthermore, our method can be generalized to other systems hosting QSL states.

Acknowledgments

First and foremost I would like to thank my supervisor Prof. Matthias Punk, who got me excited about condensed matter physics in his excellent lectures and proposed this fascinating topic to me. I very much appreciate his constant support throughout this thesis and am particularly grateful for his open door and many hours of discussions, from which I could learn a lot about technical details as well as ‘how to think about physics on a larger scale’.

I would also like to thank Prof. Jan von Delft and all members of his chair for their hospitality and the extraordinary working conditions. Special thanks go to my office fellows and companions on the way to our master degrees, David Moser, Gianni Del Bimbo, and Santiago Aguirre, for challenging me to come to a better understanding not only of my model but of physics in general. I also want to thank Florian Stabler for many discussions about analytical methods in CMP and technical details of L^AT_EX, and Julian Thonni for our specialized discussions about spin liquids, which helped me a lot in understanding the ‘bigger picture’.

Furthermore, I want to thank Etienne Staub for proof-reading my thesis and challenging me with an experimentalist’s questions. Finally, I would like to thank my family for their support throughout the writing of this thesis, particularly, on days when things did not go smoothly.

Contents

1	Introduction	1
2	Theoretical Background	3
2.1	Quantum Phase Transitions and Quantum Spin Liquids	3
2.1.1	Quantum Phase Transitions	3
2.1.2	Quantum Spin Liquids	4
2.2	The Heisenberg-Kitaev Model	6
2.2.1	QSL States in the Triangular Heisenberg-Kitaev Model	8
2.2.2	Connection to Real Materials	10
2.3	Renormalization Group Fundamentals	10
2.3.1	Functional Renormalization Group	12
3	Effective Action of the Heisenberg-Kitaev Model	15
3.1	Schwinger Boson Description of the Model	15
3.1.1	Hubbard-Stratonovich Transformation	17
3.1.2	Transformation to Frequency and Momentum Space	18
3.2	Integrating Out the Schwinger Bosons	20
3.3	Saddle Point Approximation for A and λ	21
3.3.1	Self-Consistent Solution of the Saddle-Point Equations	23
3.3.2	Spinon Dispersion and Gap Closing	25
3.4	Expansion of the $\text{Tr} \log$ -term around $T^\gamma = 0$	25
3.4.1	Gaussian Fluctuations	26
3.4.2	Fourth Order Contribution	31
3.5	General Properties of the Effective Action	33
4	Mean-Field Analysis	35
5	Renormalization Group Analysis	39
5.1	Tree Level Scaling	39
5.2	One-Loop Approximation - Functional Renormalization Group	41
5.2.1	Flow Equations for the Parameters	41
5.2.2	Fixed Points of the fRG Flow in $d = 2 - \epsilon$ Dimensions	47
5.3	Interpretation	49
6	Summary & Outlook	53

A Singlet & Triplet Operator Identities	57
B Gauge Theory of the HK-Model on the Triangular Lattice	59
C Fourth Order Contribution to the Effective Action	61
D Technical Results for fRG Calculations	63
D.1 Expressions Used in fRG Calculations	63
D.2 Evaluation of Integrals	64
D.2.1 $I_{\gamma,\gamma'}^{(1)}, \gamma \neq \gamma'$	64
D.2.2 $I_{\gamma,\gamma}^{(1)}$	66
References	69

1

Introduction

Since the early days of quantum mechanics, the intrinsic ‘quantumness’ of spin has posed an interesting challenge for theoretical and experimental physicists. In particular, the insight that the spin and magnetic properties of a system are intertwined at a microscopic level gave rise to a new field of physics, nowadays called ‘quantum magnetism’, that describes magnetic properties from a quantum mechanical point of view [3].

The simplest models of quantum magnetism involve localized spins on a lattice, which are often derived from underlying microscopic models for the electrons in a solid, as for example the fermionic Hubbard model [4]. Already, these seemingly easy spin models provide an interesting playground for the study of (strongly-correlated) quantum many-body systems. Consequently, an enormous number of approaches has been used to study quantum magnets numerically (e.g. Quantum Monte Carlo [5], DMRG [6], tensor network methods [7], exact diagonalization [8]) and analytically (e.g. large N expansion [9], slave-particle mean-field theory [1,10]). At the same time, the close connection to real materials has led to many experimental studies of spin systems in solid-state systems as well as realizations in cold atom experiments [11].

In recent years, the field of quantum magnetism has seen a renaissance with the discovery of topologically ordered phases. Loosely speaking, this kind of order is characterized by the absence of a local order parameter describing a broken symmetry, and therefore has to be studied and understood globally [12,13]. One class of topologically ordered states are so-called quantum spin liquid states, which can arise as ground states of frustrated spin models. The possibility to formulate the underlying models in terms of lattice gauge theories has given rise to analogies to high energy physics, most prominently Higgs mechanisms and particle confinement [14].

Again, a new perspective presents itself by combining lattice symmetries with topologically ordered states. In this way, *symmetry enriched topological phases* can be defined, which are characterized by both, topological properties as well as the representation of the symmetry group of the underlying lattice. These phases can be (partially) classified using the projective symmetry group [1] or group cohomology [15].

An example of a system hosting different symmetry enriched topological phases, and in particular different quantum spin liquid states, is the Heisenberg-Kitaev model on the triangular lattice. Kos and Punk [2] used Schwinger boson mean-field theory to analyze this model. For a totally symmetric mean-field ansatz they found the system to host three quantum spin liquid ground states, which are separated by quantum phase transitions. However, the details of the phase transitions remained unclear. The nature of one of these

quantum phase transitions will be discussed in this thesis. To this end, we will derive an effective action for the relevant degrees of freedom in chapter 3 using a Schwinger boson representation of the spin degrees of freedom. To get a first understanding of the possible phases, we perform a mean-field analysis of the resulting effective action in chapter 4. In chapter 5, we use the functional renormalization group to derive one-loop renormalization group flow equations and use them to understand the critical behavior of the theory.

We confirm the existence of the quantum phase transition using analytical tools without relying on numerical methods. Furthermore, we derive a critical theory characterizing the phase transition and argue that it is indeed second order by both mean-field and RG arguments.

Before we start our endeavor, we will review some theoretical background on quantum phase transitions, quantum spin liquids and renormalization group methods in chapter 2.

2

Theoretical Background

To set the stage for our discussion of quantum phase transitions in the Heisenberg-Kitaev model, some theoretical foundations are introduced in this chapter. First, a very short exposition of quantum phase transitions is given. For a deeper understanding we refer to the literature (e.g. Sachdev's book on quantum phase transitions [16]). We discuss in some detail magnetic (dis)order on the square and triangular lattice to obtain a working definition of quantum spin liquids. Afterwards, we define some basic notation and the Heisenberg and Kitaev models, before we turn to a short review of earlier work on the Heisenberg-Kitaev model on the triangular lattice and discuss connections to real materials. Eventually, we introduce basic concepts of the renormalization group method and the functional renormalization group.

2.1. Quantum Phase Transitions and Quantum Spin Liquids

2.1.1. Quantum Phase Transitions

As is well-known from statistical physics, when lowering the temperature, many systems undergo phase transitions from (thermally) disordered to ordered phases. Such a phase transition is driven by thermal fluctuations which contribute more at high temperatures and therefore lead to disorder in this regime. When lowering the temperature, the thermal fluctuations become increasingly negligible and the system will finally reach its ground state. This idea gave rise to Landau's theory of phase transitions formulated in terms of order parameters and symmetry breaking. Today we know some exceptions to this theory even for thermal phase transitions, in particular in low dimensions. However for a rough understanding of the difference between classical and quantum phase transitions this simplified picture is sufficient at this point.

In quantum mechanical systems, additional quantum fluctuations play an important role. When lowering the temperature, these quantum fluctuations become more and more important [16] and at zero temperature, they are the only kind of fluctuations that persist. If the system depends on some non-thermal control parameter, the ground state of the system may depend on this non-thermal parameter. Then, by changing this parameter, the system may undergo what is called a *quantum phase transition* (QPT) and the point of the phase transition is called a *quantum critical point* (QCP). These transitions are clearly driven by quantum fluctuations as they occur at zero temperature, $T = 0$. A generic phase diagram for a system undergoing a QPT is given in Fig. 2.1.

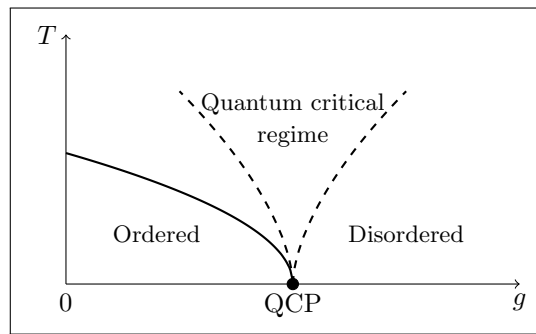


Fig. 2.1. Schematic phase diagram around a quantum critical point (QCP), where T denotes the temperature and g denotes a non-thermal control parameter. The solid line indicates a classical second order phase transition around which the classical theory of thermal fluctuations may be applied. The dashed line indicates the crossover into the quantum critical regime, where the finite-temperature behavior is affected by the QCP. (Figure adapted from [16])

In addition to the QPT at zero temperature, there is a *quantum critical regime*, where the finite-temperature properties of the system are controlled by the QCP. In this regime, quantum and thermal fluctuations are equally important and a classical description of the system cannot be used. It is important to mention that the crossover behavior around this quantum critical regime is *not* a thermal phase transition but really a crossover. The quantum critical regime is of great interest due to the interplay of quantum and thermal fluctuations. Even more, as any experiment will perform measurements at temperatures $T > 0$, understanding the influence of the QCP on the behavior in the quantum critical regime is very important for a correct interpretation of such measurements.

2.1.2. Quantum Spin Liquids

For spin systems, phase transitions can often be described by a local order parameter measuring magnetic order in the system. To illustrate this situation, consider Ising spins on the square lattice with an anti-ferromagnetic nearest-neighbor interaction. We want to find the ground state of this model. For the first spin we have the freedom to have it point parallel to the z -axis or anti-parallel.¹ For the neighboring spins the orientation is restricted by the first spin due to the anti-ferromagnetic interaction: all neighboring spins of the initial spin have to point in the opposite direction as the initial one. Repeating this argument for all lattice sites, we finally arrive at the well-known Néel-ordered state depicted in Fig. 2.2a. The order parameter in this case would be the staggered magnetization, $\langle \frac{1}{N} \sum_i (-1)^i \sigma_i^z \rangle$, where σ_i^z is the value of the Ising variable at site i and N is the number of lattice sites. For the Néel-ordered state the staggered magnetization takes a finite value whereas it is zero in the disordered phase.

However, for the triangular lattice the situation changes drastically. Consider again Ising spins with anti-ferromagnetic nearest-neighbor interaction. After positioning the first spin, the second neighboring spin is forced to point in the opposite direction as the first one. The third spin necessarily neighbors one spin pointing upwards and one pointing downwards, therefore it is not clear how to align the third spin in an optimal way (see Fig. 2.2b), a feature known as *geometric frustration*.

¹We choose the z -axis to be perpendicular to the lattice plane.

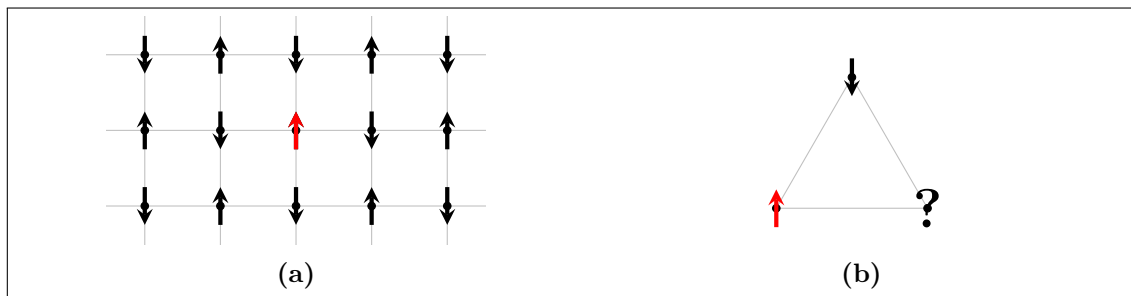


Fig. 2.2. Spin alignment for the anti-ferromagnetic Ising model. (a) Néel-ordered ground state on the square lattice. (b) Geometric frustration on the triangular lattice. The red spin indicates the first spin placed on the lattice.

Allowing for superpositions of various states in the quantum case, this problem can be overcome in the so-called *resonating valence bond* (RVB) state. For a given lattice, consider a state where pairs of neighboring spins combine into spin singlets. Such a state is called a *valence bond state* and is illustrated in Fig. 2.3. A single valence bond state clearly breaks the lattice symmetries, however a superposition of all possible valence bond states restores the initial symmetries. Therefore, such a superposition seems to be a good candidate for a state without broken symmetries and without long-range order. Such a superposition is called a (short-ranged) RVB state and was first proposed by Anderson in 1973 [17, 18].

The described RVB state is the prototype of so-called *quantum spin liquid* (QSL) states which break *no* symmetries [19]. Quantum spin liquids are indeed qualitatively different from other states of matter. They do not break symmetries of the system and thus cannot be described by Landau's theory of phase transitions which involves spontaneous symmetry breaking as a key ingredient. In fact, they are *topologically ordered* in the sense that they have degenerate ground states which cannot be distinguished in terms of local observables [12].

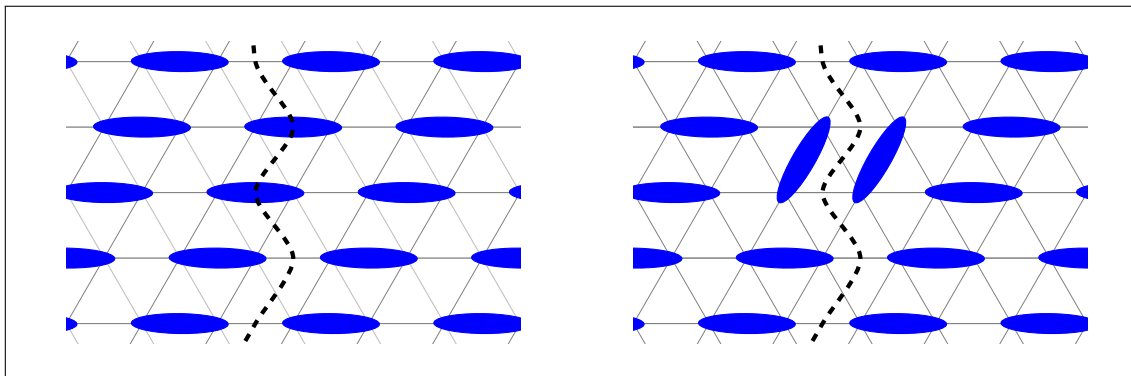


Fig. 2.3. Examples of valence bond states on the triangular lattice. The blue ellipses indicate the singlets. The state in the right panel can be obtained from the state in the left one by the action of a local operator. The number of singlets crossed by the dashed path has the same parity for all states obtained under the action of local operators. (Figure adapted and expanded from [20])

This degeneracy can most easily be understood in the context of a valence bond state as indicated in Fig. 2.3. Imagine the triangular lattice to be realized on a torus. Consider the left panel of the figure and draw a closed path intersecting some of the bonds in the middle. Thus, the path might cross some of the singlets, where we are mainly interested in the parity of the number of crossings (in the figure the path crosses 2 singlets, i.e. an even number). Acting on the state with a local operator which effectively flips two of the singlets, we obtain another valence bond state like the one in the right panel. Again, examining the path defined before for the new state, we see that it crosses some singlets and the parity of this number did not change. Since this is in fact true for any local operator, the Hilbert space is split into two parts of opposite parity,

$$\mathcal{H} = \mathcal{H}_{\text{even}} \oplus \mathcal{H}_{\text{odd}},$$

and we cannot distinguish states in one summand of the Hilbert space by any local measurement. Note, that the periodic boundary conditions for the path are crucial for this argument. As the possible closed paths in a given space are dictated by the topology of this space, it is clear that the splitting of the Hilbert space is a topological statement. Thus, it is expected to be unaffected by local properties and changes of the system.

In particular, the ground state degeneracy is robust against any local perturbation and excitations are gapped. Hallmark signs of topological order are a high degree of entanglement and non-local and fractionalized excitations [21]. In the RVB picture the fractionalization of an excitation can be understood intuitively. Starting from a valence bond state, imagine breaking one of the singlets by flipping one of the spins, thereby obtaining an excitation with $\Delta S = 1$. The two resulting spins can independently propagate through the system. These excitations are called ‘spinons’ which carry spin $1/2$ but no charge.

2.2. The Heisenberg-Kitaev Model

Having discussed the basic ideas of quantum spin liquids, we now want to find a model which might host such a special state of matter. In particular, we are looking for models of localized spins on a lattice as these were studied in the context of ‘quantum magnetism’ for quite some time [3]. One of the simplest models describing localized spins is the Heisenberg model, which consists of spin- S particles on a lattice interacting according to the Hamiltonian

$$\mathcal{H}_{\text{H}} = \sum_{\substack{i,j \\ i \neq j}} J_{ij} \vec{S}_i \cdot \vec{S}_j,$$

where i, j denote the lattice sites and \vec{S}_i is the spin operator on site i . The couplings J_{ij} could in principle be chosen arbitrarily, however we restrict our discussion to the case of site-independent nearest-neighbor interactions, such that the Heisenberg Hamiltonian simplifies to

$$\mathcal{H}_{\text{H}} = J_{\text{H}} \sum_{\langle ij \rangle} \vec{S}_i \cdot \vec{S}_j, \quad (2.1)$$

where $\langle ij \rangle$ denotes the sum over nearest-neighbors. Furthermore, we will discuss the *antiferromagnetic* Heisenberg model where $J_{\text{H}} > 0$. Note, that the Heisenberg Hamiltonian in Eq. (2.1) preserves SU(2) spin-rotation symmetry.

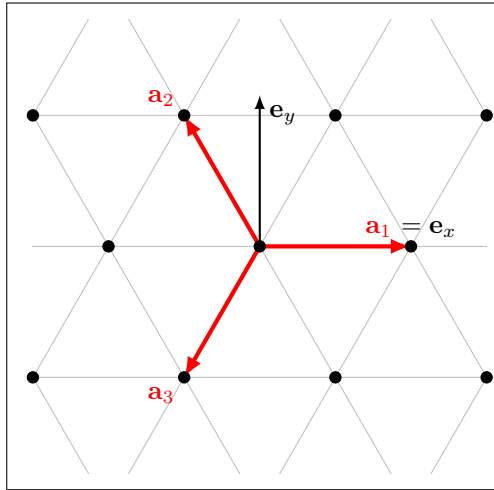


Fig. 2.4. Definition of the triangular lattice vectors \mathbf{a}_γ and the Cartesian coordinate system $\mathbf{e}_{x,y}$ for lattice constant $a = 1$.

For the Kagomé lattice it was found that the ground state of the anti-ferromagnetic Heisenberg model is indeed a spin liquid [22, 23]. The previous discussion of the Ising model on the triangular lattice indicates some interesting physics on this lattice as well. However, for the triangular Heisenberg model with spin-1/2 constituents it is known that the ground state is characterized by the magnetic ‘120-degree order’. Nevertheless, using or adding other interactions one can prevent the system from magnetically ordering even at zero temperature.

One particular model hosting QSL states was proposed by Kitaev in Ref. [24]. Even though the model was initially studied on the hexagonal lattice, it can be equally well defined on the triangular lattice. To this end, we define the triangular lattice vectors \mathbf{a}_γ as shown in Fig. 2.4. The Kitaev model again consists of interacting spins with the anisotropic interaction

$$\mathcal{H}_K = J_1 \sum_{1\text{-links}} S_i^1 S_j^1 + J_2 \sum_{2\text{-links}} S_i^2 S_j^2 + J_3 \sum_{3\text{-links}} S_i^3 S_j^3,$$

where the sums are over the nearest-neighboring lattice sites along the indicated link. The couplings $J_{1,2,3}$ can again take any value, however we consider the symmetric case, $J_1 = J_2 = J_3 = J_K > 0$, and rewrite the Kitaev Hamiltonian in the more compact form

$$\mathcal{H}_K = J_K \sum_{\gamma \parallel \langle ij \rangle} S_i^\gamma S_j^\gamma. \quad (2.2)$$

Here, the notation $\gamma \parallel \langle ij \rangle$ indicates the sum over neighboring sites along a link in direction $\gamma \in \{1, 2, 3\}$.

To understand the interplay of different types of interaction, we will study the physics of spins on a triangular lattice interacting via both a Heisenberg and a Kitaev term,

$$\mathcal{H}_{\text{HK}} = J_H \sum_{\langle ij \rangle} \vec{S}_i \cdot \vec{S}_j + J_K \sum_{\gamma \parallel \langle ij \rangle} S_i^\gamma S_j^\gamma, \quad (2.3)$$

in this thesis.

2.2.1. QSL States in the Triangular Heisenberg-Kitaev Model

Earlier studies of the Heisenberg-Kitaev model on the triangular lattice showed that the properties of the system depend strongly on the size of the spin, S . For $S = 1/2$ Becker et al. calculated phase diagrams for both the classical and the quantum version of the model [25]. It turned out that the model hosts a variety of different phases depending on the ratio of the Heisenberg and the Kitaev coupling. Without going into the physical properties of the individual phases, we show the phase diagram for the quantum model in Fig. 2.5, where the parametrization

$$J_H = \cos \alpha, \quad J_K = \sin \alpha,$$

is used and the couplings were normalized, such that $J_H^2 + J_K^2 = 1$. Earlier analyses of Heisenberg models on triangular and Kagomé lattices [9,14] have shown that, by lowering the value of the spin to (unphysically) small values, the ground state might become a QSL state. Furthermore, further-neighbor interactions were found to stabilize the QSLs as they might increase frustration of the system. Thus, QSL ground states might actually be realized in real materials as discussed in the next section.

Guided by these results Kos and Punk [2, 26] studied the ground state behavior of the triangular Heisenberg-Kitaev model at small spin values using Schwinger boson mean-field theory (SBMFT). They found three different spin liquid phases in the sector $J_H, J_K > 0$, which they identified as symmetry enriched topological (SET) phases. Ground state phase diagrams for three different spin values can be found in Fig. 2.6a. Note that the phase transition between the different spin liquid phases seems to depend on the value of the spin. In particular, the transition between SL1 and SL2 occurs at a smaller ratio J_K/J_H for larger spin values. The nature of the quantum phase transitions between the different QSL phases remained unclear and will be addressed in this thesis.

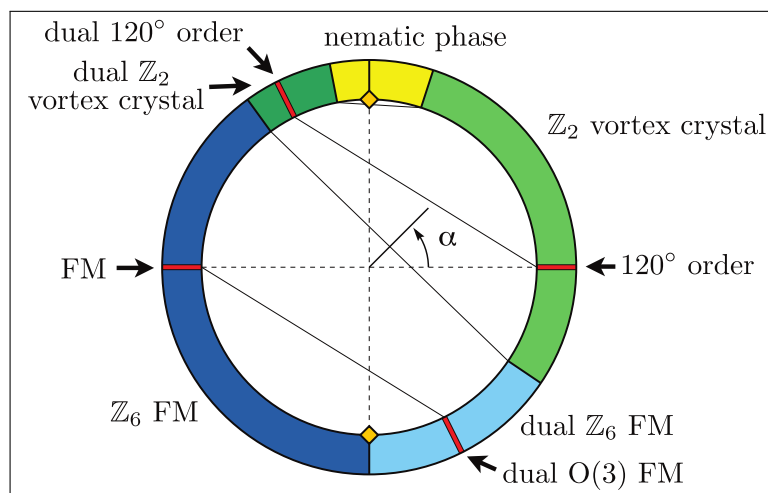


Fig. 2.5. Phase diagram of the Heisenberg-Kitaev model on the triangular lattice for $S = 1/2$ as obtained by Becker et al., using the parametrization $J_H = \cos \alpha$, $J_K = \sin \alpha$. (Figure taken from [25])

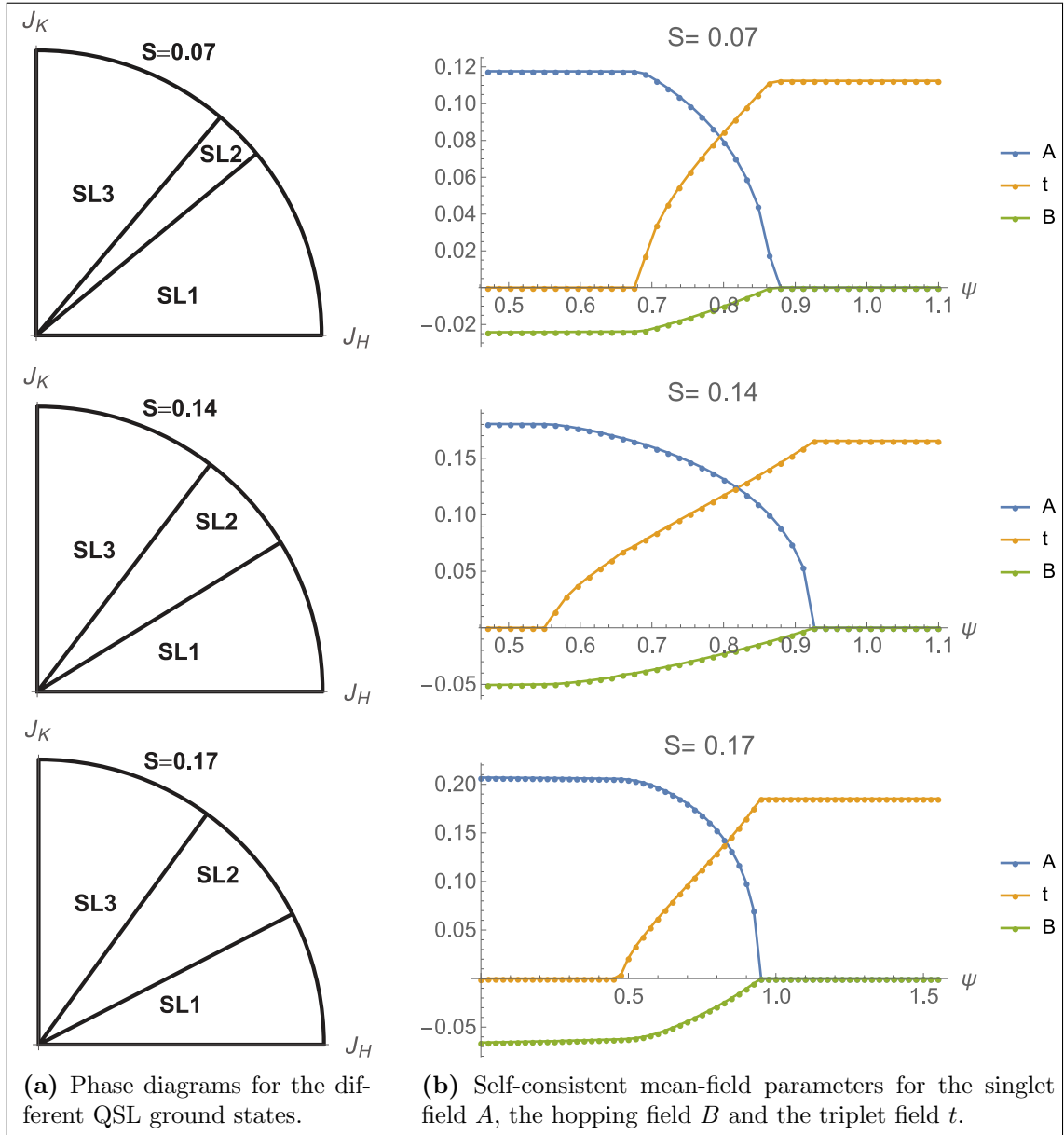


Fig. 2.6. Phase diagrams and self-consistent mean-field parameters as obtained by Kos and Punk [2] using the parametrization $J_H = \cos \psi$, $J_K = \sin \psi$. Here, SL1, SL2, and SL3 denote the three different QSL phases obtained in SBMFT using totally symmetric ansätze, defined by the different fields taking (non-)zero values. (Figures taken from [2])

2.2.2. Connection to Real Materials

So far, our discussion of quantum spin liquids was rather abstract and we did not connect our theoretical concepts to real materials. However, several promising candidates for QSL states in real materials have been studied using numerical and experimental techniques [27]. For example, in the compound κ -(BEDT-TTF)₂Cu₂(CN)₃, in which an almost isotropic triangular Heisenberg model is realized, QSL behavior was found using ¹H NMR and static susceptibility measurements [28]. Using neutron scattering, Cs₂CuCl₄ was found to host a QSL phase and spinon excitations [29], where a description by an anisotropic Heisenberg interaction applies. A recent example of a triangular lattice compound possibly hosting a QSL ground state is LiYbS₂, where magnetic susceptibility and ⁷Li NMR measurements indicate the absence of magnetic long range order down to 2 K [30].

Strong spin-orbit coupling could give rise to a Kitaev-type interaction in certain Mott insulating materials. Often, this Kitaev interaction is accompanied by a residual Heisenberg interaction, thus the system can be described by an effective Heisenberg-Kitaev model. A possible class of materials realizing this idea are the iridates A₂IrO₃, A = Na, Li [31]. Analyzing thermodynamic measurements, α -Li₂IrO₃ was estimated to be close to a spin-liquid regime, whereas Na₂IrO₃ seems to be in a magnetically ordered regime [32]. Instead of a triangular lattice, these materials form a hexagonal lattice. However, the Ir⁴⁺-ions in the compound Ba₃IrTi₂O₉ were found to form a triangular lattice and could theoretically be described by a spin-1/2 Heisenberg-Kitaev model [25]. Indeed, experimental measurements of the magnetic susceptibility did not find magnetic ordering down to 2 K [33]. Even more, heat capacity measurements give no indication for magnetic order down to 0.35 K. These measurements suggest that Ba₃IrTi₂O₉ hosts a quantum spin liquid described by the Heisenberg-Kitaev model on a triangular lattice.

2.3. Renormalization Group Fundamentals

Having introduced quantum phase transitions and QSL states, we now take a different perspective on the system under study. The Heisenberg-Kitaev model is a theory of pure interaction in the sense that the Hamiltonian only contains interaction terms and no kinetic term. Thus, we are more or less directly in the regime of strong interactions. A meaningful analysis of interacting theories is notoriously difficult. A convenient method to gain knowledge about the behavior in the limit of weak interactions is perturbation theory, especially in combination with diagrammatic techniques [34, 35]. However, in the regime of strong coupling, perturbation theory is doomed to fail and a different method has to be used. A method which turned out to be particularly useful is the *renormalization group* (RG), which was mainly developed by Wilson. Here, we will only sketch the main idea following reference [36] and refer to the literature for a more detailed discussion [37–40].

In condensed matter physics, we are mainly interested in the long-range behavior of a system so that it seems natural to integrate out fast, short-range fluctuations in order to obtain an effective theory for the slow, long-range fluctuations. However, the separation of fast and slow fluctuations is in general not clear a priori and instead, one introduces a scale $\Lambda = \Lambda_0/b$ in momentum space which separates fast and slow fluctuations, where Λ_0 is some ultraviolet (UV) scale at which the parameters of the theory are known, and b

parametrizes the recursive step discussed next.

The recursive RG step starts with the integration over the fast field components and yields a new effective action for the slow field components. At this stage, approximations like a loop expansion are needed in most cases. The choice of reasonable approximations strongly influences the effectiveness of the RG method. Rescaling momenta and frequencies in such a way that the kinetic term of the theory becomes scale-invariant yields a mapping from the old couplings \mathbf{g} to a set of new couplings $\mathbf{g}' = \tilde{R}(\mathbf{g})$. Now, for the new effective theory the RG step is repeated and again the fast field components are integrated out. Repeating this argument recursively, one obtains a flow for the couplings which is parametrized by the rescaling parameter b .

Introducing the infinitesimal, logarithmic flow parameter $l = \log b$ one obtains the *Gell-Mann–Low equation* or *β -function* for the change of the couplings under the RG step:

$$\frac{d\mathbf{g}}{dl} = R(\mathbf{g}), \quad \text{where } R(\mathbf{g}) = \lim_{l \rightarrow 0} l^{-1} \left(\tilde{R}(\mathbf{g}) - \mathbf{g} \right).$$

We identify the Gell-Mann–Low equation as a set of flow equations for the couplings which might have fixed points which do not change under the RG step, thus parametrizing a scale-invariant action. Now, the correlation length ξ describing the exponential decay of field correlations is a natural length scale for a given system. Importantly, only $\xi = 0$ and $\xi = \infty$ are compatible with the argument of scale-invariance. However, the divergence of the correlation length can be seen as a hallmark of a second order phase transition. Therefore, the study of fixed points of the RG flow might help to understand phase transitions of the system under study.

The fixed point structure of the flow equations can be investigated further. Linearizing the flow equations around the fixed point \mathbf{g}^* one might use the eigenvalues λ_α and left-eigenvectors ϕ_α of the resulting matrix to define scaling fields,

$$v_\alpha = \phi_\alpha^T (\mathbf{g} - \mathbf{g}^*),$$

satisfying the property

$$\frac{dv_\alpha}{dl} = \lambda_\alpha v_\alpha.$$

We distinguish three different types of RG eigenvalues and scaling fields:

- $\lambda_\alpha > 0$: The flow is directed away from the fixed point and the corresponding scaling field is called *relevant*.
- $\lambda_\alpha < 0$: The flow is directed towards the fixed point and the corresponding scaling field is called *irrelevant*.
- $\lambda_\alpha = 0$: In this case, the scaling field is stationary under the flow and is called *marginal*.

Using this classification of RG eigenvalues, we can also distinguish different types of fixed points:

- *Stable fixed points* with only irrelevant and marginal scaling fields. These describe stable phases of matter, as any small deviation from the (fine-tuned) fixed point is decreased upon the RG flow, driving the system back to the stable fixed point.

- *Unstable fixed points* with only relevant scaling fields. They do not describe special phases of matter, but are highly important for the global structure of the RG flow.
- *Generic fixed points* involving both relevant and irrelevant scaling fields. These turn out to be particularly important for the understanding of phase transitions. The irrelevant scaling fields span the so-called *critical manifold*. Starting on the critical manifold the couplings get attracted to the fixed point. However, even the slightest deviation from the critical manifold introduces some relevant parameter and drives the flow away from the fixed point to either some other fixed point or to the strongly interacting regime.
- *Critical fixed points* as a special case of the previous type, with one relevant and an arbitrary number of irrelevant scaling fields, where the relevant perturbation drives a phase transition. This class of fixed points is clearly the most interesting one for the analysis of critical phenomena and indicates a second order phase transition.

Furthermore, the RG eigenvalues can be used to calculate critical exponents which can be measured in experiments. Thus, the RG not only allows for qualitative statements but also for *quantitative* predictions which can be tested in experiments.

This superficial introduction to the philosophy of the renormalization group already indicates its effectiveness in the study of critical phenomena in the strongly correlated regime. However, RG methods can be used not only in condensed matter physics but also in high-energy physics and statistical physics. Also, many different implementations exist for both numerical and analytical approaches. In the next section, we will shortly discuss the *functional renormalization group* (fRG) as a particularly versatile method due to its flexibility in the choice of the separation between slow and fast modes. Our discussion follows [21, 41]. For a more detailed introduction to the fRG we refer to the literature [41].

2.3.1. Functional Renormalization Group

Consider a field theory containing the fields φ_α , where α is some (multi-)index labeling the fields (e.g. momentum, spin, Hermitian conjugates, ...), coupled to source fields J_α . We write the partition function as functional integral:

$$\mathcal{Z}[J] = \int \mathcal{D}\varphi_\alpha e^{-S[\varphi] + \int_\alpha J_\alpha \varphi_\alpha}.$$

Next, we decompose the action into a Gaussian part,

$$S_0[\varphi] = -\frac{1}{2} \int_{\alpha, \alpha'} \varphi_\alpha (G_0^{-1})_{\alpha\alpha'} \varphi_{\alpha'},$$

and an interaction part $S_1[\varphi]$, such that

$$S[\varphi] = S_0[\varphi] + S_1[\varphi].$$

From the generating functional for connected correlators,

$$W[J] = \log \mathcal{Z}[J],$$

one can derive the vacuum expectation values of the fields φ_α ,

$$\frac{\delta W[J]}{\delta J_\alpha} = \langle \varphi_\alpha \rangle =: \phi_\alpha, \tag{2.4}$$

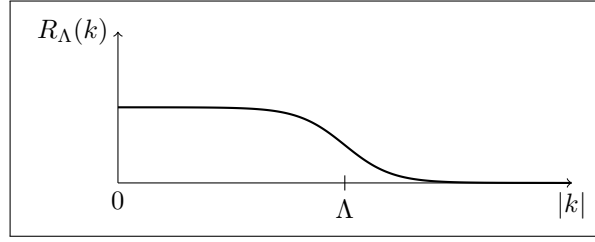


Fig. 2.7. Schematic plot of a regulator satisfying the necessary conditions.

and we define the effective action Γ as the Legendre transform of $W[J]$,

$$\Gamma[\phi] = \int_{\alpha} J_{\alpha} \phi_{\alpha} - W[J],$$

where $J_{\alpha} = J_{\alpha}[\phi]$ can be obtained by inverting Eq. (2.4). The functional derivatives of Γ with respect to ϕ_{α} give the one-particle irreducible n -point correlation functions with their full momentum and frequency dependence.²

We formalize the RG step of integrating out the fast modes by introducing a cutoff Λ such that we obtain a cutoff-dependent generating functional

$$\mathcal{Z}_{\Lambda}[J] = \int \mathcal{D}\varphi_{\alpha} e^{-S_{0,\Lambda}[\varphi] - S_1[\varphi] + \int_{\alpha} J_{\alpha} \varphi_{\alpha}},$$

where, in the cutoff-dependent Gaussian action $S_{0,\Lambda}$, the propagator G_0 is modified by some regulator R_{Λ} ,

$$G_{0,\Lambda}^{-1}(k) = G_0^{-1}(k) - R_{\Lambda}(k),$$

satisfying the conditions

$$R_{\Lambda}(k) \rightarrow \begin{cases} \infty & \text{for } \Lambda \rightarrow \infty, \\ 0 & \text{for } |k| \gg \Lambda \text{ or } \Lambda \rightarrow 0 \text{ (}|k| \text{ fixed)}, \\ > 0 & \text{for } |k| \rightarrow 0. \end{cases}$$

A schematic plot for such a regulator can be found in Fig. 2.7.

Using the regularized propagator, we define the cutoff-dependent effective action

$$\Gamma_{\Lambda}[\phi] := \int_{\alpha} J_{\alpha} \phi_{\alpha} - W_{\Lambda}[J] - \underbrace{\frac{1}{2} \int_{\alpha, \alpha'} \phi_{\alpha} (R_{\Lambda})_{\alpha\alpha'} \phi_{\alpha'}}_{\Delta S_{\Lambda}[\phi]}, \quad (2.5)$$

which is a modified Legendre transform of the cutoff-dependent generating functional, such that

$$\Gamma_{\Lambda}[\phi] = \begin{cases} S[\phi] & \text{for } \Lambda \rightarrow \infty, \\ \Gamma[\phi] & \text{for } \Lambda \rightarrow 0, \end{cases}$$

where $S[\phi]$ is the classical action at some initial UV scale.

²In our analytical approach we will neglect the external momentum and frequency dependence and restrict the correlation functions to be some parameters flowing under the RG.

Taking the derivative of Eq. (2.5) with respect to the cutoff Λ followed by some manipulations [41] one arrives at the *Wetterich equation*,

$$\partial_\Lambda \Gamma_\Lambda[\phi] = \frac{1}{2} \text{Tr} \left[\left(\mathbf{\Gamma}_\Lambda^{(2)} + \mathbf{R}_\Lambda \right)^{-1} \partial_\Lambda \mathbf{R}_\Lambda \right], \quad (2.6)$$

where the trace is performed over all indices and where we used the matrix notation³

$$\left(\mathbf{\Gamma}_\Lambda^{(2)} \right)_{\alpha\alpha'} := \frac{\delta}{\delta\phi_\alpha} \Gamma_\Lambda \frac{\overleftarrow{\delta}}{\delta\phi_{\alpha'}}.$$

The Wetterich equation is an exact equation for the flow of the effective action and defines an infinite hierarchy of flow equations for the n -point correlation functions. In order to obtain a closed set of equations, this hierarchy has to be truncated at some order n . For our analysis, we will use the *one-loop approximation*, and keep only the n -point correlation functions up to $n = 4$, neglecting all higher order correlation functions. For an action S including terms up to fourth order in the fields, this corresponds to

$$\Gamma_\Lambda = S,$$

where the parameters in S are now taken to be Λ -dependent. Thus, one can derive flow equations for the parameters as functional derivatives of the Wetterich equation with respect to the fields ϕ_α .

³The arrow above the second derivative indicates that the derivative acts from the left. This distinction is not needed for purely bosonic theories, however in the case of fermionic fields additional minus signs can arise. Since in this thesis we only use bosonic fields, we do not discuss this in further detail.

3

Chapter 3

Effective Action of the Heisenberg-Kitaev Model

Starting from the Heisenberg-Kitaev Hamiltonian,

$$\mathcal{H}_{\text{HK}} = J_{\text{H}} \sum_{\langle ij \rangle} \vec{S}_i \cdot \vec{S}_j + J_{\text{K}} \sum_{\gamma \parallel \langle ij \rangle} S_i^\gamma S_j^\gamma, \quad (3.1)$$

we want to study quantum phase transitions between different quantum spin liquid ground states on the triangular lattice discovered earlier [2]. We concentrate on the QPT at relatively small Kitaev coupling, that is the transition from SL1 to SL2 in the nomenclature of the aforementioned reference. To this end, we want to derive a critical theory describing some order parameter-like quantity characterizing the QPT.

We start by rewriting the model in terms of Schwinger bosons for which we obtain an action containing quartic interactions. We decouple this action by a Hubbard-Stratonovich transformation and integrate out the remaining Schwinger bosons. At this point, we can use a saddle point approximation as consistency check and compare our intermediate results to those by Kos and Punk. We use the saddle point approximation for some of the degrees of freedom and perform a gradient expansion of the two-point vertex for the triplet fields. Thus, we obtain an effective theory expected to characterize the critical behavior at the QPT.

3.1. Schwinger Boson Description of the Model

Since the model consists only of interaction terms and therefore does not allow for a perturbative expansion in some small parameter, we have to use another approach. In earlier works [2, 9, 42], Schwinger boson approaches turned out to be particularly useful to study frustrated spin systems. Therefore, we employ spin-1/2 bosons, b_\uparrow, b_\downarrow , and express the spin operator at lattice site i as

$$\vec{S}_i = \frac{1}{2} b_{i\alpha}^\dagger \vec{\sigma}_{\alpha\beta} b_{i\beta},$$

where $\vec{\sigma}$ is the vector of Pauli matrices and $b_{i\alpha}^{(\dagger)}$ are the creation/annihilation operators for a boson with spin α at site i .¹ For this representation to be faithful, the constraint

$$b_{i\alpha}^\dagger b_{i\alpha} = 2S \quad \forall i \quad (3.2)$$

¹If not explicitly mentioned otherwise, summation over spin indices is implied throughout this thesis.

has to be satisfied, where S is the total spin.

Using the Schwinger boson operators, we define a singlet (a_{ij}) and three triplet operators (t_{ij}^γ) on nearest-neighbor bonds,

$$\begin{aligned} a_{ij} &= \frac{1}{2} b_{i\alpha} \epsilon_{\alpha\beta} b_{j\beta} = \frac{i}{2} b_{i\alpha} \sigma_{\alpha\beta}^2 b_{j\beta} \\ t_{ij}^1 &= \frac{i}{2} b_{i\alpha} \sigma_{\alpha\beta}^3 b_{j\beta} \\ t_{ij}^2 &= -\frac{1}{2} b_{i\alpha} \delta_{\alpha\beta} b_{j\beta} \\ t_{ij}^3 &= -\frac{i}{2} b_{i\alpha} \sigma_{\alpha\beta}^1 b_{j\beta}, \end{aligned}$$

where ϵ is the anti-symmetric tensor of rank 2. These operators satisfy the identities

$$a_{ji} = -a_{ij}, \quad t_{ji}^\gamma = t_{ij}^\gamma$$

and

$$\begin{aligned} \vec{S}_i \cdot \vec{S}_j &= -2a_{ij}^\dagger a_{ij} + S^2 \\ S_i^\gamma S_j^\gamma &= -t_{ij}^{\gamma\dagger} t_{ij}^\gamma - a_{ij}^\dagger a_{ij} + S^2, \end{aligned}$$

which hold true for arbitrary spin S (see appendix A). With the new link operators the Heisenberg-Kitaev Hamiltonian reads

$$\mathcal{H}_{\text{HK}} = - (2J_{\text{H}} + J_{\text{K}}) \sum_{\langle ij \rangle} a_{ij}^\dagger a_{ij} - J_{\text{K}} \sum_{\gamma \parallel \langle ij \rangle} t_{ij}^{\gamma\dagger} t_{ij}^\gamma + \underbrace{(J_{\text{H}} + J_{\text{K}}) \sum_{\langle ij \rangle} S^2}_{\text{const.}}$$

We include the constraint in Eq. (3.2) in the Hamiltonian via Lagrange multipliers λ_i , define the new couplings

$$J_1 := 2J_{\text{H}} + J_{\text{K}}, \quad J_2 := J_{\text{K}},$$

and drop the constant term to get

$$\mathcal{H} = -J_1 \sum_{\langle ij \rangle} a_{ij}^\dagger a_{ij} - J_2 \sum_{\gamma \parallel \langle ij \rangle} t_{ij}^{\gamma\dagger} t_{ij}^\gamma + \sum_i \lambda_i (b_{i\alpha}^\dagger b_{i\alpha} - 2S).$$

We relax the constraint to hold only on average, i.e. $\lambda_i = \lambda$. In principle, this allows doubly-occupied or unoccupied sites, which correspond to unphysical states in the enlarged Hilbert space of the Schwinger boson representation. However, studies involving the related pseudo-fermion representation showed that, using the relaxed constraint, the ground state remains in the physical Hilbert space, where all sites are singly-occupied [43]. A similar behavior is expected for our Schwinger boson representation as well, thus justifying the approximation.²

²The validity of this approximation can also be seen from gauge theoretical considerations: It is possible to describe the anti-ferromagnetic Heisenberg model in terms of a U(1) lattice gauge theory [12,21]. In this description the (now time-dependent) field $\lambda_i(\tau)$ plays the role of the temporal component of the gauge field. It turns out that in the present case the fluctuations of the gauge field are gapped and therefore approximating $\lambda_i(\tau)$ by its expectation value should not change the theory significantly. We comment on the gapped gauge fluctuations later on when discussing the validity of a saddle point approximation.

In this approximation, the Hamiltonian in the Schwinger boson representation takes the form

$$\mathcal{H}_{\text{SB}} = -J_1 \sum_{\langle ij \rangle} a_{ij}^\dagger a_{ij} - J_2 \sum_{\gamma \parallel \langle ij \rangle} t_{ij}^{\gamma\dagger} t_{ij}^\gamma + \lambda \sum_i b_{i\alpha}^\dagger b_{i\alpha} - 2\lambda N S. \quad (3.3)$$

Here, from a formal point of view, S can take any real value and it was seen earlier, that below some critical value, $S_{\text{crit}} < 1/2$, spin liquid states can emerge. We will briefly discuss this in the context of the saddle point approximation below.

In SBMFT this Hamiltonian would be the starting point for replacing the singlet and triplet operators by their mean-field values, expanding in the fluctuations around the mean-field and again rewriting the fluctuations in terms of Schwinger boson operators. This was done by Kos and Punk in their previous work [2]. Here, we will not use the mean-field approximation but instead use a Hubbard-Stratonovich transformation to decouple the quartic interactions of the Schwinger bosons in the next section. This allows for a more systematic treatment of the fluctuations around the mean-field solution.

3.1.1. Hubbard-Stratonovich Transformation

Using a functional integral approach, the partition function can be written as

$$\mathcal{Z} = \int \mathcal{D}[\bar{b}, b, \lambda] e^{-\mathcal{S}_{\text{SB}}[b, \lambda]},$$

$$\mathcal{S}_{\text{SB}}[b, \lambda] = \int_0^\beta d\tau \left(\sum_i \bar{b}_{i\alpha}(\tau) \partial_\tau b_{i\alpha}(\tau) + \mathcal{H}_{\text{SB}}[\bar{b}(\tau), b(\tau)] \right).$$

The Hamiltonian for the Schwinger bosons contains terms quartic in the bosons, $b_{i\sigma}$.³ To decouple this quartic interaction, we perform a Hubbard-Stratonovich transformation using the identity

$$1 = \int \mathcal{D}[\bar{A}, A] e^{-J_1 \sum_{\langle ij \rangle} \int_0^\beta d\tau \bar{A}_{ij}(\tau) A_{ij}(\tau)},$$

and shifting the A -field according to the rules

$$A_{ij}(\tau) \rightarrow A_{ij}(\tau) - \frac{1}{2} b_{i\alpha}(\tau) \epsilon_{\alpha\beta} b_{j\beta}(\tau) = A_{ij}(\tau) - a_{ij}(\tau)$$

$$\bar{A}_{ij}(\tau) \rightarrow \bar{A}_{ij}(\tau) - \frac{1}{2} \bar{b}_{i\alpha}(\tau) \epsilon_{\alpha\beta} \bar{b}_{j\beta}(\tau) = \bar{A}_{ij}(\tau) - \bar{a}_{ij}(\tau).$$

Introducing analogous Hubbard-Stratonovich fields T^γ for the triplets t^γ , we decouple all quartic terms in the pairing channel.⁴ Decoupling in the pairing channel seems reasonable as we want to construct an RVB-like ground state consisting mostly of spin singlets and some (rather dilute) triplets. Flint and Coleman [42] argued that an additional decoupling in the hopping channel yields more reliable results and a more accurate description in large N descriptions. However, for our Schwinger boson representation, where $N = 2$, the inclusion of the hopping term is mainly used to improve numerical stability. Therefore, we treat numerical accuracy for a simpler description involving only the pairing channel.

³Recall that a_{ij} and t_{ij} are both quadratic in b .

⁴To avoid confusion, from now on temperature is always expressed by the inverse temperature β and $T^{(\gamma)}$ always refers to the triplet field.

Note, that the triplet fields T^γ are only non-zero on the corresponding γ -links, i.e.

$$T_{ij}^\gamma = T_{ij}^\gamma \delta_{\mathbf{r}_j, \mathbf{r}_i \pm \mathbf{a}_\gamma}.$$

Thus, we obtain the equivalent action

$$\begin{aligned} \mathcal{S}[b, \lambda, A, T^\gamma] = \int_\tau \left\{ \sum_i \bar{b}_{i\alpha} (\partial_\tau + \lambda) b_{i\alpha} + \sum_{\langle ij \rangle} \left(J_1 |A_{ij}|^2 + J_2 \sum_\gamma |T_{ij}^\gamma|^2 \right) \right. \\ \left. - \sum_{\langle ij \rangle} \left(\frac{J_1}{2} \epsilon_{\alpha\beta} \bar{A}_{ij} + \frac{J_2 i}{2} \sigma_{\alpha\beta}^3 \bar{T}_{ij}^1 - \frac{J_2}{2} \delta_{\alpha\beta} \bar{T}_{ij}^2 - \frac{J_2 i}{2} \sigma_{\alpha\beta}^1 \bar{T}_{ij}^3 \right) b_{i\alpha} b_{j\beta} + \text{c.c.} \right\} \\ - 2\lambda N S \beta, \end{aligned} \quad (3.4)$$

where we dropped the imaginary time arguments for convenience and introduced the notation

$$\int_\tau = \int_0^\beta d\tau.$$

3.1.2. Transformation to Frequency and Momentum Space

Defining the fields $b_{i\alpha}(\omega_n)$ and $A_{ij}(\Omega)$ in frequency space via

$$\begin{aligned} b_{i\alpha}(\tau) &= \frac{1}{\sqrt{\beta}} \sum_{\omega_n} b_{i\alpha}(\omega_n) e^{i\omega_n \tau}, \\ A_{ij}(\Omega) &= \int_\tau e^{-i\Omega \tau} A_{ij}(\tau), \end{aligned}$$

and analogously for $T_{ij}^\gamma(\Omega)$, we can write the action in frequency space as

$$\begin{aligned} \mathcal{S}[b, \lambda, A, T^\gamma] = \sum_{\omega_n} \left\{ \sum_i \bar{b}_{i\alpha}(\omega_n) (i\omega_n + \lambda) b_{i\alpha}(\omega_n) + \frac{1}{\beta} \sum_{\langle ij \rangle} \left(J_1 |A_{ij}(\omega_n)|^2 + J_2 \sum_\gamma |T_{ij}^\gamma(\omega_n)|^2 \right) \right\} \\ - \frac{1}{\beta} \sum_{\omega_n, \omega_{n'}} \sum_{\langle ij \rangle} \left\{ \left(\frac{J_1}{2} \epsilon_{\alpha\beta} \bar{A}_{ij}(\omega_n + \omega_{n'}) + \frac{J_2 i}{2} \sigma_{\alpha\beta}^3 \bar{T}_{ij}^1(\omega_n + \omega_{n'}) \right. \right. \\ \left. \left. - \frac{J_2}{2} \delta_{\alpha\beta} \bar{T}_{ij}^2(\omega_n + \omega_{n'}) - \frac{J_2 i}{2} \sigma_{\alpha\beta}^1 \bar{T}_{ij}^3(\omega_n + \omega_{n'}) \right) b_{i\alpha}(\omega_n) b_{j\beta}(\omega_{n'}) \right. \\ \left. + \text{c.c.} \right\} \\ - 2\lambda N S \beta. \end{aligned}$$

Similarly, we define the fields in momentum space via

$$\begin{aligned} b_{i\alpha}(\omega_n) &= \frac{1}{\sqrt{N}} \sum_{\mathbf{k}} e^{-i\mathbf{k}\mathbf{r}_i} b_{\mathbf{k}\alpha}(\omega_n), \\ \bar{A}_{\mathbf{K}}^\gamma(\Omega) &= \sum_i \bar{A}_{i, i+\gamma}(\Omega) e^{-i\mathbf{K}\mathbf{r}_i}, \end{aligned}$$

and analogously for $T_{\mathbf{K}}^\gamma(\Omega)$.

The momentum space expressions for the coupling of the Schwinger bosons to the Hubbard-Stratonovich fields are somewhat non-trivial due to the geometry of the triangular lattice:

$$\begin{aligned}
& \frac{J_1 \epsilon_{\alpha\beta}}{2\beta} \sum_{\omega_n, \omega_{n'}} \sum_{\langle ij \rangle} \bar{A}_{ij}(\omega_n + \omega_{n'}) b_{i\alpha}(\omega_n) b_{j\beta}(\omega_{n'}) \\
&= \frac{J_1 \epsilon_{\alpha\beta}}{2N\beta} \sum_{\omega_n, \omega_{n'}} \sum_{\mathbf{k}, \mathbf{k}'} \sum_{\langle ij \rangle} \bar{A}_{ij}(\omega_n + \omega_{n'}) e^{-i(\mathbf{k}\mathbf{r}_i + \mathbf{k}'\mathbf{r}_j)} b_{\mathbf{k}\alpha}(\omega_n) b_{\mathbf{k}'\beta}(\omega_{n'}) \\
&= \frac{J_1 \epsilon_{\alpha\beta}}{4N\beta} \sum_{\omega_n, \omega_{n'}} \sum_{\mathbf{k}, \mathbf{k}'} \sum_{i, \pm\gamma} \bar{A}_{i, i\pm\gamma}(\omega_n + \omega_{n'}) e^{-i(\mathbf{k} + \mathbf{k}')\mathbf{r}_i \mp i\mathbf{k}'\mathbf{a}_\gamma} b_{\mathbf{k}\alpha}(\omega_n) b_{\mathbf{k}'\beta}(\omega_{n'}) \\
&= \frac{J_1 \epsilon_{\alpha\beta}}{4N\beta} \sum_{\omega_n, \omega_{n'}} \sum_{\mathbf{k}, \mathbf{k}'} \sum_{i, \gamma} \bar{A}_{i, i+\gamma}(\omega_n + \omega_{n'}) e^{-i(\mathbf{k} + \mathbf{k}')\mathbf{r}_i} \left(e^{-i\mathbf{k}'\mathbf{a}_\gamma} - e^{i\mathbf{k}'\mathbf{a}_\gamma} \right) b_{\mathbf{k}\alpha}(\omega_n) b_{\mathbf{k}'\beta}(\omega_{n'}) \\
&= -i \frac{J_1 \epsilon_{\alpha\beta}}{2N\beta} \sum_{\omega_n, \omega_{n'}} \sum_{\mathbf{k}, \mathbf{k}'} \sum_{i, \gamma} \bar{A}_{i, i+\gamma}(\omega_n + \omega_{n'}) e^{-i(\mathbf{k} + \mathbf{k}')\mathbf{r}_i} \sin(ak'_\gamma) b_{\mathbf{k}\alpha}(\omega_n) b_{\mathbf{k}'\beta}(\omega_{n'}) \\
&= -i \frac{J_1}{2N\beta} \epsilon_{\alpha\beta} \sum_{\omega_n, \omega_{n'}} \sum_{\mathbf{k}, \mathbf{k}'} \sum_{\gamma} \sin(ak'_\gamma) \bar{A}_{\mathbf{k}+\mathbf{k}'}^\gamma(\omega_n + \omega_{n'}) b_{\mathbf{k}\alpha}(\omega_n) b_{\mathbf{k}'\beta}(\omega_{n'}).
\end{aligned}$$

Here, we used the notation

$$ak_\gamma = \mathbf{a}_\gamma \cdot \mathbf{k},$$

where \mathbf{a}_γ is any of the lattice vectors and a is the lattice constant. The factor of two in the second equality is needed to compensate for overcounting when changing from a sum over nearest-neighbors to a sum over *all* lattice sites. Note in particular that, when changing to the sum over all lattice sites, we include bonds in both directions, $\pm\mathbf{a}_\gamma$. This is special for the triangular lattice, as, for example, on the hexagonal lattice only $+\mathbf{a}_\gamma$ bonds exist. This is the first expression in our discussion, where the lattice geometry enters the mathematical structure of the theory.

By a similar calculation one finds for the term containing $\bar{T}^\gamma bb$

$$\begin{aligned}
& \frac{J_2}{2N\beta} \sum_{\omega_n, \omega_{n'}} \sum_{\langle ij \rangle} \bar{T}_{ij}^\gamma(\omega_n + \omega_{n'}) b_{i\alpha}(\omega_n) b_{j\beta}(\omega_{n'}) \\
&= \frac{J_2}{2N\beta} \sum_{\omega_n, \omega_{n'}} \sum_{\mathbf{k}, \mathbf{k}'} \cos(ak'_\gamma) \bar{T}_{\mathbf{k}+\mathbf{k}'}^\gamma(\omega_n + \omega_{n'}) b_{\mathbf{k}\alpha}(\omega_n) b_{\mathbf{k}'\beta}(\omega_{n'}).
\end{aligned}$$

We introduce the notation $k = (\omega_k, \mathbf{k}) = (k_0, \mathbf{k})$, $b_\alpha(k) = b_{\alpha\mathbf{k}}(\omega_k)$, and

$$\sum_{\mathbf{k}} = \sum_{k_0, \mathbf{k}},$$

and write the action in frequency and momentum space as

$$\begin{aligned}
& \mathcal{S}[b, \lambda, A, T^\gamma] \\
&= \sum_{\mathbf{k}} \left\{ \bar{b}_\alpha(k) (ik_0 + \lambda) b_\alpha(k) + \frac{1}{N\beta} \sum_{\gamma} (J_1 |A^\gamma(k)|^2 + J_2 |T^\gamma(k)|^2) \right\} \\
&\quad - \frac{1}{N\beta} \sum_{k, k'} \left(-i \frac{J_1}{2} \epsilon_{\alpha\beta} \left(\sum_{\gamma} \sin(ak'_\gamma) \bar{A}^\gamma(k+k') \right) + i \frac{J_2}{2} \cos(ak'_1) \sigma_{\alpha\beta}^3 \bar{T}^1(k+k') \right. \\
&\quad \quad \left. - \frac{J_2}{2} \cos(ak'_2) \delta_{\alpha\beta} \bar{T}^2(k+k') - \frac{J_2 i}{2} \cos(ak'_3) \sigma_{\alpha\beta}^1 \bar{T}^3(k+k') \right) b_\alpha(k) b_\beta(k') + \text{c.c.} \\
&\quad - 2\lambda N S \beta. \tag{3.5}
\end{aligned}$$

The diagrammatic Feynman rules for this theory are illustrated in Fig. 3.1. We represent Schwinger boson propagators by solid lines and propagators for the A (T^γ) fields by dashed (solid) double lines.

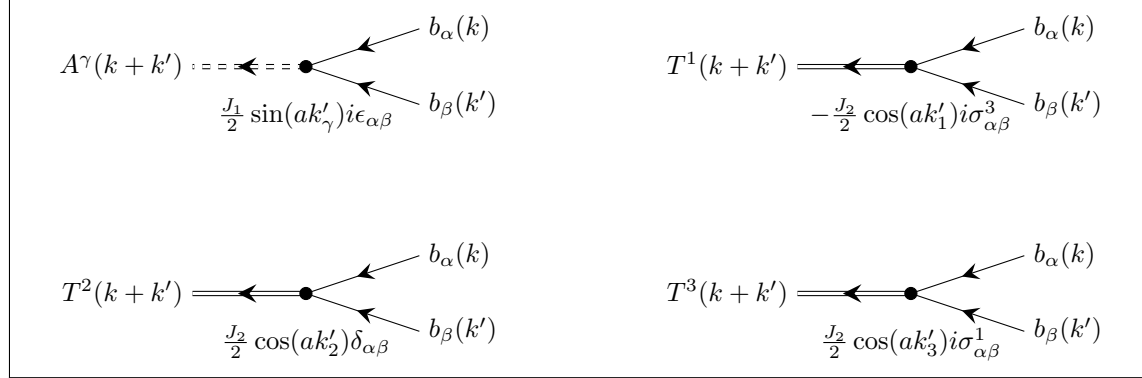


Fig. 3.1. Diagrammatic Feynman rules for the action Eq. (3.5) of the Schwinger bosons. Solid single lines represent Schwinger bosons, dashed (solid) double lines represent the A (T^γ) fields.

3.2. Integrating Out the Schwinger Bosons

Since the action in Eq. (3.5) is quadratic in the Schwinger bosons, we can formally integrate them out via a functional Gauss integral. We rewrite the action in terms of pseudo-spinors,

$$\Psi(k) = \left(b_\uparrow(k), b_\downarrow(k), b_\uparrow^\dagger(-k), b_\downarrow^\dagger(-k) \right)^T,$$

and introduce the notation

$$\delta_{k,k'} = \delta_{k_0,k'_0} \delta_{\mathbf{k}\mathbf{k}'}$$

Since the components of the pseudo-spinor $\Psi(k)$ are *not* linearly independent, a simple summation over all 3-momenta k would lead to double-counting and therefore a change of the partition function. In order to compensate for double-counting, we only sum over half the momentum space, $k_\alpha = \mathbf{n}_\alpha \cdot \mathbf{k} \geq 0$ for some (arbitrary) direction specified by the unit vector \mathbf{n}_α . We indicate the restricted sum by \sum' , such that the action reads

$$\begin{aligned} \mathcal{S}[\Psi, \lambda, A, T^\gamma] &= \frac{1}{2N\beta} \sum'_{k,k'} \bar{\Psi}(k) \mathbf{G}_{k,k'}^{-1} \Psi(k') \\ &+ \frac{1}{N\beta} \sum_k \sum_\gamma (J_1 |A^\gamma(k)|^2 + J_2 |T^\gamma(k)|^2) - 2N\beta\lambda S, \end{aligned} \quad (3.6)$$

where

$$\begin{aligned}
\left(\mathbf{G}_{k,k'}^{-1}\right)_{11} &= N\beta (ik_0 + \lambda) \delta_{kk'} \mathbb{1}_2, \\
\left(\mathbf{G}_{k,k'}^{-1}\right)_{12} &= -J_1\sigma^2 \sum_{\gamma} \sin(ak'_\gamma) A^\gamma(k-k') \\
&\quad + J_2 (i\sigma^3 \cos(ak'_1) T^1(k-k') - \mathbb{1}_2 \cos(ak'_2) T^2(k-k') - i\sigma^1 \cos(ak'_3) T^3(k-k')), \\
\left(\mathbf{G}_{k,k'}^{-1}\right)_{21} &= -J_1\sigma^2 \sum_{\gamma} \sin(ak'_\gamma) \bar{A}^\gamma(k'-k) \\
&\quad + J_2 (-i\sigma^3 \cos(ak'_1) \bar{T}^1(k'-k) - \mathbb{1}_2 \cos(ak'_2) \bar{T}^2(k'-k) + i\sigma^1 \cos(ak'_3) \bar{T}^3(k'-k)), \\
\left(\mathbf{G}_{k,k'}^{-1}\right)_{22} &= N\beta (-ik_0 + \lambda) \delta_{kk'} \mathbb{1}_2
\end{aligned}$$

is the inverse Green's function of the pseudo-spinor Ψ .

Integrating out the bosonic pseudo-spinor Ψ we get

$$\begin{aligned}
\mathcal{Z} &= \int \mathcal{D} [\bar{\Psi}, \Psi, \lambda, \bar{A}, A, \bar{T}^\gamma, T^\gamma] e^{-\mathcal{S}[\Psi, \lambda, A, T^\gamma]} \\
&= \int \mathcal{D} [\lambda, \bar{A}, A, \bar{T}^\gamma, T^\gamma] e^{-\frac{1}{N\beta} \sum_{k,\gamma} (J_1 |A^\gamma(k)|^2 + J_2 |T^\gamma(k)|^2) + 2N\beta\lambda S} \det \left(\frac{1}{2N\beta} \mathbf{G}^{-1} \right)^{-1} \\
&= \int \mathcal{D} [\lambda, \bar{A}, A, \bar{T}^\gamma, T^\gamma] e^{-\tilde{\mathcal{S}}[\lambda, A, T^\gamma]},
\end{aligned}$$

where we defined

$$\tilde{\mathcal{S}}[\lambda, A, T^\gamma] := \frac{1}{N\beta} \sum_{k,\gamma} (J_1 |A^\gamma(k)|^2 + J_2 |T^\gamma(k)|^2) - 2N\beta\lambda S + \text{Tr} \log \left(\frac{1}{2N\beta} \mathbf{G}^{-1} \right). \quad (3.7)$$

Here, the trace has to be performed over frequencies, momenta and spinor indices, but *without* any additional prefactors since these are already included in the Green's function,

$$\text{Tr} \rightarrow \sum_k' \text{tr}_4.$$

3.3. Saddle Point Approximation for A and λ

Before we continue our derivation of an effective field theory, we want to use a saddle point approximation to get a first understanding of the system. Thus, we get mean-field estimates for the singlet field A and the Lagrange multiplier λ . In particular, we will see that the assumption $J_1 A/\lambda \ll 1$ - which will turn out to be very useful in our further discussion - can be satisfied by tuning the spin value S . Furthermore, we can use the saddle point approximation to compare our theory to the qualitative behavior found by Kos and Punk [2] and use this as a consistency check on our way towards a theory beyond Schwinger boson mean-field theory.

The projective symmetry group (PSG) analysis performed by Kos and Punk motivates a spatially and temporally homogeneous mean-field ansatz,

$$A_{ij}(\omega) = \pm A \delta_{\omega,0} \delta_{j,i\pm\gamma}, \quad T_{ij}^\gamma(\omega) = T \delta_{\omega,0} \delta_{j,i\pm\gamma},$$

where A can be chosen as real. Therefore, we have

$$A^\gamma(k) = AN\beta\delta_{k,0}, \quad T^\gamma(k) = TN\beta\delta_{k,0}.$$

In the saddle point approximation, the action simplifies to

$$\tilde{\mathcal{S}}_{\text{MF}}[\lambda, A, T^\gamma] = N\beta \left(3J_1 A^2 + 3J_2 |T|^2 - 2\lambda S + \frac{1}{N\beta} \text{Tr} \log \left(\frac{1}{2N\beta} \mathbf{G}_{\text{MF}}^{-1} \right) \right),$$

and the saddle point equations read

$$\frac{\partial \tilde{\mathcal{S}}_{\text{MF}}}{\partial \lambda} \stackrel{!}{=} 0, \quad \frac{\partial \tilde{\mathcal{S}}_{\text{MF}}}{\partial A} \stackrel{!}{=} 0, \quad \frac{\partial \tilde{\mathcal{S}}_{\text{MF}}}{\partial T} \stackrel{!}{=} 0.$$

Performing the derivatives, we get

$$\begin{aligned} 0 &\stackrel{!}{=} -2S + \frac{1}{N\beta} \text{Tr} \left(\mathbf{G}_{\text{MF}} \frac{\partial \mathbf{G}_{\text{MF}}^{-1}}{\partial \lambda} \right), & 0 &\stackrel{!}{=} 6J_1 A + \frac{1}{N\beta} \text{Tr} \left(\mathbf{G}_{\text{MF}} \frac{\partial \mathbf{G}_{\text{MF}}^{-1}}{\partial A} \right), \\ 0 &\stackrel{!}{=} J_2 \bar{T} + \frac{1}{N\beta} \text{Tr} \left(\mathbf{G}_{\text{MF}} \frac{\partial \mathbf{G}_{\text{MF}}^{-1}}{\partial T} \right). \end{aligned}$$

A self-consistent solution of the saddle point equations using numerical methods was undertaken in reference [2], whereas here we restrict ourselves to an approximative, analytical discussion. We are interested in the quantum phase transition where the A -field has a finite expectation value throughout the transition, and the T field acquires a finite expectation value at some parameters (J_1, J_2) . Thus, to get a feeling for the values of A and λ , we consider the case where $T = 0$ in order to estimate their mean-field values. The saddle point equation for λ takes the form

$$2S = \frac{1}{N\beta} \text{Tr} \left(\mathbf{G}_{\text{MF}}|_{T=0} \frac{\partial \mathbf{G}_{\text{MF}}^{-1}}{\partial \lambda} \Big|_{T=0} \right) = \text{Tr} (\mathbf{G}_{\text{MF}}|_{T=0}).$$

Here, we have to be careful when evaluating the various traces. Since the Matsubara summation over $\pm 1/k_0$ is formally divergent, we have to regularize the divergence by introducing the convergence generating factors $e^{ik_0 0^+}$ [36] in the inverse Green's function,

$$\left(\mathbf{G}_{\text{MF}}^{-1}|_{T=0} \right)_{kk'} = N\beta\delta_{kk'} \begin{pmatrix} (ik_0 + \lambda) e^{ik_0 0^+} \mathbb{1}_2 & -J_1 \sigma^2 \tilde{A}_{\mathbf{k}} \\ -J_1 \sigma^2 \tilde{A}_{\mathbf{k}} & (-ik_0 + \lambda) e^{-ik_0 0^+} \mathbb{1}_2 \end{pmatrix},$$

where we used

$$\tilde{A}_{\mathbf{k}} := A \sum_{\gamma} \sin(ak_{\gamma}).$$

Now, we can safely perform the trace in spinor space and get

$$2S = \frac{2}{N\beta} \sum_k' \frac{1}{k_0^2 + \lambda^2 - J_1^2 \tilde{A}_{\mathbf{k}}^2} \left((-ik_0 + \lambda) e^{-ik_0 0^+} + (ik_0 + \lambda) e^{ik_0 0^+} \right).$$

As we are interested in the ground state behavior of the system, we take the zero temperature limit and replace the Matsubara sum by an integral,

$$\frac{1}{\beta} \sum_{k_0} \rightarrow \int_{-\infty}^{\infty} \frac{dk_0}{2\pi}.$$

The frequency integral can be evaluated using the residue theorem and we get

$$\begin{aligned} 2S &= \frac{2}{N} \sum_{\mathbf{k}}' \frac{\lambda - \sqrt{\lambda^2 - J_1^2 \tilde{A}_{\mathbf{k}}^2}}{\sqrt{\lambda^2 - J_1^2 \tilde{A}_{\mathbf{k}}^2}} \\ &= \frac{2}{N} \sum_{\mathbf{k}}' \frac{\lambda}{\sqrt{\lambda^2 - J_1^2 \tilde{A}_{\mathbf{k}}^2}} - \frac{2}{N} \sum_{\mathbf{k}}'. \end{aligned}$$

Using the symmetry of the summands under $k_x \rightarrow -k_x$, the saddle point equation for λ reads

$$\begin{aligned} 2S &= \frac{1}{N} \sum_{\mathbf{k}} \frac{\lambda}{\sqrt{\lambda^2 - J_1^2 \tilde{A}_{\mathbf{k}}^2}} - 1 \\ \Leftrightarrow 2S + 1 &= \frac{1}{N} \sum_{\mathbf{k}} \frac{\lambda}{\sqrt{\lambda^2 - J_1^2 \tilde{A}_{\mathbf{k}}^2}}. \end{aligned} \quad (3.8)$$

Due to the matrix structure, all Matsubara sums in the saddle point equation for A converge and the convergence generating factor is not needed:

$$\begin{aligned} 6J_1 A &= \frac{4J_1^2 A}{N\beta} \sum_{\mathbf{k}}' \frac{\left(\sum_{\gamma} \sin(ak_{\gamma})\right)^2}{k_0^2 + \lambda^2 - J_1^2 \tilde{A}_{\mathbf{k}}^2} \\ &= \frac{2J_1^2 A}{N} \sum_{\mathbf{k}}' \frac{\left(\sum_{\gamma} \sin(ak_{\gamma})\right)^2}{\sqrt{\lambda^2 - J_1^2 \tilde{A}_{\mathbf{k}}^2}} \\ &= \frac{J_1^2 A}{N} \sum_{\mathbf{k}} \frac{\left(\sum_{\gamma} \sin(ak_{\gamma})\right)^2}{\sqrt{\lambda^2 - J_1^2 \tilde{A}_{\mathbf{k}}^2}}. \end{aligned} \quad (3.9)$$

3.3.1. Self-Consistent Solution of the Saddle-Point Equations

Instead of a (numerical) evaluation of the sums over momenta in the saddle point Eqs. (3.8) and (3.9), we stay with the qualitative behavior of these equations. Assuming that $J_1 A / \lambda \ll 1$, we expand the summands in powers of this ratio and get the approximate equations

$$\begin{aligned} 2S + 1 &\approx \frac{1}{N} \sum_{\mathbf{k}} \left(1 + \frac{J_1^2 A^2}{2\lambda^2} \left(\sum_{\gamma} \sin(ak_{\gamma}) \right)^2 \right) \\ &= 1 + \frac{J_1^2 A^2}{2\lambda^2} \sum_{\mathbf{k}} \left(\sum_{\gamma} \sin(ak_{\gamma}) \right)^2, \\ 6 &\approx \frac{J_1}{\lambda N} \sum_{\mathbf{k}} \left(\left(\sum_{\gamma} \sin(ak_{\gamma}) \right)^2 + \frac{J_1^2 A^2}{2\lambda^2} \left(\sum_{\gamma} \sin(ak_{\gamma}) \right)^4 \right). \end{aligned}$$

Taking the thermodynamic limit and replacing the momentum sums by integrals over the first Brillouin zone,

$$\frac{1}{N} \sum_{\mathbf{k}} \rightarrow \frac{1}{V_{\text{BZ}}} \int_{\text{BZ}} d^2k,$$

we find

$$\frac{1}{N} \sum_{\mathbf{k}} \left(\sum_{\gamma} \sin(ak_{\gamma}) \right)^2 = \frac{3}{2}, \quad \frac{1}{N} \sum_{\mathbf{k}} \left(\sum_{\gamma} \sin(ak_{\gamma}) \right)^4 = \frac{45}{8}.$$

Thus, we can rewrite the saddle point equation for λ as

$$2S \approx \frac{3 J_1^2 A^2}{4 \lambda^2} \Rightarrow \frac{J_1^2 A^2}{\lambda^2} = \frac{8}{3} S, \quad (3.10)$$

and inserting this in the saddle point equation for A we get

$$6 \approx \frac{3 J_1}{2 \lambda} + J_1 \frac{15 S}{2} \Rightarrow \lambda = \frac{J_1}{4 - 5 S}. \quad (3.11)$$

In particular, we see from the first equation that by decreasing S the ratio $J_1 A / \lambda$ decreases. Therefore, we are able to fulfill the assumption $J_1 A / \lambda \ll 1$ by tuning S .

The calculations above rely on the assumption that $J_1 A / \lambda \ll 1$. Therefore, our approximation will definitely break down for $S \gtrsim \frac{3}{8} = 0.375$. Indeed, previous works [9, 14] found that above some critical spin value the spin liquid description is no longer valid. We will briefly discuss this in the next section.

We can use the expressions above to estimate A and λ for some values of S and compare our estimates to the results obtained by Kos and Punk. We do not necessarily expect the numerical values to coincide, since the inclusion of a hopping parameter B for the Schwinger bosons in their work may affect the values of A and λ . Furthermore, our approximate equations are only valid in the limit $J_1 A / \lambda \ll 1$, whereas the numerical results take into account higher order corrections which become more and more relevant away from this limit. Nevertheless, the increasing value of A with increasing spin value S implied by Eqs. (3.10) and (3.11) agrees with the results of the numerical analysis. Therefore, we believe our approximation to capture the essential physics in the limit of small spin S .

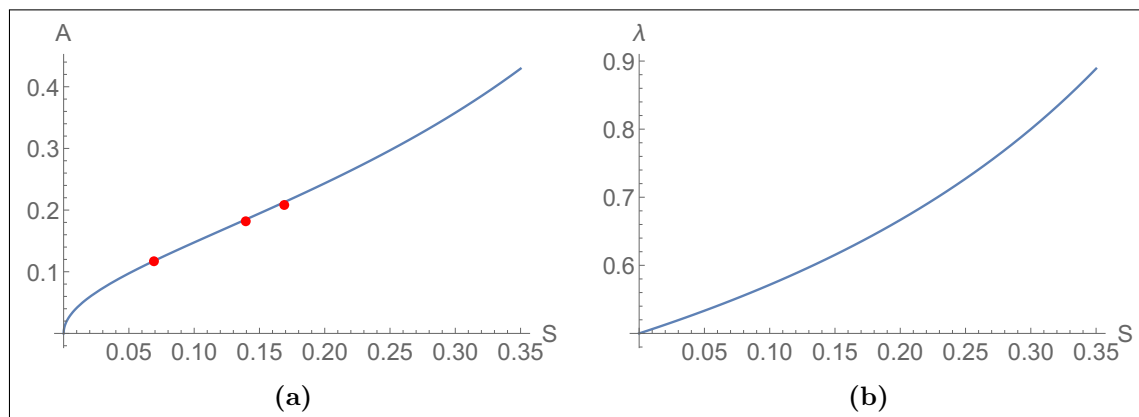


Fig. 3.2. Mean-field values of (a) A and (b) λ as functions of the spin value S ($J_1 = 2$). The red dots in (a) indicate the numerical values from Ref. [2]. Note in particular the qualitative agreement of decreasing A with decreasing S .

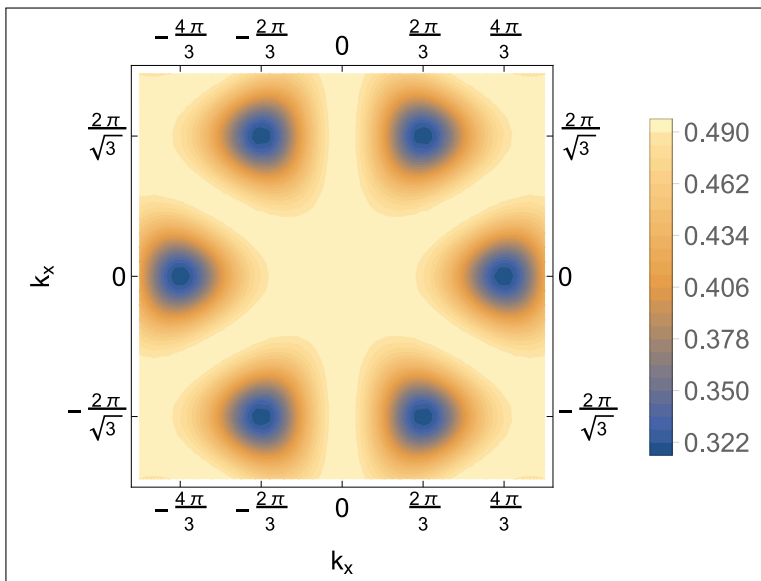


Fig. 3.3. Spinon dispersion for $\lambda = 1$, $J_1 A/\lambda = 0.3$ and lattice constant $a = 1$. The minima are located at the K -points, whereas the maximum is located at the Γ -point.

3.3.2. Spinon Dispersion and Gap Closing

Returning to the action in Eq. (3.6) before integrating out the Schwinger bosons, we can understand the qualitative change taking place at the critical spin value S_{crit} . The Hamiltonian corresponding to the action $\mathcal{S}[\Psi, \lambda, A, T^\gamma]$ can be diagonalized via a Bogoliubov transformation giving rise to a new set of bosonic operators $\gamma_{\mathbf{k}}^{(\dagger)}$. We interpret them as spinons carrying spin 1/2. For the case $T = 0$ the spinon dispersion relation is given by

$$\omega_{\text{spinon}}(\mathbf{k}) = \frac{1}{2} \sqrt{\lambda^2 - J_1^2 \tilde{A}_{\mathbf{k}}^2},$$

which is plotted in Fig. 3.3 for $\lambda = 1$, $J_1 A/\lambda = 0.3$. The minima of the spinon dispersion are located at the K -points of the first Brillouin zone, for example at $(k_x, k_y) = (4\pi/3a, 0)$, where the value is given by

$$\Delta_{\text{gap}} = \omega_{\text{spinon}}(4\pi/3a, 0) = \frac{1}{2} \sqrt{\lambda^2 - \frac{27}{4} J_1^2 A^2} = \frac{\lambda}{2} \sqrt{1 - \frac{27 J_1^2 A^2}{\lambda^2}}.$$

Therefore, the spinons are gapped as long as $J_1^2 A^2/\lambda^2 < 4/27$. As soon as the spinon gap closes, our approach of integrating out the Schwinger bosons fails, as the spinons start to form a Bose condensate with $\langle b_{\mathbf{k}_K} \rangle \neq 0$, where \mathbf{k}_K denotes the K -points. This condensation leads to the 120-degree-order of the triangular Heisenberg model as discussed in Ref. [2]. As long as the spinons are gapped, there is no magnetic order and a spin liquid state forms. Therefore, we call the regime $J_1 A/\lambda \ll 1$ the ‘spin liquid regime’ which can be reached by lowering the spin length S .

3.4. Expansion of the $\text{Tr} \log$ -term around $T^\gamma = 0$

As mentioned before, we want to discuss the quantum phase transition, where A has a finite expectation value, and T^γ plays the role of an order parameter acquiring a finite expectation value at some parameters. The phase fluctuations of A are gapped and therefore

at low energy the essential physics is captured by the (gapless) fluctuations of the triplet fields, T^γ .⁵

Deep in the spin liquid regime we can expand the term

$$\text{Tr} \log \left(\frac{1}{2N\beta} \mathbf{G}^{-1} \right)$$

in powers of T^γ as its fluctuations around 0 will be small compared to $\lambda/J_1 A$. We decompose the inverse Green's function as

$$\mathbf{G}^{-1} = \mathbf{G}_0^{-1} + \mathbf{D},$$

where

$$\mathbf{G}_{0;k,k'}^{-1} := N\beta\delta_{kk'} \begin{pmatrix} (\lambda + ik_0)\mathbb{1}_2 & -J_1 A \sigma^2 \sum_\gamma \sin(ak_\gamma) \\ -J_1 A \sigma^2 \sum_\gamma \sin(ak_\gamma) & (\lambda - ik_0)\mathbb{1}_2 \end{pmatrix}$$

and \mathbf{D} accordingly. Starting from this decomposition, we expand the Tr log-term as

$$\begin{aligned} \text{Tr} \log \left(\frac{1}{2N\beta} \mathbf{G}^{-1} \right) &= \text{Tr} \log \left(\frac{1}{2N\beta} (\mathbf{G}_0^{-1} + \mathbf{D}) \right) \\ &= \text{Tr} \log \left(\frac{1}{2N\beta} \mathbf{G}_0^{-1} \right) - \underbrace{\sum_{n=1}^{\infty} \frac{(-1)^n}{n} \text{Tr} [(\mathbf{G}_0 \mathbf{D})^n]}_{=: \tilde{\mathcal{S}}^{(n)}}. \end{aligned}$$

The linear term ($n = 1$) vanishes when evaluating the trace as expected for an expansion around the saddle point. In order to study the effect of T^γ fluctuations we start by discussing the Gaussian fluctuations.

3.4.1. Gaussian Fluctuations

The algebraic form of the second order contribution in T^γ can be anticipated from the diagrams in Fig. 3.4. Since the inverse 'bare' Green's function \mathbf{G}_0^{-1} is not diagonal in the Schwinger boson basis, one gets a somewhat unusual form for the Schwinger boson propagator. Working in the mean-field approximation with respect to A and λ , we think of the Schwinger bosons as coupled to the A -field and thus have to use

$$\omega(\mathbf{k}) = \sqrt{\lambda^2 - J_1^2 \tilde{A}_{\mathbf{k}}^2}$$

for the denominator of the Green's function.

At second order in T^γ we have

$$\begin{aligned} \tilde{\mathcal{S}}^{(2)} &= -\frac{1}{2} \text{Tr} [\mathbf{G}_0 \mathbf{D} \mathbf{G}_0 \mathbf{D}] \\ &= -\frac{1}{2} \sum'_{k,l,m,n} \text{tr}_4 [\mathbf{G}_{0;k,l} \mathbf{D}_{l,m} \mathbf{G}_{0;m,n} \mathbf{D}_{n,k}]. \end{aligned}$$

⁵Some comments on the $U(1)$ gauge structure of the theory justifying this approximation can be found in appendix B.

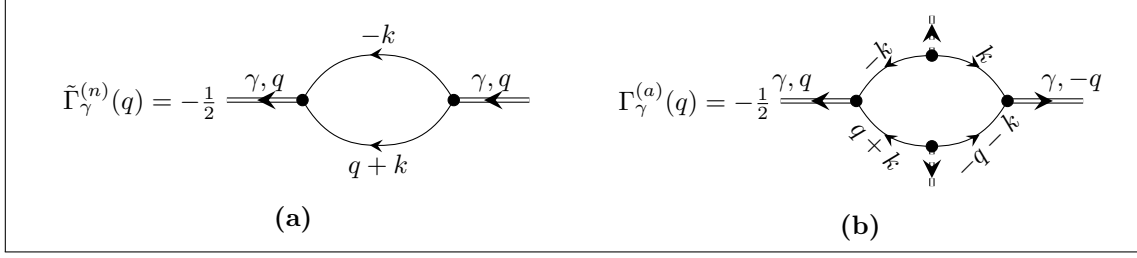


Fig. 3.4. Contributions to the (a) normal ((b) anomalous) two-point vertex from the second order expansion of the Tr log-term. For the anomalous term, coupling of Schwinger bosons to A -fields is needed as expected from the evaluation of the matrix products in the algebraic method. Recall, that the A -field only has a $k = 0$ -mode in the mean-field approximation.

Inverting the inverse ‘bare’ Green’s function we get

$$\begin{aligned} \mathbf{G}_{0;k,l} &= \frac{\delta_{k,l}}{N\beta} \frac{1}{k_0^2 + \omega^2(\mathbf{k})} \begin{pmatrix} (\lambda - ik_0) \mathbb{1}_2 & J_1 \tilde{A}_{\mathbf{k}} \sigma^2 \\ J_1 \tilde{A}_{\mathbf{k}} \sigma^2 & (\lambda + ik_0) \mathbb{1}_2 \end{pmatrix} \\ &= \frac{\delta_{k,l}}{N\beta} \begin{pmatrix} G_k^{(n)} \mathbb{1}_2 & G_k^{(a)} \sigma^2 \\ G_k^{(a)} \sigma^2 & G_{-k}^{(n)} \mathbb{1}_2 \end{pmatrix}. \end{aligned}$$

Thus, we can write the second order contribution as

$$\tilde{\mathcal{S}}^{(2)} = -\frac{1}{2N^2\beta^2} \sum'_{k,l} \text{tr}_4 [\mathbf{G}_{0;k,k} \mathbf{D}_{k,l} \mathbf{G}_{0;l,l} \mathbf{D}_{l,k}].$$

We define

$$\begin{aligned} \tilde{\mathbf{T}}(k-l) &= i\sigma^3 \cos(al_1) T^1(k-l) - \mathbb{1}_2 \cos(al_2) T^2(k-l) - i\sigma^1 \cos(al_3) T^3(k-l), \\ \tilde{\tilde{\mathbf{T}}}(l-k) &= -i\sigma^3 \cos(al_1) \tilde{T}^1(l-k) - \mathbb{1}_2 \cos(al_2) \tilde{T}^2(l-k) + i\sigma^1 \cos(al_3) \tilde{T}^3(l-k), \end{aligned}$$

and write

$$\mathbf{D}_{k,l} = -J_2 \begin{pmatrix} 0 & \tilde{\mathbf{T}}(k-l) \\ \tilde{\tilde{\mathbf{T}}}(l-k) & 0 \end{pmatrix}.$$

Evaluating the matrix product and performing the trace in spinor space we get

$$\begin{aligned} \tilde{\mathcal{S}}^{(2)} &= -\frac{J_2^2}{2N^2\beta^2} \sum'_{k,l} \left\{ G_k^{(a)} G_l^{(a)} \left(\text{tr}_2 \left[\sigma^2 \tilde{\mathbf{T}}(l-k) \sigma^2 \tilde{\mathbf{T}}(k-l) \right] + \text{tr}_2 \left[\sigma^2 \tilde{\mathbf{T}}(k-l) \sigma^2 \tilde{\mathbf{T}}(l-k) \right] \right) \right. \\ &\quad \left. + \left(G_k^{(n)} G_{-l}^{(n)} \text{tr}_2 \left[\tilde{\mathbf{T}}(k-l) \tilde{\tilde{\mathbf{T}}}(k-l) \right] + G_l^{(n)} G_{-k}^{(n)} \text{tr}_2 \left[\tilde{\mathbf{T}}(l-k) \tilde{\tilde{\mathbf{T}}}(l-k) \right] \right) \right\}. \end{aligned}$$

Using the Pauli matrix trace identity

$$\text{tr}_2 \left[\sigma^\alpha \sigma^\beta \right] = 2\delta_{\alpha\beta},$$

we can rewrite this expression as

$$\tilde{\mathcal{S}}^{(2)} = \frac{1}{N\beta} \sum_{q,\gamma} \left(\tilde{\Gamma}_\gamma^{(n)}(q) \tilde{T}^\gamma(q) T^\gamma(q) + \Gamma_\gamma^{(a)}(q) (\tilde{T}^\gamma(q) \tilde{T}^\gamma(-q) + \text{c.c.}) \right),$$

where we defined the two-point vertices $\Gamma_\gamma^{(n)}$ and $\Gamma_\gamma^{(a)}$ via⁶

$$\begin{aligned}\Gamma_\gamma^{(n)}(q) &:= J_2 + \tilde{\Gamma}_\gamma^{(n)}(q), \\ \tilde{\Gamma}_\gamma^{(n)}(q) &:= -\frac{J_2^2}{N\beta} \sum_k'' \frac{(\lambda - ik_0)(\lambda + ik_0 + iq_0) \cos(ak_\gamma) \cos(a(k_\gamma + q_\gamma))}{(k_0^2 + \omega^2(\mathbf{k}))((k_0 + q_0)^2 + \omega^2(\mathbf{k} + \mathbf{q}))},\end{aligned}\quad (3.12)$$

$$\begin{aligned}\sum_k'' &:= \sum_k - \sum_{\substack{k \\ -q_\gamma < k_\gamma < 0}} - \sum_{\substack{k \\ 0 < k_\gamma < -q_\gamma}}, \\ \Gamma_\gamma^{(a)}(q) &:= -\frac{J_2^2}{N\beta} \sum_{k_\gamma \geq \max(0, q_\gamma)} \frac{J_1^2 \tilde{A}_{\mathbf{k}} \tilde{A}_{\mathbf{k}+\mathbf{q}} \cos(ak_\gamma) \cos(a(k_\gamma + q_\gamma))}{(k_0^2 + \omega^2(\mathbf{k}))((k_0 + q_0)^2 + \omega^2(\mathbf{k} + \mathbf{q}))}.\end{aligned}\quad (3.13)$$

Instability of the Normal Two-Point Vertex

The normal two-point vertex can be understood as the inverse normal propagator for the T^γ -fields. Therefore, a potential instability will be indicated by a sign change of the normal two-point vertex at vanishing external frequency and momenta. Therefore, we perform the Matsubara sum over k_0 and evaluate the vertex at $q = 0$ to get

$$\Gamma_\gamma^{(n)}(0) = J_2 \left(1 - \frac{J_2}{4N} \sum_{\mathbf{k}} \frac{\lambda^2 + \omega^2(\mathbf{k})}{\omega(\mathbf{k})^3} \cos^2(ak_\gamma) \right).$$

Here, we used that for $q = 0$ the sum $\sum_{\mathbf{k}}''$ simplifies to a normal sum over momenta.

Since the summand in the previous expression is positive, $\Gamma_\gamma^{(n)}(0)$ vanishes for some value $J_{2,\text{crit}}$ where the Gaussian action becomes unstable so that we have to take into account higher order contributions to obtain a stable theory. The precise value of $J_{2,\text{crit}}$ could be obtained by evaluating the sum over \mathbf{k} numerically, however an estimate value can be obtained deep in the spin liquid regime without integrating the full expression. We expand the summand in powers of $J_1 A/\lambda$ and keep only terms up to second order:

$$\Gamma_\gamma^{(n)}(0) \approx J_2 \left(1 - \frac{J_2}{2\lambda N} \sum_{\mathbf{k}} \left(1 + \frac{J_1^2 A^2}{\lambda^2} \left(\sum_{\alpha} \sin(ak_\alpha) \right)^2 \right) \cos^2(ak_\gamma) \right).$$

Replacing the momentum sums by integrals over the first Brillouin zone and evaluating the integrals, we get

$$\Gamma_\gamma^{(n)}(0) \approx J_2 \left(1 - \frac{J_2}{4\lambda} \left(1 + \frac{5 J_1^2 A^2}{4 \lambda^2} \right) \right).$$

Inserting the expressions for A and λ obtained from the saddle point approximation above, we can solve the equation

$$\Gamma_\gamma^{(n)}(0) = 0$$

for J_2 and find (apart from the trivial solution $J_2 = 0$)

$$J_{2,\text{crit}} = \frac{12J_1}{(4 - 5S)(3 + 10S)}.$$

⁶For the normal two-point vertex we add the contribution J_2 which was present in the action already before expanding the $\text{Tr} \log$ -term. Therefore, we distinguish the ‘full’ normal two-point vertex Γ_n^γ and the contribution from the second order terms in the $\text{Tr} \log$ -expansion. For the anomalous two-point vertex only a contribution of the second type exists.

Using the definitions of $J_{1/2}$ and the parametrization $J_H = \cos \alpha$, $J_K = \sin \alpha$, we define the critical angle α_{crit} via

$$\alpha_{\text{crit}} := \arctan \left(\frac{2J_{2,\text{crit}}}{J_1 - J_{2,\text{crit}}} \right).$$

In particular, the critical angle does not depend on the value of J_1 or J_H but is only a function of the spin, as expected. For the spin values $S = 0.07$ (0.14, 0.17) discussed above we find $\alpha_{\text{crit}} = 1.508$ (1.467, 1.454). The tendency of smaller α_{crit} for larger S , which was one of the key results of Kos and Punk [2] (see also Fig. 2.6), is correctly captured by our estimate. As discussed for the saddle point values of A and λ , we do not expect numerical agreement due to the differences in the parametrization of the model itself and the assumption to be deep in the spin liquid.

Gradient Expansion of the Normal Two-Point Vertex

We want to derive a time-dependent Ginzburg-Landau action [44, 45] as effective action for the fluctuations of T^γ around their mean-field values, $T_{\text{MF}}^\gamma = 0$. To this end, we perform a gradient expansion of the two-point vertex,

$$\Gamma_\gamma^{(n)}(q) \approx \Gamma_\gamma^{(n)}(0) + q_0 \partial_{q_0} \Gamma_\gamma^{(n)}(0) + \sum_\alpha q_\alpha \partial_{q_\alpha} \Gamma_\gamma^{(n)}(0) + \frac{1}{2} \sum_{\alpha, \beta} q_\alpha q_\beta \partial_{q_\alpha} \partial_{q_\beta} \Gamma_\gamma^{(n)}(0).$$

We already determined the contribution $\Gamma_\gamma^{(n)}(0)$ above. For the frequency term we get

$$\begin{aligned} q_0 \partial_{q_0} \Gamma_\gamma^{(n)}(0) &= iq_0 \frac{J_2^2}{4N} \sum_{\mathbf{k}} \frac{\lambda}{\omega^3(\mathbf{k})} \\ &\approx iq_0 \frac{J_2^2}{4\lambda^2 N} \sum_{\mathbf{k}} \left(1 + \frac{3}{2} \frac{J_1^2 \tilde{A}_{\mathbf{k}}^2}{\lambda^2} \right) \cos^2(ak_\gamma) \\ &= iq_0 \frac{J_2^2}{8\lambda^2} \left(1 + \frac{15}{8} \frac{J_1^2 A^2}{\lambda^2} \right), \end{aligned}$$

where we kept only terms up to second order in $J_1 A / \lambda \ll 1$.

The term linear in the momenta vanishes by symmetry. For the term quadratic in \mathbf{q} we have to distinguish four different index combinations:

- $\alpha = \beta = \gamma$,
- $\alpha = \beta \neq \gamma$,
- twice the contribution from $\alpha \neq \beta = \gamma$,
- α, β, γ all different, $\alpha \neq \beta \neq \gamma \neq \alpha$.

The corresponding contributions are

$$\begin{aligned}
\frac{1}{2} q_\gamma^2 \partial_{q_\gamma}^2 \Gamma_\gamma^{(n)}(0) &\approx q_\gamma^2 \frac{J_2^2 a^2}{8\lambda} \left(1 + \frac{9}{16} \frac{J_1^2 A^2}{\lambda^2} \right), \\
\frac{1}{2} \sum_{\alpha \neq \gamma} q_\alpha^2 \partial_{q_\alpha}^2 \Gamma_\gamma^{(n)}(0) &\approx \sum_{\alpha \neq \gamma} q_\alpha^2 \frac{J_2^2 a^2}{8\lambda} \frac{1}{8} \frac{J_1^2 A^2}{\lambda^2}, \\
\frac{2}{2} \sum_{\alpha \neq \gamma} q_\alpha q_\gamma \partial_{q_\alpha} \partial_{q_\gamma} \Gamma_\gamma^{(n)}(0) &\approx \sum_{\alpha \neq \gamma} q_\alpha q_\gamma \frac{J_2^2 a^2}{8\lambda} \frac{1}{8} \frac{J_1^2 A^2}{\lambda^2}, \\
\frac{1}{2} \sum_{\substack{\alpha, \beta, \gamma \\ \text{distinct}}} q_\alpha q_\beta \partial_{q_\alpha} \partial_{q_\beta} \Gamma_\gamma^{(n)}(0) &\approx \sum_{\substack{\alpha, \beta, \gamma \\ \text{distinct}}} q_\alpha q_\beta \frac{J_2^2 a^2}{8\lambda} \frac{1}{8} \frac{J_1^2 A^2}{\lambda^2},
\end{aligned}$$

where we always approximated the expressions up to second order in $J_1 A/\lambda$. Note, that the term involving q_γ^2 gives the dominant contribution deep in the spin liquid regime. We will return to this point later.

Since the velocities in the final action have to be independent of the index γ in order to preserve the lattice symmetries, it is sufficient to consider the case $\gamma = 1$ for which we can rewrite the full quadratic contribution as

$$\begin{aligned}
&\frac{J_2^2 a^2}{8\lambda} \left(q_1^2 \left(1 + \frac{9}{16} \frac{J_1^2 A^2}{\lambda^2} \right) + \frac{1}{8} \frac{J_1^2 A^2}{\lambda^2} \sum_{\alpha \neq 1} (q_\alpha^2 + q_\alpha q_1) + \frac{1}{8} \frac{J_1^2 A^2}{\lambda^2} \sum_{\substack{\alpha, \beta, 1 \\ \text{distinct}}} q_\alpha q_\beta \right) \\
&= \frac{J_2^2 a^2}{8\lambda} \left(q_1^2 \left(1 + \frac{7}{16} \frac{J_1^2 A^2}{\lambda^2} \right) + \frac{1}{8} \frac{J_1^2 A^2}{\lambda^2} \left(\underbrace{q_1^2 + q_2^2 + q_3^2}_{=\sum_\alpha q_\alpha^2 = \frac{3}{2}(q_x^2 + q_y^2)} + \underbrace{q_1 q_2 + q_1 q_3 + 2q_2 q_3}_{=-\frac{1}{2}(q_x^2 + 3q_y^2)} \right) \right) \\
&= \frac{J_2^2 a^2}{8\lambda} \left(1 + \frac{9}{16} \frac{J_1^2 A^2}{\lambda^2} \right) q_1^2
\end{aligned}$$

Note, in particular, that any contribution containing q_2, q_3 vanishes at this level of accuracy so that the propagator is extremely anisotropic. Nevertheless, we expect higher order terms in $J_1 A/\lambda$ to give a contribution for these directions, however these contributions will not be taken into account here. Combining our previous results, we arrive at the following normal part of the action:

$$\frac{1}{N\beta} \sum_{q; \gamma} \bar{T}^\gamma(q) (r + Z i q_0 + c q_\gamma^2) T^\gamma(q),$$

where we defined the phenomenological parameters

$$\begin{aligned}
r &= J_2 \left(1 - \frac{J_2}{4\lambda} \left(1 + \frac{5}{4} \frac{J_1^2 A^2}{\lambda^2} \right) \right), \\
Z &= \frac{J_2^2}{8\lambda^2} \left(1 + \frac{15 J_1^2 A^2}{8\lambda^2} \right), \\
c &= \frac{J_2^2 a^2}{8\lambda} \left(1 + \frac{9}{16} \frac{J_1^2 A^2}{\lambda^2} \right).
\end{aligned}$$

Gradient Expansion of the Anomalous Two-Point Vertex

The same approach can be used to approximate the anomalous two-point vertex,

$$\begin{aligned}\Gamma_\gamma^{(a)}(q) &= -\frac{J_1^2 J_2^2}{N\beta} \sum_{k_\gamma \geq \max(0, q_\gamma)} \frac{\tilde{A}_\mathbf{k} \tilde{A}_{\mathbf{k}+\mathbf{q}} \cos(ak_\gamma) \cos(a(k_\gamma + q_\gamma))}{(k_0^2 + \omega^2(\mathbf{k})) \left((k_0 + q_0)^2 + \omega^2(\mathbf{k} + \mathbf{q}) \right)} \\ &= -\frac{J_1^2 J_2^2}{N} \sum_{k_\gamma \geq \max(0, q_\gamma)} \frac{\tilde{A}_\mathbf{k} \tilde{A}_{\mathbf{k}+\mathbf{q}} \cos(ak_\gamma) \cos(a(k_\gamma + q_\gamma)) (\omega(\mathbf{k} + \mathbf{q}) + \omega(\mathbf{k}))}{2\omega(\mathbf{k})\omega(\mathbf{k} + \mathbf{q}) \left((\omega(\mathbf{k} + \mathbf{q}) + \omega(\mathbf{k}))^2 + q_0^2 \right)},\end{aligned}$$

where we get the gradient expansion

$$\Gamma_\gamma^{(a)}(q) \approx \frac{J_2^2}{64\lambda} \frac{J_1^2 A^2}{\lambda^2} \left(-5 + 4a^2 q_\gamma^2 + a^2 \sum_{\alpha \neq \gamma} q_\alpha^2 \right).$$

Thus, the effective action up to Gaussian fluctuations reads

$$\begin{aligned}\mathcal{S}^{(2)}[T^\gamma; \lambda, A] &= 3J_1 N \beta A^2 - 2N\beta \lambda S + \text{tr} \log \left(\frac{1}{2N\beta} \mathbf{G}_0^{-1} \right) \\ &\quad + \frac{1}{N\beta} \sum_{q;\gamma} \bar{T}^\gamma(q) (r + Zi q_0 + cq_\gamma^2) T^\gamma(q) \\ &\quad + \frac{1}{N\beta} \sum_{q;\gamma} \left(t + c^{(a)} \left(3q_\gamma^2 + \sum_\alpha q_\alpha^2 \right) \right) (\bar{T}^\gamma(q) \bar{T}^\gamma(-q) + T^\gamma(q) T^\gamma(-q)),\end{aligned}$$

where we defined

$$\begin{aligned}t &= -\frac{5J_2^2}{64\lambda} \frac{J_1^2 A^2}{\lambda^2}, \\ c^{(a)} &= \frac{J_2^2 a^2}{64\lambda} \frac{J_1^2 A^2}{\lambda^2}.\end{aligned}$$

Deep in the spin liquid regime the anomalous terms do not contribute much, whereas the normal terms are dominant. In particular, we can approximate the Gaussian action as

$$\mathcal{S}_{\text{eff}}^{(2)}[T^\gamma; A, \lambda] = \frac{1}{N\beta} \sum_{q;\gamma} \bar{T}^\gamma(q) (r + Zi q_0 + cq_\gamma^2) T^\gamma(q) + \mathcal{O} \left(\frac{J_1^2 A^2}{\lambda^2} \right).$$

3.4.2. Fourth Order Contribution

Since the third order terms in T^γ vanish by spin structure arguments, we continue our discussion at fourth order. The key idea of the diagrammatic representation for this expression is given in Fig. 3.5. Here, various different spin combinations are possible and give rise to the somewhat complicated algebraic form. A more detailed derivation of this expression is given in appendix C.

Deep in the spin liquid regime, $J_1^2 A^2 / \lambda^2 \ll 1$, we can neglect the off-diagonal terms of the

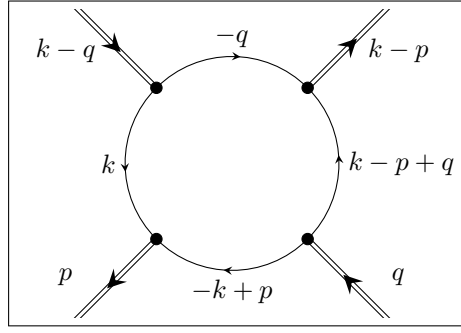


Fig. 3.5. Diagram illustrating the key idea of the fourth order contribution. Note, that the spin arguments were omitted for convenience, however they give rise to the non-trivial structure in Eq. (3.14).

Schwinger boson Green's function and get

$$\begin{aligned}
 \tilde{\mathcal{S}}^{(4)} &= -\frac{1}{4} \text{Tr} [\mathbf{G}_0 \mathbf{D} \mathbf{G}_0 \mathbf{D} \mathbf{G}_0 \mathbf{D} \mathbf{G}_0 \mathbf{D}] \\
 &\approx -\frac{2J_2^4}{4(N\beta)^4} \sum'_{k,l,m,n} G_k^{(n)} G_{0,-l}^{(n)} G_{0,m}^{(n)} G_{0,-n}^{(n)} \text{tr}_2 \left[\tilde{\mathbf{T}}(k-l) \tilde{\mathbf{T}}(m-l) \tilde{\mathbf{T}}(m-n) \tilde{\mathbf{T}}(k-n) \right] \\
 &= -\frac{J_2^4}{2N^4\beta^4} \sum_{\substack{q_1, q_2, q_3 \\ \alpha, \beta, \gamma, \delta}} \sum''_k G_{0,k}^{(n)} G_{0,-k+q_1}^{(n)} G_{0,k+q_3}^{(n)} G_{0,-k+q_2-q_3}^{(n)} \\
 &\quad \text{tr}_2 \left[\sigma^{\tau(\alpha)} \sigma^{\tau(\beta)} \sigma^{\tau(\gamma)} \sigma^{\tau(\delta)} \right] \text{sgn}(\alpha) \text{sgn}^*(\beta) \text{sgn}(\gamma) \text{sgn}^*(\delta) \\
 &\quad \cos(a(k_\alpha - q_{1,\alpha})) \cos(a(k_\beta + q_{3,\beta})) \cos(a(k_\gamma - q_{2,\gamma} + q_{3,\gamma})) \cos(ak_\delta) \\
 &\quad T^\alpha(q_1) \bar{T}^\beta(q_1 + q_3) T^\gamma(q_2) \bar{T}^\delta(q_2 - q_3),
 \end{aligned}$$

where we used

$$\sum''_k = \sum_{k_{\gamma} \geq \max(0, q_{1,\gamma}, q_{2,\gamma} - q_{3,\gamma}, -q_{3,\gamma})}$$

and defined

$$\text{sgn}(\alpha) = \begin{cases} i & \alpha = 1 \\ -1 & \alpha = 2 \\ -i & \alpha = 3 \end{cases}, \quad \tau(\alpha) = \begin{cases} 3 & \alpha = 1 \\ 0 & \alpha = 2 \\ 1 & \alpha = 3, \end{cases} \quad \sigma^0 = \mathbb{1}.$$

Using Pauli matrix identities and neglecting the frequency and momentum dependence of the four-point vertices, we can write the fourth order contribution as

$$\begin{aligned}
 \tilde{\mathcal{S}}^{(4)} &= -\frac{4u}{(N\beta)^3} \sum_{q_1, q_2, q_3} \sum_{\gamma, \gamma'} T^\gamma(q_1) \bar{T}^\gamma(q_1 + q_3) T^{\gamma'}(q_2) \bar{T}^{\gamma'}(q_2 - q_3) \\
 &\quad + \frac{2u}{(N\beta)^3} \sum_{q_1, q_2, q_3} \sum_{\gamma, \gamma'} T^\gamma(q_1) \bar{T}^{\gamma'}(q_1 + q_3) T^\gamma(q_2) \bar{T}^{\gamma'}(q_2 - q_3) \\
 &\quad - \frac{u}{(N\beta)^3} \sum_{q_1, q_2, q_3} \sum_{\gamma} T^\gamma(q_1) \bar{T}^\gamma(q_1 + q_3) T^\gamma(q_2) \bar{T}^\gamma(q_2 - q_3), \quad (3.14)
 \end{aligned}$$

where we defined

$$u := \frac{J_2^4}{64\lambda^3}.$$

Summing up all contributions up to fourth order, we finally arrive at the effective action for the T^γ -fields deep in the spin liquid regime:

$$\begin{aligned} \mathcal{S}_{\text{eff}}[T^\gamma; \lambda, A] &= \frac{1}{N\beta} \sum_{q;\gamma} \bar{T}^\gamma(q) (r + Zi q_0 + c q_\gamma^2) T^\gamma(q) \\ &\quad - 2u \frac{1}{N^3 \beta^3} \sum_{\substack{k,p,q \\ \gamma,\gamma'}} \left(2\bar{T}^\gamma(k-p)\bar{T}^{\gamma'}(p)T^\gamma(q)T^{\gamma'}(k-q) \right. \\ &\quad \quad \left. - \bar{T}^\gamma(k-p)\bar{T}^\gamma(p)T^{\gamma'}(q)T^{\gamma'}(k-q) \right) \\ &\quad - u \frac{1}{N^3 \beta^3} \sum_{\substack{k,p,q \\ \gamma}} \bar{T}^\gamma(k-p)\bar{T}^\gamma(p)T^\gamma(q)T^\gamma(k-q). \end{aligned} \quad (3.15)$$

3.5. General Properties of the Effective Action

We conclude the derivation of the effective action by a short discussion of its general properties. First of all, we note that the action in Eq. (3.15) is only valid deep in the spin liquid regime, where $J_1 A/\lambda \ll 1$. This was the key assumption of our derivation and restricts the validity of our result. Beyond this limit higher orders in $J_1 A/\lambda$ become increasingly relevant. In particular, the anomalous terms, $\propto (T^\gamma)^2, (\bar{T}^\gamma)^2$, become relevant and the action gets much more complicated. Furthermore, one would probably have to take into account an isotropic dispersion, thus changing the qualitative form of the action even more.

Deep in the spin liquid regime, we found a theory of three interacting bosonic species T^γ of the same mass. Each of them disperses anisotropically in the corresponding spatial direction \mathbf{a}_γ . This might show some quasi-one-dimensional features of the system which could be addressed in future studies. The bosons behave non-relativistically as their dispersion relation is given by

$$\omega(\mathbf{q}) \propto q_\gamma^2,$$

and the dynamical exponent is $z = 2$.

Considering for a moment the symmetric mean-field ansatz for the T^γ fields used by Kos and Punk,

$$T^\gamma(k) = N\beta\delta(k)T,$$

we get

$$\mathcal{S}_{\text{eff,MF}} = N\beta \left(3r |T|^2 - 15u |T|^4 \right).$$

Believing our result that $u > 0$, the mean-field approximation would yield an unstable action. In fact, we believe this to be wrong and suspect a sign error in the derivation of the fourth order term, or a sixth order term stabilizing the ground state. Since the

functional renormalization group analysis below will not depend on the sign of u , we do not go into further discussion of the sign of u .

For the interaction of different bosonic species different processes are possible. We define the new couplings

$$u^{(n)} := -4u, \quad u^{(a)} := 2u, \quad v := -u$$

to distinguish the interactions. Thus, we can write the effective action as

$$\begin{aligned} \mathcal{S}_{\text{eff}}[T^\gamma; \lambda, A] &= \frac{1}{N\beta} \sum_{q;\gamma} \bar{T}^\gamma(q) (r + Zi q_0 + cq_\gamma^2) T^\gamma(q) \\ &+ \frac{u^{(n)}}{N^3\beta^3} \sum_{\substack{k,p,q \\ \gamma,\gamma'}} \bar{T}^\gamma(k-p) \bar{T}^{\gamma'}(p) T^\gamma(q) T^{\gamma'}(k-q) \\ &+ \frac{u^{(a)}}{N^3\beta^3} \sum_{\substack{k,p,q \\ \gamma,\gamma'}} \bar{T}^\gamma(k-p) \bar{T}^{\gamma'}(p) T^{\gamma'}(q) T^\gamma(k-q) \\ &+ \frac{v}{N^3\beta^3} \sum_{\substack{k,p,q \\ \gamma}} \bar{T}^\gamma(k-p) \bar{T}^\gamma(p) T^\gamma(q) T^\gamma(k-q). \end{aligned} \quad (3.16)$$

The bosonic fields can interact in three different ways:

- $\underline{T^\gamma + T^{\gamma'} \rightarrow T^\gamma + T^{\gamma'}}$: In this process, the number of bosons of species γ and γ' is preserved separately, therefore we call this process a *normal interaction* characterized by $u^{(n)}$.
- $\underline{2T^\gamma \rightarrow 2T^{\gamma'}}$: In this process two bosons of species γ are transmuted into two bosons of species γ' . Therefore, the particle number for both species is *not* preserved and we call it an *anomalous interaction* characterized by $u^{(a)}$.
- $\underline{2T^\gamma \rightarrow 2T^\gamma}$: In this case, two bosons of species γ interact without transmutation to another species. Such an interaction is parametrized by $u^{(n)} + u^{(a)} + v$.

Therefore, we see that in the case $u^{(a)} = 0$ the number of bosons is preserved for all species independently, whereas for $u^{(a)} \neq 0$ this is only true for the total number of bosons.

In the case $u^{(a)} = v = 0$ the corresponding theory with an isotropic propagator was studied among others by Uzunov using perturbative renormalization group methods [46]. Wetterich [47] used the functional renormalization group to study similar systems for a broad range of parameters. They both found that the propagator does not get renormalized at any loop order. Neglecting the gradient terms, or equivalently using a homogeneous mean-field ansatz, for $u^{(a)} = v = 0$ the action is not only invariant under U(3) rotations of the fields T^γ , but also under an O(6) symmetry, as the action only contains the absolute values of the fields T^γ . For the case $v \neq 0$ the model is similar to models describing cubic symmetry breaking which were for example discussed by Aharony [48].

Note that the analogies of our theory to the aforementioned models rely on the absence of the gradient terms. The non-relativistic, anisotropic propagator as well as the anomalous interaction are expected to qualitatively change the picture beyond mean-field approximation. Therefore, we will briefly analyze the mean-field behavior of the effective action in the next chapter before we perform a renormalization group analysis using the functional renormalization group.

4

Mean-Field Analysis

A first step towards a better understanding of the phase transition indicated by the instability discussed above is to study the mean-field behavior of the critical theory. To this end, we approximate the triplet fields T^γ by a spatially and temporally homogeneous mean-field defined by

$$T^\gamma(k) = N\beta T^\gamma \delta(k). \quad (4.1)$$

The PSG analysis by Kos and Punk [2] suggests a real mean-field, such that the effective action Eq. (3.16) simplifies to

$$\mathcal{S}_{\text{MF}}[T^\gamma] = N\beta \left(r \sum_{\gamma} (T^\gamma)^2 + \sum_{\gamma, \gamma'} (u^{(n)} + u^{(a)} + \delta_{\gamma, \gamma'} v) (T^\gamma)^2 (T^{\gamma'})^2 \right).$$

Note that for real mean-fields the action does not distinguish normal and anomalous interactions of bosons. Therefore, we define the effective coupling

$$u^{\text{eff}} := u^{(n)} + u^{(a)}.$$

Furthermore, the mean-field effective action is that of the usual $O(3)$ symmetric model with a cubic symmetry breaking term, which was studied earlier [40, 48, 49].

The mean-field equations are given by

$$0 \stackrel{!}{=} \frac{\partial \mathcal{S}_{\text{MF}}}{\partial T^\gamma} = 2N\beta T^\gamma \left(r + 2 \sum_{\gamma'} (u^{\text{eff}} + v \delta_{\gamma, \gamma'}) (T^{\gamma'})^2 \right).$$

The mean-fields T^γ could in principle take different values in the three directions. Thus, we get the following solutions to the mean-field equations:

$$T^1 = T^2 = T^3 = 0, \quad (4.2)$$

$$T^1 = \pm \sqrt{-\frac{r}{2(u^{\text{eff}} + v)}}, \quad T^2 = T^3 = 0, \quad (4.3)$$

$$T^1 = T^2 = \pm \sqrt{-\frac{r}{2(2u^{\text{eff}} + v)}}, \quad T^3 = 0, \quad (4.4)$$

$$T^1 = T^2 = T^3 = \pm \sqrt{-\frac{r}{2(3u^{\text{eff}} + v)}}. \quad (4.5)$$

The choice of the non-vanishing component is somewhat arbitrary. By symmetry of the mean-field action under permutations of the field indices we can argue that the four solutions listed above in fact describe all possible phases of the system. The same is true for a change $T^\gamma \rightarrow -T^\gamma$.

It is clear that the first solution exists for all parameters r, u, v , however the other three solutions exist only for certain parameter regimes. The corresponding constraints are implied by the assumption of a real mean-field and are given by

$$\frac{r}{u^{\text{eff}} + v} < 0, \quad (4.6)$$

$$\frac{r}{2u^{\text{eff}} + v} < 0, \quad (4.7)$$

$$\frac{r}{3u^{\text{eff}} + v} < 0. \quad (4.8)$$

For a solution to the mean-field equations to describe a stable phase it has to be a minimum of the mean-field free energy or, equivalently, the effective action. This condition is equivalent to the (dimensionless) Hessian matrix,

$$h_{\alpha\beta} := \frac{1}{N\beta} \left(\frac{\partial^2 \tilde{\mathcal{S}}_{\text{MF}}}{\partial T^\alpha \partial T^\beta} \right),$$

being positive definite or, equivalently, having only positive eigenvalues. Here, the derivatives are evaluated at the respective solution of the mean-field equations. The matrix elements of the Hessian matrix are given by

$$h_{\alpha\beta} = 2\delta_{\alpha\beta} \left(r + 2u^{\text{eff}} \sum_{\gamma} (T^\gamma)^2 + 6v (T^\alpha)^2 \right) + 8u^{\text{eff}} T^\alpha T^\beta.$$

We will now discuss the stability of the possible solutions, Eqs. (4.2)-(4.5). A summary of this discussion can be found in Tab. 4.1.

For the trivial solution Eq. (4.2), $T^\gamma = 0$, we get

$$h_{\alpha\beta}^{(1)} = 2r\delta_{\alpha\beta},$$

which has only eigenvalue $2r$. Thus, we conclude that the trivial solution $T^\gamma = 0$ is stable for $r \geq 0$ and arbitrary values of u^{eff} and v .

For the solution Eq. (4.3) with one non-vanishing component, $T^1 = \sqrt{-\frac{r}{2(u^{\text{eff}}+v)}}$, we get

$$h_{\alpha\beta}^{(2)} = 2r\delta_{\alpha\beta} \left(\frac{v}{u^{\text{eff}} + v} - \delta_{\alpha,1} \left(2 + \frac{v}{u^{\text{eff}} + v} \right) \right),$$

which has eigenvalues

$$\frac{2rv}{u^{\text{eff}} + v}, \quad -4r.$$

Therefore, we conclude that this solution is stable for

$$r < 0, \quad v < 0, \quad u^{\text{eff}} + v > 0.$$

For the solution Eq. (4.4) with two non-vanishing components the Hessian matrix has eigenvalues

$$-\frac{4rv}{2u^{\text{eff}} + v}, \quad \frac{2rv}{2u^{\text{eff}} + v}, \quad -4r,$$

which clearly cannot all be positive at the same time. Thus, we conclude that this solution is nowhere stable.

Finally, for solution Eq. (4.5) the Hessian matrix has eigenvalues

$$-\frac{4rv}{3u^{\text{eff}} + v}, \quad -4r,$$

so that we conclude that this solution is stable for

$$r < 0, \quad v > 0, \quad 3u^{\text{eff}} + v > 0.$$

MF solution	Stability conditions
$T^1 = T^2 = T^3 = 0$	$r \geq 0$
$T^1 = \sqrt{-\frac{r}{2(u^{\text{eff}}+v)}}, T^2 = T^3 = 0$	$r < 0, v < 0, u^{\text{eff}} + v > 0$
$T^1 = T^2 = \sqrt{-\frac{r}{2(2u^{\text{eff}}+v)}}, T^3 = 0$	nowhere stable
$T^1 = T^2 = T^3 = \sqrt{-\frac{r}{2(3u^{\text{eff}}+v)}}$	$r < 0, v > 0, 3u^{\text{eff}} + v > 0$

Tab. 4.1. Solutions to the mean-field equations and corresponding stability conditions for the parameters for real mean-fields T^γ .

Next, we use the relations $u^{(n)} = -4u, u^{(a)} = 2u, v = -u$ from our microscopic derivation and get

$$u^{\text{eff}} = -2u.$$

Thus, we can rewrite the stability condition for the first non-trivial solution, Eq. (4.3), as

$$r < 0, \quad u > 0, \quad u < 0,$$

which is clearly inconsistent. Therefore, we conclude that this solution is not a valid mean-field solution. For the third non-trivial solution, Eq. (4.5), we get the stability condition

$$r < 0, \quad u < 0.$$

Using the parameters r and u , we obtain the following mean-field structure:

- $r \geq 0, u \in \mathbb{R}$: The mean-field solution is given by the trivial one,

$$T^1 = T^2 = T^3 = 0.$$

- $r < 0, u < 0$: The mean-field solution is given by

$$T^1 = T^2 = T^3 = \sqrt{\frac{r}{14u}}.$$

- $r < 0, u > 0$: In this case, the only solution to the mean-field equations is

$$T^1 = T^2 = T^3 = 0.$$

However, this solution is unstable, as it is a maximum of the mean-field free energy as can be seen from the Hessian having only the eigenvalue $2r < 0$. Therefore, no stable mean-field solution exists.

The results of our mean-field analysis resemble those of Kos and Punk [2]. In the regime $u < 0$ we interpret the qualitative change of the mean-field solution to describe a second order phase transition from a QSL phase with $T^\gamma = 0$ to a QSL phase with $T^\gamma \neq 0$. The phase transition is driven by the parameter r or, in terms of microscopic quantities, by the ratio of the Heisenberg coupling, J_H , and the Kitaev coupling, J_K . We can see this as a sanity check that the effective action Eq. (3.16) captures the essential physics correctly. Thus, we expect the value of u to be actually negative as already discussed at the end of the derivation of the effective action.

In order to get a better understanding of the phase transition and, in particular, the dependence on the potentially independent parameters $u^{(n)}, u^{(a)}$, and v , we perform a renormalization group analysis in the next chapter.

5

Renormalization Group Analysis

We want to use a renormalization group (RG) approach to get a better understanding of the quantum phase transition occurring at $J_{2,\text{crit}}$. In order to get a fairly simple RG procedure, we assume the system to be deep in the spin liquid regime and use the effective action Eq. (3.16) derived above. Since we do not expect any symmetry to protect the specific relation between the coupling constants for the quartic interactions, we treat them as independent parameters, so that we want to derive RG flow equations for

$$Z, c, r, u^{(n)}, u^{(a)}, \text{ and } v,$$

and determine the resulting fixed point structure.

To this end, we first consider the tree level scaling behavior of the parameters using power counting arguments and then use the functional renormalization group (fRG) to obtain the one-loop flow equations. Note that in this approximation, we expect the wave function renormalization factor Z and the velocity c to not get renormalized. Thus, it seems appropriate to rescale the fields in such a way that the velocity can be set $c = 1$. To get flow equations beyond tree level for c and Z one would need higher loop orders.

Using the one-loop fRG flow equations, we perform an ϵ -expansion in $d = 2 - \epsilon$ dimensions and determine the fixed points of the flow numerically. Linearizing the flow equations around the fixed points and determining the RG eigenvalues, we study the stability properties of the fixed points.

5.1. Tree Level Scaling

We start our RG analysis by performing a power counting analysis. Since we also want to determine the critical dimension of the theory, we generalize the dimension to arbitrary d . Furthermore, we take the thermodynamic limit to replace momentum sums by integrals and take the zero temperature limit,

$$\frac{1}{N} \sum_{\mathbf{k}} \rightarrow \int \frac{d^d k}{(2\pi)^d}, \quad \frac{1}{\beta} \sum_{k_0} \rightarrow \int_{-\infty}^{\infty} \frac{dk_0}{(2\pi)}.$$

Thus, we arrive at the new form of the action,

$$\begin{aligned}
\mathcal{S}_{\text{eff}}[T^\gamma; \lambda, A] &= \sum_\gamma \int_q \bar{T}^\gamma(q) (r + Zi q_0 + q_\gamma^2) T^\gamma(q) \\
&+ \sum_{\gamma, \gamma'} \int_{k, p, q} \left(u^{(n)} \bar{T}^\gamma(k-p) \bar{T}^{\gamma'}(p) T^\gamma(q) T^{\gamma'}(k-q) \right. \\
&\quad \left. + u^{(a)} \bar{T}^\gamma(k-p) \bar{T}^\gamma(p) T^{\gamma'}(q) T^{\gamma'}(k-q) \right) \\
&+ v \sum_\gamma \int_{k, p, q} \bar{T}^\gamma(k-p) \bar{T}^\gamma(p) T^\gamma(q) T^\gamma(k-q), \tag{5.1}
\end{aligned}$$

where we used the notation

$$\int_k := \int_{-\infty}^{\infty} \frac{dk_0}{(2\pi)} \int \frac{d^d k}{(2\pi)^d}.$$

For our power counting analysis, we rescale the momenta as $\mathbf{k}' = b\mathbf{k}$ and the frequencies as $k'_0 = b^z k_0$, where $z = 2$ is the dynamical exponent. At the same time, the fields are rescaled as

$$T^{\gamma'}(k') = b^{-\Delta_T} T^\gamma(k).$$

Requiring the kinetic term to be scale invariant, we get

$$\Delta_T = \frac{d+z+2}{2} = \frac{d+4}{2},$$

i.e.

$$T^{\gamma'}(k') = b^{-(d+z+2)/2} T^\gamma(k) = b^{-(d+4)/2} T^\gamma(k),$$

so that we get for the scaling behavior of the couplings at tree level

$$\begin{aligned}
r' &= b^2 r, \\
u^{(n)'} &= b^{4-d-z} u^{(n)} = b^{2-d} u^{(n)}, \\
u^{(a)'} &= b^{4-d-z} u^{(a)} = b^{2-d} u^{(a)}, \\
v' &= b^{4-d-z} v = b^{2-d} v.
\end{aligned}$$

We see that the mass parameter r is always relevant as expected. The quartic couplings are relevant in $d < 2$, a fact which we will investigate further in the one-loop approximation using the functional renormalization group (fRG). From our scaling analysis, we conclude that the critical dimension is $d_c = 2$ which is the dimension of the physical system. Typically, the marginal parameters give rise to logarithmic corrections to the scaling behavior at the (upper) critical dimension [40]. Nevertheless, we expect the RG flow slightly below the critical dimension to still capture the essential physics [50]. Therefore, we will perform an ϵ -expansion in $d = 2 - \epsilon$ below.

5.2. One-Loop Approximation - Functional Renormalization Group

The one-loop RG flow can be obtained using fRG and the truncation

$$\Gamma_\Lambda[T^\gamma] = \mathcal{S}_{\Lambda, \text{eff}}[T^\gamma; \lambda, A],$$

where we promoted the parameters to cutoff-dependent parameters $r_\Lambda, Z_\Lambda, \dots$. Next, we will derive flow equations for these parameters by taking functional derivatives of the Wetterich equation (2.6) with respect to the fields T^γ . For simplicity, we return to the case $d = 2$ in our derivation and generalize only the final flow equations to arbitrary dimensions.

We define the inverse propagator,

$$G_{\Lambda, q, \gamma}^{-1} := - (r_\Lambda + Z_\Lambda i q_0 + q_\gamma^2)$$

and the regularized inverse propagator,

$$G_{R, q, \gamma}^{-1} := G_{\Lambda, q, \gamma}^{-1} - R_{\Lambda, q, \gamma},$$

where $R_{\Lambda, q, \gamma}$ is some regulator function specified below. Defining the matrices

$$\left(\Gamma_\Lambda^{(2)} \right)_{p, q; \alpha, \beta} = \begin{pmatrix} \frac{\delta^2 \Gamma_\Lambda}{\delta T^\alpha(p) \delta T^\beta(q)} & \frac{\delta^2 \Gamma_\Lambda}{\delta T^\alpha(p) \delta T^\beta(q)} \\ \frac{\delta^2 \Gamma_\Lambda}{\delta T^\alpha(p) \delta T^\beta(q)} & \frac{\delta^2 \Gamma_\Lambda}{\delta T^\alpha(p) \delta T^\beta(q)} \end{pmatrix},$$

$$(R_\Lambda)_{p, q; \alpha, \beta} = \delta_{\alpha\beta} \delta_{p, q} R_{\Lambda, p, \alpha} \begin{pmatrix} 0 & 1 \\ 1 & 0 \end{pmatrix},$$

and $M := \Gamma_\Lambda^{(2)} + R_\Lambda$, we can write the Wetterich equation (2.6) as

$$\partial_\Lambda \Gamma_\Lambda = \frac{1}{2} \text{Tr} [M^{-1} \partial_\Lambda R_\Lambda].$$

Some expressions needed for our calculations related to these objects are listed in appendix D.1.

5.2.1. Flow Equations for the Parameters

We derive the fRG flow equations as functional derivatives of the Wetterich equation using the identities

$$\begin{aligned} G_{\Lambda, k, \gamma}^{-1} &= - \int_{k'} \frac{\delta^2 \Gamma_\Lambda}{\delta \bar{T}^\gamma(k) \delta T^\gamma(k')} \Big|_{T=0}, \\ r_\Lambda &= - \lim_{k \rightarrow 0} G_{\Lambda, k, \gamma}^{-1}, \\ Z_\Lambda &= i \lim_{k \rightarrow 0} \partial_{k_0} G_{\Lambda, k, \gamma}^{-1}, \\ u_\Lambda^{(n)} &= \frac{1}{12} \sum_{\gamma \neq \gamma'} \int_{p_4} \lim_{p_1, \dots, p_3 \rightarrow 0} \frac{\delta^4 \Gamma_\Lambda}{\delta \bar{T}^\gamma(p_1) \delta \bar{T}^{\gamma'}(p_2) \delta T^\gamma(p_3) \delta T^{\gamma'}(p_4)} \Big|_{T=0}, \\ u_\Lambda^{(a)} &= \frac{1}{24} \sum_{\gamma \neq \gamma'} \int_{p_4} \lim_{p_1, \dots, p_3 \rightarrow 0} \frac{\delta^4 \Gamma_\Lambda}{\delta \bar{T}^\gamma(p_1) \delta \bar{T}^\gamma(p_2) \delta T^{\gamma'}(p_3) \delta T^{\gamma'}(p_4)} \Big|_{T=0}, \\ u_\Lambda^{(n)} + u_\Lambda^{(a)} + v_\Lambda &= \frac{1}{12} \sum_\gamma \int_{p_4} \lim_{p_1, \dots, p_3 \rightarrow 0} \frac{\delta^4 \Gamma_\Lambda}{\delta \bar{T}^\gamma(p_1) \delta \bar{T}^\gamma(p_2) \delta T^\gamma(p_3) \delta T^\gamma(p_4)} \Big|_{T=0}. \end{aligned}$$

Flow Equation for $G_{\Lambda,k,\gamma}^{-1}$

We start by determining the flow equation of the inverse propagator:

$$\begin{aligned}
\partial_\Lambda G_{\Lambda,k,\gamma}^{-1} &= - \int_{k'} \frac{\delta^2}{\delta \bar{T}^\gamma(k) \delta T^\gamma(k')} \Big|_{T=0} \partial_\Lambda \Gamma_\Lambda \\
&= \frac{1}{2} \sum_{\alpha,\beta} \int_{k',p,q} \text{tr}_2 \left[\left(\frac{\delta^2 M}{\delta \bar{T}^\gamma(k) \delta T^\gamma(k')} \right)_{p,q;\alpha,\beta} (M^{-1}|_{T=0} \partial_\Lambda R_\Lambda M^{-1}|_{T=0})_{q,p;\beta,\alpha} \right] \\
&= \frac{1}{2} \sum_\alpha \int_{k',p} \frac{\partial_\Lambda R_{\Lambda,p,\alpha}}{G_{R,p,\alpha}^2} \text{tr}_2 \left[\left(\frac{\delta^2 M}{\delta \bar{T}^\gamma(k) \delta T^\gamma(k')} \right)_{p,p;\alpha,\alpha} \begin{pmatrix} 0 & 1 \\ 1 & 0 \end{pmatrix} \right] \\
&= 2 \int_{k'} (2\pi)^{(d+1)} \delta(k - k') \sum_\alpha \left(u_\Lambda^{(n)} (\delta_{\alpha\gamma} + 1) + 2 \left(u_\Lambda^{(a)} + v_\Lambda \right) \delta_{\alpha\gamma} \right) \int_p \frac{\partial_\Lambda R_{\Lambda,p,\alpha}}{G_{R,p,\alpha}^{-2}} \\
&= 2 \sum_\alpha \left(u_\Lambda^{(n)} (\delta_{\alpha\gamma} + 1) + 2 \left(u_\Lambda^{(a)} + v_\Lambda \right) \delta_{\alpha\gamma} \right) \int_p \frac{\partial_\Lambda R_{\Lambda,p,\alpha}}{G_{R,p,\alpha}^{-2}},
\end{aligned}$$

where we used the Eqs. (D.1) and (D.4) to evaluate the trace.

Next, we use a regulator implementing a sharp cutoff in momentum space ,

$$R_{\Lambda,p,\alpha} = R_{\Lambda,p} = \Lambda^2 \Theta(\Lambda^2 - \mathbf{p}^2) \quad (5.2)$$

and its derivative

$$\partial_\Lambda R_{\Lambda,p,\alpha} = 2\Lambda (\Theta(\Lambda^2 - \mathbf{p}^2) + \Lambda^2 \delta(\Lambda^2 - \mathbf{p}^2)). \quad (5.3)$$

Thus, the frequency integral

$$\int_{-\infty}^{\infty} \frac{dp_0}{2\pi} \frac{2\Lambda (\Theta(\Lambda^2 - \mathbf{p}^2) + \Lambda^2 \delta(\Lambda^2 - \mathbf{p}^2))}{(r_\Lambda + Z_\Lambda i p_0 + p_\alpha^2 + \Lambda^2 \Theta(\Lambda^2 - \mathbf{p}^2))^2}$$

can be evaluated using the residue theorem. To this end, we note that the only pole of the integrand lies in the upper half plane, as long as $r_\Lambda > -\Lambda^2$. As we are later on interested in the behavior for small $|r_\Lambda/\Lambda^2|$, this condition will be satisfied. Closing the contour in the lower half plane, the integral vanishes.

Therefore, we conclude that

$$\partial_\Lambda G_{\Lambda,k,\gamma}^{-1} = 0, \quad (5.4)$$

i.e. the inverse propagator does not get renormalized. This resembles the fact that for non-relativistic, interacting bosons at $T = 0$ the self-energy is known to not get renormalized [46, 47]. Since this result holds at all orders in perturbation theory, we expect Eq. (5.4) to stay true even beyond our one-loop approximation.

Flow Equations for r_Λ and Z_Λ

Using the fRG flow for the inverse propagator, it is immediately clear that the mass parameter r_Λ and the wave function renormalization factor Z_Λ do not get renormalized as well,

$$\partial_\Lambda r_\Lambda = 0, \quad (5.5)$$

$$\partial_\Lambda Z_\Lambda = 0. \quad (5.6)$$

Flow Equation for $u_\Lambda^{(n)}$

Next, we want to derive the flow equations for the quartic couplings, starting with $u_\Lambda^{(n)}$:

$$\begin{aligned}
\partial_\Lambda u_\Lambda^{(n)} &= \frac{1}{12} \sum_{\gamma \neq \gamma'} \int_{p_4} \lim_{p_1, \dots, p_3 \rightarrow 0} \frac{\delta^4}{\delta \bar{T}^\gamma(p_1) \delta \bar{T}^{\gamma'}(p_2) \delta T^\gamma(p_3) \delta T^{\gamma'}(p_4)} \Big|_{T=0} \partial_\Lambda \Gamma_\Lambda \\
&= \frac{1}{24} \sum_{\gamma \neq \gamma'} \int_{p_4} \lim_{p_1, \dots, p_3 \rightarrow 0} \text{Tr} \left[\left(\frac{\delta^2 M}{\delta \bar{T}^\gamma(p_1) \delta \bar{T}^{\gamma'}(p_2)} M^{-1} \Big|_{T=0} \frac{\delta^2 M}{\delta T^\gamma(p_3) \delta T^{\gamma'}(p_4)} \right. \right. \\
&\quad \left. \left. + \frac{\delta^2 M}{\delta T^\gamma(p_3) \delta T^{\gamma'}(p_4)} M^{-1} \Big|_{T=0} \frac{\delta^2 M}{\delta \bar{T}^\gamma(p_1) \delta \bar{T}^{\gamma'}(p_2)} \right. \right. \\
&\quad \left. \left. + 2 \frac{\delta^2 M}{\delta \bar{T}^\gamma(p_1) \delta T^{\gamma'}(p_4)} M^{-1} \Big|_{T=0} \frac{\delta^2 M}{\delta \bar{T}^{\gamma'}(p_2) \delta T^\gamma(p_3)} \right) \right. \\
&\quad \left. \left. + 2 \frac{\delta^2 M}{\delta \bar{T}^\gamma(p_1) \delta T^\gamma(p_3)} M^{-1} \Big|_{T=0} \frac{\delta^2 M}{\delta \bar{T}^{\gamma'}(p_2) \delta T^{\gamma'}(p_4)} \right) \right. \\
&\quad \left. (M^{-1} \Big|_{T=0} \partial_\Lambda R_\Lambda M^{-1} \Big|_{T=0}) \right].
\end{aligned}$$

We evaluate the summands separately, using the Eqs. (D.1)-(D.4). For the first term we get

$$\begin{aligned}
&\frac{1}{24} \sum_{\gamma \neq \gamma'} \int_{p_4} \lim_{p_1, \dots, p_3 \rightarrow 0} \text{Tr} \left[\frac{\delta^2 M}{\delta \bar{T}^\gamma(p_1) \delta \bar{T}^{\gamma'}(p_2)} M^{-1} \Big|_{T=0} \frac{\delta^2 M}{\delta T^\gamma(p_3) \delta T^{\gamma'}(p_4)} (M^{-1} \Big|_{T=0} \partial_\Lambda R_\Lambda M^{-1} \Big|_{T=0}) \right] \\
&= -\frac{4u_\Lambda^{(n)2}}{24} \sum_{\substack{\gamma \neq \gamma' \\ \alpha\beta}} \int_{k,l,p_4} \lim_{p_1, \dots, p_3 \rightarrow 0} \frac{\partial_\Lambda R_{\Lambda,k,\alpha}}{G_{R,k,\alpha}^{\gamma-2} G_{R,l,\beta}^{\gamma-1}} (\delta_{\alpha\gamma} \delta_{\beta\gamma'} + \delta_{\beta\gamma} \delta_{\alpha\gamma'})^2 \\
&\quad \times (2\pi)^{(d+1)} \delta(p_1 + p_2 - k - l) (2\pi)^{(d+1)} \delta(p_3 + p_4 - l - k) \\
&= -\frac{u_\Lambda^{(n)2}}{3} \sum_{\substack{\gamma \neq \gamma' \\ \alpha\beta}} \delta_{\alpha\gamma} \delta_{\beta\gamma'} \int_k \frac{\partial_\Lambda R_{\Lambda,k,\alpha}}{G_{R,k,\alpha}^{\gamma-2} G_{R,-k,\beta}^{\gamma-1}} \\
&= -\frac{u_\Lambda^{(n)2}}{3} \sum_{\gamma \neq \gamma'} \underbrace{\int_k \frac{\partial_\Lambda R_{\Lambda,k,\gamma}}{G_{R,k,\gamma}^{\gamma-2} G_{R,-k,\gamma'}^{\gamma-1}}}_{:=I_{\gamma,\gamma'}^{(1)}},
\end{aligned}$$

and the second term gives the same contribution. By a similar calculation, we get for the third term

$$\begin{aligned}
&\frac{2}{24} \sum_{\gamma \neq \gamma'} \int_{p_4} \lim_{p_1, \dots, p_3 \rightarrow 0} \text{Tr} \left[\frac{\delta^2 M}{\delta \bar{T}^\gamma(p_1) \delta T^{\gamma'}(p_4)} M^{-1} \Big|_{T=0} \frac{\delta^2 M}{\delta \bar{T}^{\gamma'}(p_2) \delta T^\gamma(p_3)} (M^{-1} \Big|_{T=0} \partial_\Lambda R_\Lambda M^{-1} \Big|_{T=0}) \right] \\
&= -\frac{2(u_\Lambda^{(n)2} + 4u_\Lambda^{(a)2})}{3} \sum_{\gamma \neq \gamma'} \underbrace{\int_k \frac{\partial_\Lambda R_{\Lambda,k,\gamma}}{G_{R,k,\gamma}^{\gamma-2} G_{R,k,\gamma'}^{\gamma-1}}}_{:=I_{\gamma,\gamma'}^{(2)}},
\end{aligned}$$

and for the fourth term

$$\begin{aligned} & \frac{2}{24} \sum_{\gamma \neq \gamma'} \int_{p_4} \lim_{p_1, \dots, p_3 \rightarrow 0} \text{Tr} \left[\frac{\delta^2 M}{\delta \bar{T}^\gamma(p_1) \delta T^\gamma(p_3)} M^{-1} \Big|_{T=0} \frac{\delta^2 M}{\delta \bar{T}^{\gamma'}(p_2) \delta T^{\gamma'}(p_4)} (M^{-1} \Big|_{T=0} \partial_\Lambda R_\Lambda M^{-1} \Big|_{T=0}) \right] \\ &= -\frac{2}{3} \sum_{\substack{\gamma \neq \gamma' \\ \alpha}} u_\Lambda^{(n)} \left(u_\Lambda^{(n)} (1 + 2\delta_{\alpha\gamma}) + 4(u_\Lambda^{(a)} + v_\Lambda) \delta_{\alpha\gamma} \right) I_{\alpha, \alpha}^{(2)}. \end{aligned}$$

Summing up all contributions, we obtain

$$\begin{aligned} \partial_\Lambda u_\Lambda^{(n)} &= -\frac{u_\Lambda^{(n)2}}{3} \sum_{\gamma \neq \gamma'} I_{\gamma, \gamma'}^{(1)} - \frac{2(u_\Lambda^{(n)2} + 4u_\Lambda^{(a)2})}{3} \sum_{\gamma \neq \gamma'} I_{\gamma, \gamma'}^{(2)} \\ &\quad - \frac{2u_\Lambda^{(n)}}{3} \sum_{\substack{\gamma \neq \gamma' \\ \alpha}} \left(u_\Lambda^{(n)} (1 + 2\delta_{\alpha\gamma}) + 4(u_\Lambda^{(a)} + v_\Lambda) \delta_{\alpha\gamma} \right) I_{\alpha, \alpha}^{(2)}. \end{aligned}$$

Again, using the regulator specified in Eq. (5.2), we see that the integral $I_{\gamma, \gamma'}^{(2)}$ vanishes when performing the frequency integral by the same argument as above. Therefore, we are left with the first summand involving the integral $I_{\gamma, \gamma'}^{(1)}$. Referring to the appendix D.2.1 for the evaluation of the integral, we know that the value of $I_{\gamma, \gamma'}^{(1)}$ does not depend on the indices $\gamma \neq \gamma'$ but only on the fact that they are different. Therefore, we define $I_\Lambda^{(\neq)}(r) := I_{\gamma, \gamma'}^{(1)}$ and rewrite the flow equation for $u_\Lambda^{(n)}$ as

$$\partial_\Lambda u_\Lambda^{(n)} = -2I_\Lambda^{(\neq)}(r) u_\Lambda^{(n)2}. \quad (5.7)$$

Note that $I_\Lambda^{(\neq)}(r)$ depends on the mass parameter r and the cutoff Λ . A diagrammatic representation of the flow equations for all parameters is shown in Fig. 5.1, where only the diagrams with a non-zero contribution are included.

Flow Equation for $u_\Lambda^{(a)}$

A similar calculation gives for $u_\Lambda^{(a)}$

$$\begin{aligned} \partial_\Lambda u_\Lambda^{(a)} &= \frac{1}{24} \sum_{\gamma \neq \gamma'} \int_{p_4} \lim_{p_1, \dots, p_3 \rightarrow 0} \frac{\delta^4}{\delta \bar{T}^\gamma(p_1) \delta \bar{T}^\gamma(p_2) \delta T^{\gamma'}(p_3) \delta T^{\gamma'}(p_4)} \Big|_{T=0} \partial_\Lambda \Gamma_\Lambda \\ &= \frac{1}{48} \sum_{\gamma \neq \gamma'} \int_{p_4} \lim_{p_1, \dots, p_3 \rightarrow 0} \text{Tr} \left[\left(\frac{\delta^2 M}{\delta \bar{T}^\gamma(p_1) \delta \bar{T}^\gamma(p_2)} M^{-1} \Big|_{T=0} \frac{\delta^2 M}{\delta T^{\gamma'}(p_3) \delta T^{\gamma'}(p_4)} \right. \right. \\ &\quad \left. \left. + \frac{\delta^2 M}{\delta T^{\gamma'}(p_3) \delta T^{\gamma'}(p_4)} M^{-1} \Big|_{T=0} \frac{\delta^2 M}{\delta \bar{T}^\gamma(p_1) \delta \bar{T}^\gamma(p_2)} \right. \right. \\ &\quad \left. \left. + 4 \frac{\delta^2 M}{\delta \bar{T}^\gamma(p_1) \delta T^{\gamma'}(p_4)} M^{-1} \Big|_{T=0} \frac{\delta^2 M}{\delta \bar{T}^\gamma(p_2) \delta T^{\gamma'}(p_3)} \right) \right. \\ &\quad \left. (M^{-1} \Big|_{T=0} \partial_\Lambda R_\Lambda M^{-1} \Big|_{T=0}) \right]. \end{aligned}$$

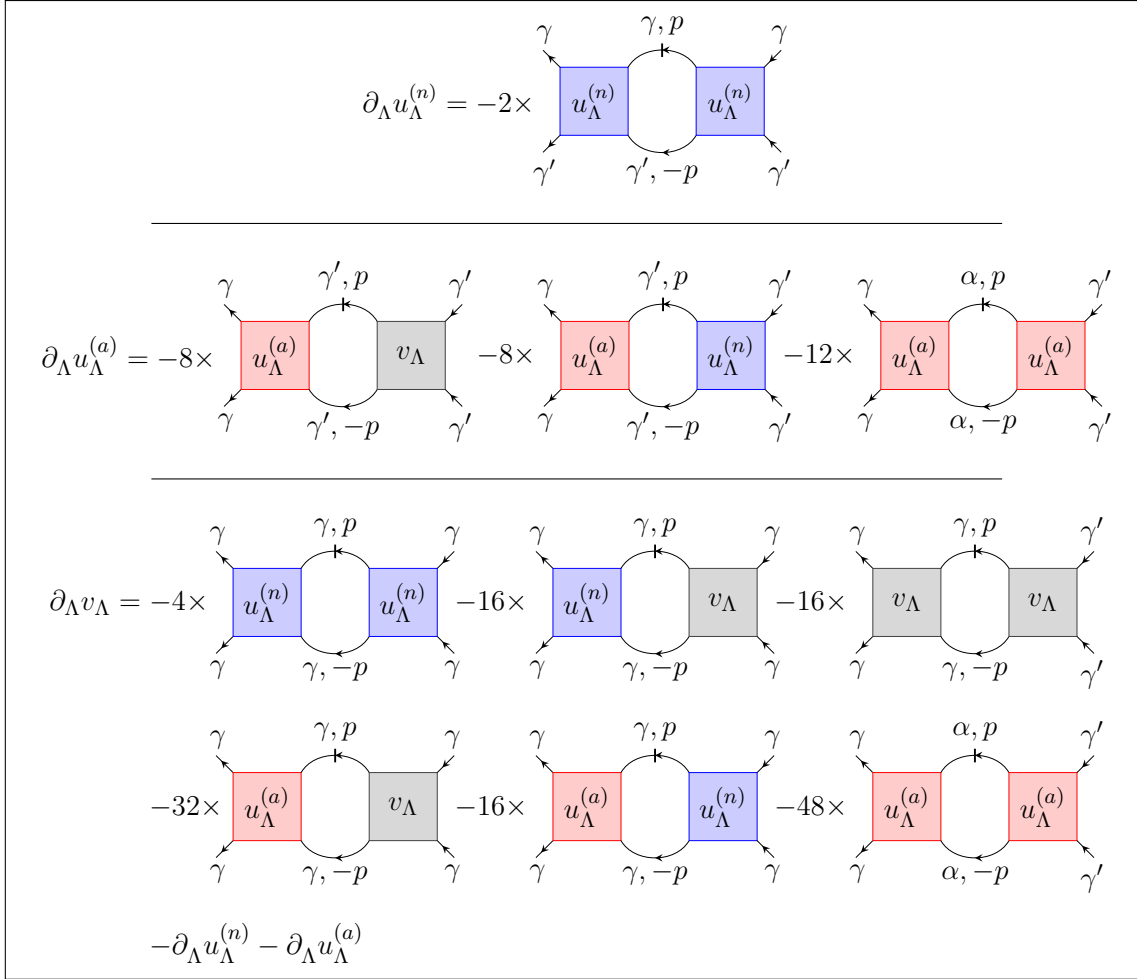


Fig. 5.1. Diagrammatic representation of the one-loop fRG flow equations (5.7), (5.8) and (5.9), where solid lines indicate triplet propagators and the vertical line represents a regulator insertion. In our approximation all external frequencies and momenta vanish. The combinatorial prefactors can be obtained by carefully summing over admissible index combinations and topologically distinct diagrams. Only diagrams giving a non-zero contribution were included.

For the first summand we get

$$\begin{aligned} & \frac{1}{48} \sum_{\gamma \neq \gamma'} \int_{p_4} \lim_{p_1, \dots, p_3 \rightarrow 0} \text{Tr} \left[\frac{\delta^2 M}{\delta \bar{T}^\gamma(p_1) \delta \bar{T}^\gamma(p_2)} M^{-1} \Big|_{T=0} \frac{\delta^2 M}{\delta T^{\gamma'}(p_3) \delta T^{\gamma'}(p_4)} (M^{-1} \Big|_{T=0} \partial_\Lambda R_\Lambda M^{-1} \Big|_{T=0}) \right] \\ &= -\frac{1}{3} \sum_{\substack{\gamma \neq \gamma' \\ \alpha}} u_\Lambda^{(a)} \left(2 \left(u_\Lambda^{(n)} + v_\Lambda \right) \delta_{\alpha\gamma} + u_\Lambda^{(a)} \right) I_{\alpha,\alpha}^{(1)}, \end{aligned}$$

and the same expression is obtained for the second summand. For the third summand we get

$$\begin{aligned} & \frac{4}{48} \sum_{\gamma \neq \gamma'} \int_{p_4} \lim_{p_1, \dots, p_3 \rightarrow 0} \text{Tr} \left[\frac{\delta^2 M}{\delta \bar{T}^\gamma(p_1) \delta T^{\gamma'}(p_4)} M^{-1} \Big|_{T=0} \frac{\delta^2 M}{\delta \bar{T}^\gamma(p_2) \delta T^{\gamma'}(p_3)} (M^{-1} \Big|_{T=0} \partial_\Lambda R_\Lambda M^{-1} \Big|_{T=0}) \right] \\ &= -\frac{8}{3} u_\Lambda^{(n)} u_\Lambda^{(a)} \sum_{\gamma \neq \gamma'} I_{\gamma,\gamma'}^{(2)}. \end{aligned}$$

Combining these terms, we obtain

$$\partial_\Lambda u_\Lambda^{(a)} = -\frac{2}{3} \sum_{\substack{\gamma \neq \gamma' \\ \alpha}} u_\Lambda^{(a)} \left(2 \left(u_\Lambda^{(n)} + v_\Lambda \right) \delta_{\alpha\gamma} + u_\Lambda^{(a)} \right) I_{\alpha,\alpha}^{(1)} - \frac{8}{3} u_\Lambda^{(n)} u_\Lambda^{(a)} \sum_{\gamma \neq \gamma'} I_{\gamma,\gamma'}^{(2)}.$$

Using the regulator in Eq. (5.2), we know that the integral $I_{\gamma,\gamma'}^{(2)}$ vanishes as before and referring to appendix D.2.2 for the evaluation of $I_{\alpha,\alpha}^{(1)}$ we get that $I_\Lambda^{(=)}(r) := I_{\alpha,\alpha}^{(1)}$ is independent of α , so that we can write the flow equation for $u_\Lambda^{(a)}$ as

$$\partial_\Lambda u_\Lambda^{(a)} = -4I^{(=)}(r) u_\Lambda^{(a)} \left(2 \left(u_\Lambda^{(n)} + v_\Lambda \right) + 3u_\Lambda^{(a)} \right). \quad (5.8)$$

Again, $I_\Lambda^{(=)}(r)$ is a function of r and Λ .

Flow Equation for v_Λ

Finally, we have

$$\begin{aligned} & \partial_\Lambda \left(u_\Lambda^{(n)} + u_\Lambda^{(a)} + v_\Lambda \right) \\ &= \frac{1}{12} \sum_\gamma \int_{p_4} \lim_{p_1, \dots, p_3 \rightarrow 0} \frac{\delta^4}{\delta \bar{T}^\gamma(p_1) \delta \bar{T}^\gamma(p_2) \delta T^\gamma(p_3) \delta T^\gamma(p_4)} \Big|_{T=0} \partial_\Lambda \Gamma_\Lambda \\ &= \frac{1}{24} \sum_\gamma \int_{p_4} \lim_{p_1, \dots, p_3 \rightarrow 0} \text{Tr} \left[\left(\frac{\delta^2 M}{\delta T^\gamma(p_3) \delta T^\gamma(p_4)} M^{-1} \Big|_{T=0} \frac{\delta^2 M}{\delta \bar{T}^\gamma(p_1) \delta \bar{T}^\gamma(p_2)} \right. \right. \\ & \quad \left. \left. + \frac{\delta^2 M}{\delta \bar{T}^\gamma(p_1) \delta \bar{T}^\gamma(p_2)} M^{-1} \Big|_{T=0} \frac{\delta^2 M}{\delta T^\gamma(p_3) \delta T^\gamma(p_4)} \right. \right. \\ & \quad \left. \left. + 4 \frac{\delta^2 M}{\delta \bar{T}^\gamma(p_1) \delta T^\gamma(p_3)} M^{-1} \Big|_{T=0} \frac{\delta^2 M}{\delta \bar{T}^\gamma(p_2) \delta T^\gamma(p_4)} \right) \right. \\ & \quad \left. (M^{-1} \Big|_{T=0} \partial_\Lambda R_\Lambda M^{-1} \Big|_{T=0}) \right]. \end{aligned}$$

Again, we evaluate the summands separately. For the first term we get

$$\begin{aligned} & \frac{1}{24} \sum_\gamma \int_{p_4} \lim_{p_1, \dots, p_3 \rightarrow 0} \text{Tr} \left[\frac{\delta^2 M}{\delta T^\gamma(p_3) \delta T^\gamma(p_4)} M^{-1} \Big|_{T=0} \frac{\delta^2 M}{\delta \bar{T}^\gamma(p_1) \delta \bar{T}^\gamma(p_2)} M^{-1} \Big|_{T=0} \partial_\Lambda R_\Lambda M^{-1} \Big|_{T=0} \right] \\ &= -2 \left(\left(u_\Lambda^{(n)} + 2 \left(u_\Lambda^{(a)} + v_\Lambda \right) \right)^2 + 8u_\Lambda^{(a)2} \right) I_{\gamma,\gamma}^{(1)}, \end{aligned}$$

and the same result is obtained for the second term. As before, the third term vanishes when evaluating the frequency integral. Using $I^{(=)}(r)$, we can rewrite the flow equation for v_Λ as

$$\begin{aligned}\partial_\Lambda v_\Lambda &= -4I^{(=)}(r) \left(\left(u_\Lambda^{(n)} + 2 \left(u_\Lambda^{(a)} + v_\Lambda \right) \right)^2 + 8u_\Lambda^{(a)2} \right) - \partial_\Lambda u_\Lambda^{(n)} - \partial_\Lambda u_\Lambda^{(a)} \\ &= -4I^{(=)}(r) \left(9u_\Lambda^{(a)2} + 2u_\Lambda^{(a)} \left(u_\Lambda^{(n)} + 3v_\Lambda \right) + \left(u_\Lambda^{(n)} + 2v_\Lambda \right)^2 \right) + 2I^{(\neq)}(r) u_\Lambda^{(n)2}.\end{aligned}\tag{5.9}$$

5.2.2. Fixed Points of the fRG Flow in $d = 2 - \epsilon$ Dimensions

In order to examine the fixed point structure of the fRG flow in $d = 2 - \epsilon$ dimensions, $\epsilon > 0$, we define the dimensionless parameters

$$\tilde{r}_\Lambda = r_\Lambda \Lambda^{-2} Z_\Lambda^{-1/2}, \quad \tilde{u}_\Lambda^{(n)} = u_\Lambda^{(n)} \Lambda^{d-2} Z_\Lambda^{-1}, \quad \tilde{u}_\Lambda^{(a)} = u_\Lambda^{(a)} \Lambda^{d-2} Z_\Lambda^{-1}, \quad \tilde{v}_\Lambda = v_\Lambda \Lambda^{d-2} Z_\Lambda^{-1},$$

and replace the dimension-dependent factor from the integrals, $\Lambda^2/2 \rightarrow \Lambda^d/d$, so that the the flow equations for the new parameters read

$$\begin{aligned}\Lambda \partial_\Lambda \tilde{r}_\Lambda &= -2\tilde{r}_\Lambda, \\ \Lambda \partial_\Lambda \tilde{u}_\Lambda^{(n)} &= (d-2) \tilde{u}_\Lambda^{(n)} + \frac{2\Lambda^{2d-3}}{dZ_\Lambda} \partial_\Lambda u_\Lambda^{(n)}, \\ \Lambda \partial_\Lambda \tilde{u}_\Lambda^{(a)} &= (d-2) \tilde{u}_\Lambda^{(a)} + \frac{2\Lambda^{2d-3}}{dZ_\Lambda} \partial_\Lambda u_\Lambda^{(a)}, \\ \Lambda \partial_\Lambda \tilde{v}_\Lambda &= (d-2) \tilde{v}_\Lambda + \frac{2\Lambda^{2d-3}}{dZ_\Lambda} \partial_\Lambda v_\Lambda.\end{aligned}$$

We introduce the logarithmic cutoff $\Lambda = \Lambda_0 e^{-s}$ and insert Eqs. (5.5)-(5.9) so that the flow equations for the dimensionless parameters read

$$\partial_s \tilde{r} = 2\tilde{r} \tag{5.10}$$

$$\partial_s \tilde{u}^{(n)} = \epsilon \tilde{u}^{(n)} + \frac{4Z_\Lambda \Lambda}{2-\epsilon} I^{(\neq)}(\tilde{r} \Lambda^2) \tilde{u}^{(n)2} \tag{5.11}$$

$$\partial_s \tilde{u}^{(a)} = \epsilon \tilde{u}^{(a)} + \frac{8Z_\Lambda \Lambda}{2-\epsilon} I^{(=)}(\tilde{r} \Lambda^2) \tilde{u}^{(a)} \left(2 \left(\tilde{u}^{(n)} + \tilde{v} \right) + 3\tilde{u}^{(a)} \right) \tag{5.12}$$

$$\begin{aligned}\partial_s \tilde{v} &= \epsilon \tilde{v} + \frac{8Z_\Lambda \Lambda}{2-\epsilon} I^{(=)}(\tilde{r} \Lambda^2) \left(9\tilde{u}^{(a)2} + 2\tilde{u}^{(a)} \left(\tilde{u}^{(n)} + 3\tilde{v} \right) + \left(\tilde{u}^{(n)} + 2\tilde{v} \right)^2 \right) \\ &\quad - \frac{4Z_\Lambda \Lambda}{2-\epsilon} I^{(\neq)}(\tilde{r} \Lambda^2) \tilde{u}^{(n)2}.\end{aligned}\tag{5.13}$$

From the fRG flow equation for \tilde{r} it is clear that all fixed points are necessarily at

$$\tilde{r}_* = 0.$$

Therefore, in order to find the fixed points of the fRG flow, we can evaluate the integrals $I_\Lambda^{(\neq/ =)}$ at $r = 0$ and get

$$\begin{aligned}I_\Lambda^{(\neq)}(0) &= -\frac{1}{\pi \Lambda Z_\Lambda} \left(\frac{1}{2\sqrt{35}} + \frac{16}{15\sqrt{15}} \right) =: -\frac{1}{\Lambda Z_\Lambda} c_1, \\ I_\Lambda^{(=)}(0) &= -\frac{1}{\pi \Lambda Z_\Lambda} \left(\frac{1}{8\sqrt{2}} + \frac{1}{3\sqrt{3}} \right) =: -\frac{1}{\Lambda Z_\Lambda} c_2.\end{aligned}$$

Thus, we can rewrite the fixed point conditions for the parameters $\tilde{u}^{(n)}, \tilde{u}^{(a)}, \tilde{v}$ as

$$\begin{aligned} 0 &= \tilde{u}_\star^{(n)} \left(\epsilon - \frac{4c_1}{2-\epsilon} \tilde{u}_\star^{(n)} \right), \\ 0 &= \tilde{u}_\star^{(a)} \left(\epsilon - \frac{8c_2}{2-\epsilon} \left(2 \left(\tilde{u}_\star^{(n)} + \tilde{v}_\star \right) + 3\tilde{u}_\star^{(a)} \right) \right), \\ 0 &= \epsilon \tilde{v}_\star + \frac{4c_1}{2-\epsilon} \tilde{u}_\star^{(n)2} - \frac{8c_2}{2-\epsilon} \left(9\tilde{u}_\star^{(a)2} + 2\tilde{u}_\star^{(a)} \left(\tilde{u}_\star^{(n)} + 3\tilde{v}_\star \right) + \left(\tilde{u}_\star^{(n)} + 2\tilde{v}_\star \right)^2 \right). \end{aligned}$$

The fixed point values for the parameters $\tilde{u}^{(n)}, \tilde{u}^{(a)}, \tilde{v}$ can be determined using Mathematica. Furthermore, we linearize the fRG flow equations around the fixed points and determine the RG eigenvalues. Expanding up to first order in ϵ , we find six fixed points. Four of them are at $\tilde{u}^{(a)} = 0$ and might be related to those of the O(6) model with cubic anisotropy discussed earlier. Therefore, we label these fixed points in analogy to the known fixed points for cubic symmetry breaking models. The fixed point structure is summarized in Tab. 5.1, and plots indicating the parameter flow are given in Fig. 5.2. The fixed points and the corresponding RG eigenvalues are the following:

- Gaussian fixed point:

$$\tilde{u}_\star^{(n)} = 0, \quad \tilde{u}_\star^{(a)} = 0, \quad \tilde{v}_\star = 0.$$

The RG eigenvalues are all positive, $2, \epsilon, \epsilon, \epsilon$, and therefore the Gaussian fixed point is unstable.

- Heisenberg-like fixed point: This fixed point seems to be related to the Heisenberg fixed point known from the study of systems with cubic symmetry breaking:

$$\tilde{u}_\star^{(n)} = 4.3642\epsilon, \quad \tilde{u}_\star^{(a)} = 0, \quad \tilde{v}_\star = -4.00026\epsilon.$$

We comment on the difference to the usual Heisenberg fixed point below. The fixed point has three relevant and one irrelevant directions with RG eigenvalues $2, 6.20\epsilon, 0.74\epsilon, -\epsilon$.

- Cubic fixed point: This fixed point seems to be related to the cubic fixed point:

$$\tilde{u}_\star^{(n)} = 4.3642\epsilon, \quad \tilde{u}_\star^{(a)} = 0, \quad \tilde{v}_\star = 0.335214\epsilon.$$

The fixed point has one relevant and three irrelevant directions with RG eigenvalues $2, -6.20\epsilon, -2.36\epsilon, -\epsilon$ and therefore is critical with the relevant parameter \tilde{r} driving a second order phase transition.

- Decoupled O(2) fixed point: Furthermore, there is a fixed point corresponding to three decoupled O(2) models for the complex order parameter:

$$\tilde{u}_\star^{(n)} = 0\epsilon, \quad \tilde{u}_\star^{(a)} = 0, \quad \tilde{v}_\star = 0.699155\epsilon.$$

This fixed point has three relevant and one irrelevant directions with RG eigenvalues $2, \epsilon, 0.5\epsilon, -\epsilon$.

- New fixed point 1: For this fixed point the anomalous interactions are crucial:

$$\tilde{u}_\star^{(n)} = 4.3642\epsilon, \quad \tilde{u}_\star^{(a)} = 1.00552\epsilon, \quad \tilde{v}_\star = -4.47418\epsilon.$$

The fixed point has two relevant and two irrelevant directions with RG eigenvalues $2, 5.40\epsilon, -1.08\epsilon, -\epsilon$.

- New fixed point 2: This fixed point is a consequence of the anomalous interactions as well:

$$\tilde{u}_\star^{(n)} = 4.3642\epsilon, \tilde{u}_\star^{(a)} = -1.50924\epsilon, \tilde{v}_\star = -0.702026\epsilon.$$

The fixed point has two relevant and two irrelevant directions with RG eigenvalues $2, 3.88\epsilon, -\epsilon, -2.25\epsilon$.

We see that the cubic fixed point is the only critical fixed point, the Gaussian fixed point is the only completely unstable fixed point and the other four fixed points are of the generic type.

	$\tilde{u}_\star^{(n)}$	$\tilde{u}_\star^{(a)}$	\tilde{v}_\star	RG eigenvalues
Gaussian fixed point	0	0	0	$2, \epsilon, \epsilon, \epsilon$
Heisenberg-like fixed point	4.3642ϵ	0	-4.00026ϵ	$2, 6.20\epsilon, 0.74\epsilon, -\epsilon$
Cubic fixed point	4.3642ϵ	0	0.335214ϵ	$2, -6.20\epsilon, -2.36\epsilon, -\epsilon$
Decoupled O(2) fixed point	0	0	0.699155ϵ	$2, \epsilon, 0.5\epsilon, -\epsilon$
New fixed point 1	4.3642ϵ	1.00552ϵ	-4.47418ϵ	$2, 5.40\epsilon, -1.08\epsilon, -\epsilon$
New fixed point 2	4.3642ϵ	-1.50924ϵ	-0.702026ϵ	$2, 3.88\epsilon, -\epsilon, -2.25\epsilon$

Tab. 5.1. Fixed points in the ϵ -expansion up to order $\mathcal{O}(\epsilon)$ for $\epsilon = 0.1$. Note that $\tilde{r}_\star = 0$ for all fixed points.

5.3. Interpretation

To interpret our results, we may compare the RG flow and the fixed point structure to earlier results in the literature and point out the important differences. To start with, we consider the case $u^{(a)} = v = 0$, i.e. the theory without anomalous interactions or cubic symmetry breaking terms. As already mentioned above, Uzunov [46] and Wetterich [47] studied such systems for the isotropically dispersing case and found that the propagator does not get renormalized. As we saw in Eq. (5.4), this property holds also for an anisotropic dispersion. Therefore, the mass does not get renormalized and the anomalous dimension is zero, $\eta \propto \partial_\Lambda Z_\Lambda = 0$. Using Eqs. (5.10) and (5.11), we get for the dimensionless parameters the flow equations

$$\begin{aligned} \partial_s \tilde{r} &= 2\tilde{r}, \\ \partial_s \tilde{u}^{(n)} &= \tilde{u}^{(n)} \left(\epsilon + \frac{4Z_\Lambda \Lambda}{2 - \epsilon} I^{(\neq)}(\tilde{r}\Lambda^2) \tilde{u}^{(n)} \right). \end{aligned}$$

Due to the anisotropic propagator, the integral $I^{(\neq)}(\tilde{r}\Lambda^2)$ is different from the expressions encountered by Uzunov and Wetterich. As in the isotropic case, the flow equations have two fixed point, the trivial Gaussian fixed point and the Heisenberg fixed point with $\tilde{u}_\star^{(n)} \neq 0$. However, as we saw above, the Heisenberg fixed point is *not* a fixed point of the full RG flow.

To understand this, we turn to the case of arbitrary v while remaining at $u^{(a)} = 0$. In the case of static fields and an isotropic kinetic term such models were studied by Aharony [48] in the context of $O(N)$ symmetric models. Our critical theory seems to be connected to the $O(6)$ symmetric model, as for $u^{(a)} = 0$ the action only contains combinations of absolute

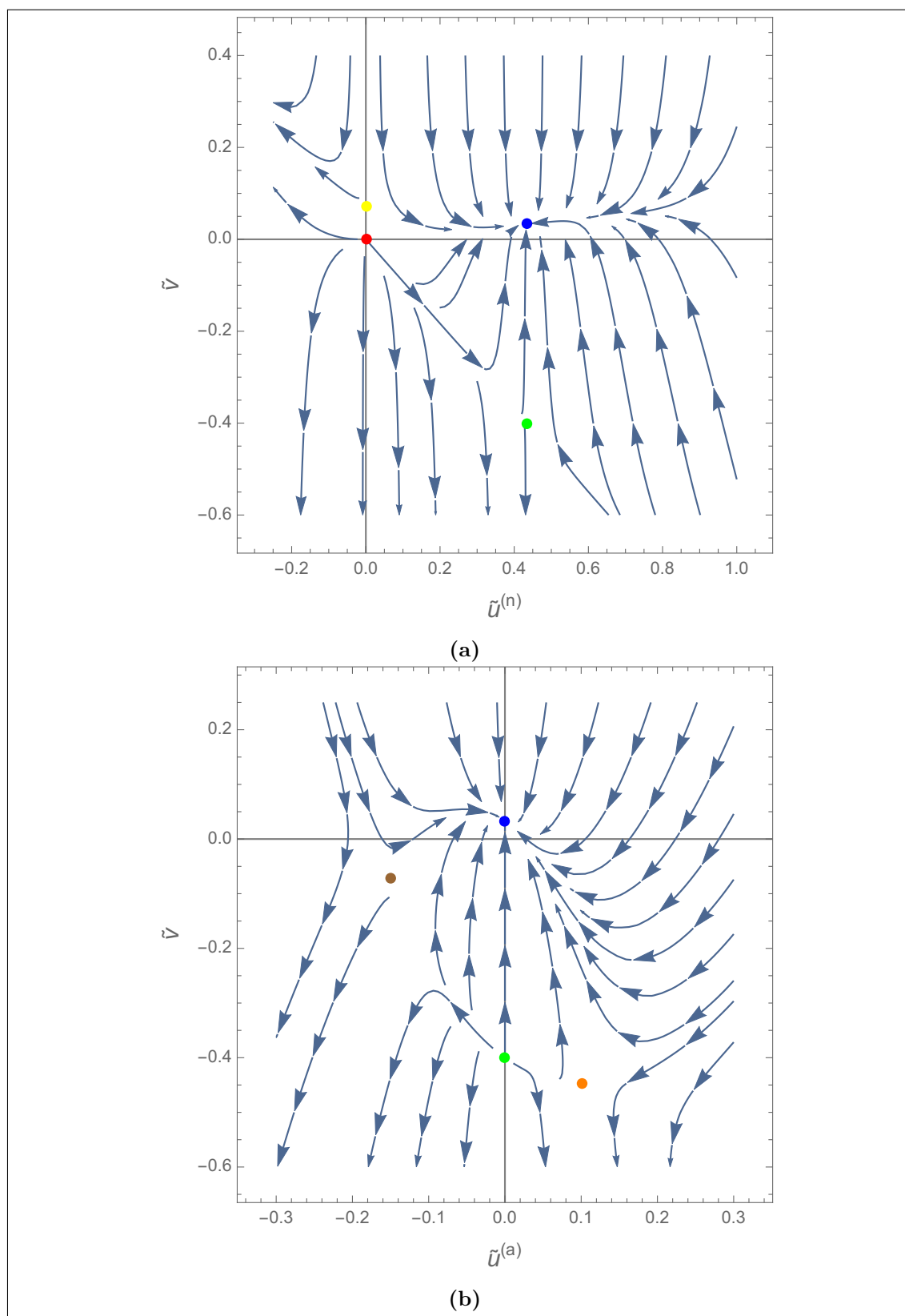


Fig. 5.2. Parameter flow (a) in the $\tilde{u}^{(n)} - \tilde{v}$ -plane for $\tilde{u}_*^{(a)} = 0$ and (b) in the $\tilde{u}^{(a)} - \tilde{v}$ -plane for $\tilde{u}_*^{(n)} \approx 4.3642\epsilon \neq 0$ and $\epsilon = 0.1$. The fixed points are indicated by the colored dots.

values of the fields. The important difference to this model is the inclusion of the linear time derivative, i.e. the dynamical exponent $z = 2$, which spoils the analogy to a classical $O(6)$ model in $d+1$ dimensions. Using the flow equations for the dimensionless parameters, Eqs. (5.10), (5.11), and (5.13), we see that the flow equations for \tilde{r} and $\tilde{u}^{(n)}$ do not involve \tilde{v} and therefore remain unchanged, and the flow equation for \tilde{v} reads

$$\partial_s \tilde{v} = \epsilon \tilde{v} + \frac{8Z_\Lambda \Lambda}{2 - \epsilon} I^{(=)}(\tilde{r}\Lambda^2) \left(\left(\tilde{u}^{(n)} + 2\tilde{v} \right)^2 \right) - \frac{4Z_\Lambda \Lambda}{2 - \epsilon} I^{(\neq)}(\tilde{r}\Lambda^2) \tilde{u}^{(n)2}.$$

Note in particular, that the flow equations for $\tilde{u}^{(n)}$ and \tilde{v} are substantially different from those for the static, ‘isotropically propagating’ cubic symmetry breaking model, where the flow of $\tilde{u}^{(n)}$ includes \tilde{v} . In particular, the present RG flow is incompatible with the Heisenberg fixed point obtained in the case $v = 0$. This is not surprising, as the symmetry of the effective action is different due to both the linear time derivative and the anisotropic kinetic term. Nevertheless, we find the four fixed points discussed above which to some extent resemble the behavior of the cubic symmetry breaking model. Note, however, that the inclusion of quantum fluctuations, i.e. the τ -dependence of the fields, and the anisotropic dispersion change the RG flow substantially. Nevertheless, there is still a fixed point which is stable in the $\tilde{u}^{(n)} - \tilde{v}$ -plane and for which the mass parameter \tilde{r} is the only relevant perturbation. Thus, we conclude that the phase transition between the QSL phases discussed by Kos and Punk is indeed a second order phase transition.

The fixed point structure and, in particular, the critical behavior seems to be surprisingly insensitive to the presence of an anomalous interaction, $u^{(a)} \neq 0$. Even if it affects the quantitative results, it does not seem to change the qualitative picture drastically. It might be interesting to study this property further in future analyses.

To conclude our discussion of the RG flow of the effective action we will briefly relate our results to the mean-field analysis above. The existence of a second order phase transition driven by the mass parameter r is a common result of both methods. Therefore, we can say for sure that the QPT discovered by Kos and Punk [2] is indeed of second order. Interestingly, the inclusion of complex fields in the RG procedure instead of real mean-field values does not change this qualitative picture. However, the RG flow itself is clearly affected by the complex structure. Starting from the RG flow it is possible to determine critical exponents, however this is left open for further studies and might be analyzed using more elaborate RG methods.

6

Chapter 6

Summary & Outlook

In this thesis, we took an analytical approach to the Heisenberg-Kitaev model on the triangular lattice. The model is known to host different quantum spin liquid ground states and is a reasonable candidate for their experimental detection. The goal of this thesis was to understand the quantum phase transition between two of these quantum spin liquid states in more detail.

In contrast to earlier studies we did not use any numerical methods but relied solely on analytical tools. We started from a Schwinger boson representation of the spins and performed a Hubbard-Stratonovich transformation to overcome the mean-field approximation used in earlier studies. We derived an effective theory for the relevant degrees of freedom by integrating out the Schwinger bosons. The resulting action describes three interacting bosonic fields dispersing in one particular direction each. Apart from *normal interactions* preserving the number of bosons of each species separately, there are also *anomalous interactions* where bosons of different species are transmuted into each other.

We confirmed the existence of the quantum phase transition by an instability of the Gaussian theory. We analyzed the mean-field behavior of the quartic theory and found an indication for the quantum phase transition to be of second order. Using the functional renormalization group, we derived one-loop RG flow equations. In particular, the RG flow has one critical fixed point, indicating a second order phase transition.

The effective action, and hence its RG flow, resembles some of the features of the $O(6)$ symmetric model with a cubic symmetry breaking term at mean-field level and to some extent even beyond. However, the dynamical exponent $z = 2$ spoils the analogy to a $d + 1$ -dimensional $O(N)$ model. Together with the anisotropic dispersion and the anomalous interactions this gives rise to some interesting behavior, like the non-renormalization property for the inverse propagator and a shift of the usual Heisenberg fixed point due to an altered symmetry of the action. Nevertheless, the critical theory seems to be surprisingly insensitive to the anomalous interactions in terms of the RG fixed point structure.

The critical theory was derived under the assumption that the system is deep in the spin liquid regime. Going beyond this approximation, we expect some isotropic contribution to the normal propagator of the effective theory. In this case, the anomalous propagator becomes relevant and therefore has to be taken into account. Together with the quasi-one-dimensional behavior of the bosons deep in the spin liquid regime, this would be an interesting line of research in future projects. Also the inclusion of higher order terms in the triplet fields might be interesting with respect to the stability of possible mean-field solutions.

Furthermore, the RG analysis of the effective theory could be taken further. In this thesis we determined the one-loop flow equations. Taking into account higher loop orders may prove fruitful to see whether the non-renormalization of the propagator remains valid as expected. Furthermore, we neglected the frequency and momentum dependence of the vertices altogether. Using modern numerical methods like the multiloop-fRG [51] it might be interesting to take into account both the full vertex structure and higher loop orders. Also, the calculation of critical exponents might be of interest in future studies.

From another point of view, realizations of the Heisenberg-Kitaev model on other lattices, in particular the hexagonal or the Kagomé lattice, could be interesting for future analysis.

We have shown that the combination of an effective action and a RG analysis in the spirit of the Landau-Ginzburg-Wilson paradigm can improve our understanding of quantum spin liquids and their phase transitions. The analytical approach used in this thesis can be generalized to study other quantum phase transitions in systems hosting quantum spin liquid phases.

A

Appendix A

Singlet & Triplet Operator Identities

Let i, j denote nearest-neighboring sites. Using Schwinger boson operators, the Heisenberg interaction can be written as

$$\begin{aligned}\vec{S}_i \cdot \vec{S}_j &= \frac{1}{4} \sum_{a=1,2,3} b_{i\alpha}^\dagger \sigma_{\alpha\beta}^a b_{i\beta} b_{j\gamma}^\dagger \sigma_{\gamma\delta}^a b_{j\delta} \\ &= \frac{1}{4} b_{i\alpha}^\dagger b_{i\beta} b_{j\gamma}^\dagger b_{j\delta} \sum_{a=1,2,3} \sigma_{\alpha\beta}^a \sigma_{\gamma\delta}^a \\ &= \frac{1}{4} b_{i\alpha}^\dagger b_{i\beta} b_{j\gamma}^\dagger b_{j\delta} (2\delta_{\alpha\delta} \delta_{\beta\gamma} - \delta_{\alpha\beta} \delta_{\gamma\delta}) \\ &= \frac{1}{2} b_{i\alpha}^\dagger b_{j\beta}^\dagger b_{i\beta} b_{j\alpha} - \frac{1}{4} b_{i\alpha}^\dagger b_{i\alpha} b_{j\beta}^\dagger b_{j\beta} \\ &= \frac{1}{2} b_{i\alpha}^\dagger b_{j\beta}^\dagger b_{i\beta} b_{j\alpha} - \frac{1}{4} n_i n_j \\ &= \frac{1}{2} b_{i\alpha}^\dagger b_{j\beta}^\dagger b_{i\beta} b_{j\alpha} - S^2.\end{aligned}$$

Here, we used the constraint in Eq. (3.2) in the last step. Note that this result holds for any spin S as long as the Schwinger bosons form a faithful, two-dimensional representation of $SU(2)$, which is ensured by the constraint.

At the same time, we have

$$\begin{aligned}a_{ij}^\dagger a_{ij} &= \frac{1}{4} \epsilon_{\alpha\beta\gamma\delta} b_{i\alpha}^\dagger b_{j\beta}^\dagger b_{i\gamma} b_{j\delta} \\ &= \frac{1}{4} b_{i\alpha}^\dagger b_{j\beta}^\dagger b_{i\gamma} b_{j\delta} (\delta_{\alpha\gamma} \delta_{\beta\delta} - \delta_{\alpha\delta} \delta_{\beta\gamma}) \\ &= \frac{1}{4} (b_{i\alpha}^\dagger b_{i\alpha} b_{j\beta}^\dagger b_{j\beta} - b_{i\alpha}^\dagger b_{j\beta}^\dagger b_{i\beta} b_{j\alpha}) \\ &= S^2 - \frac{1}{4} b_{i\alpha}^\dagger b_{j\beta}^\dagger b_{i\beta} b_{j\alpha}.\end{aligned}$$

Combining these two results, we get

$$\vec{S}_i \cdot \vec{S}_j = -2a_{ij}^\dagger a_{ij} + S^2.$$

A similar identity can be obtained for the Kitaev terms involving only one spin component,

$$S_i^\gamma S_j^\gamma = -t_{ij}^{\gamma\dagger} t_{ij}^\gamma - a_{ij}^\dagger a_{ij} + S^2.$$

This identity can be verified by explicitly calculating the contributions for $\gamma = 1, 2, 3$ separately. Again, this identity holds true for all S .

B

Appendix B

Gauge Theory of the HK-Model on the Triangular Lattice

Returning to the Schwinger boson representation of the Heisenberg-Kitaev model given in Eq. (3.3), one sees that the action has a (local) U(1) gauge symmetry [10] acting on the Schwinger bosons as

$$b_{i\alpha}(\tau) \rightarrow e^{i\theta_i} b_{i\alpha}(\tau).$$

Under this transformation the Hubbard-Stratonovich fields A and T^γ transform as

$$\begin{aligned} A_{ij}(\tau) &\rightarrow e^{i(\theta_i + \theta_j)} A_{ij}(\tau) \\ T_{ij}^\gamma(\tau) &\rightarrow e^{i(\theta_i + \theta_j)} T_{ij}^\gamma(\tau). \end{aligned}$$

The fact that two mean-field ansätze which are related by a gauge transformation cannot be distinguished by any observable¹ is the foundation of the so-called projective symmetry group (PSG) which contains all transformations which leave a given mean-field ansatz invariant. This method was developed by Wen for fermionic [1, 12] and by Wang and Vishwanath for bosonic mean-field theories [10]. In particular, PSGs allow to analyze the form of possible mean-field ansätze and are thus a very useful tool to get a first classification of possible QSL ground states. However, different QSL states can have the same PSG as it is the case, for example, for the three phases discussed by Kos and Punk [2]. A finer classification, which we will not address any further here, uses group cohomology and allows for a classification of a much broader class of topologically ordered state [15, 52, 53].

The U(1) gauge symmetry of the Heisenberg-Kitaev model can be used to restrict the form of an effective action for the A and T^γ fields significantly, as the effective action only contains gauge-invariant terms itself. Thus, the effective action for the A and T^γ fields in real space takes the form

$$\begin{aligned} \tilde{\mathcal{S}}_{\text{eff}}[A, T^\gamma] &= \sum_{\gamma \parallel \langle ij \rangle} \left(c_1(\partial_\tau) |A_{ij}|^2 + c_2(\partial_\tau) |T_{ij}^\gamma|^2 \right) \\ &+ \sum_{\text{closed loops}} \left(c_{ijkl}^{ATAT} A_{ij} \bar{T}_{jk}^{\gamma(jk)} A_{kl} \bar{T}_{li}^{\gamma(li)} + c_{ijkl}^{AATT} A_{ij} \bar{A}_{jk} T_{kl}^{\gamma(kl)} \bar{T}_{li}^{\gamma(li)} \right. \\ &\quad \left. + c_{ijkl}^{AAAA} A_{ij} \bar{A}_{jk} A_{kl} \bar{A}_{li} + c_{ijkl}^{TTTT} T_{ij}^{\gamma(ij)} \bar{T}_{jk}^{\gamma(jk)} T_{kl}^{\gamma(kl)} \bar{T}_{li}^{\gamma(li)} \right) + \dots, \end{aligned}$$

¹Any observable quantity has to be gauge invariant and therefore cannot distinguish states connected by gauge transformations.

where we dropped the time arguments of the fields. A microscopic derivation shows that the coefficients $c_{1/2}(\partial_\tau)$ contain temporal derivatives and that there are no terms including three A or three T fields. Furthermore, the lattice structure dictates the form of closed loops.

We want to justify the approximation of the singlet field A by its mean-field value while neglecting its phase fluctuations. To this end, we show that the phase fluctuations are gapped and therefore the low energy physics is correctly captured by a mean-field approximation for A . We restrict ourselves to the regime where the T^γ vanish or are negligibly small and can rewrite the effective action as

$$\tilde{\mathcal{S}}_{\text{eff}}[A; T^\gamma = 0] \approx \sum_{\gamma \parallel \langle ij \rangle} c_1(\partial_\tau) |A_{ij}|^2 + \sum_{\text{closed loops}} c_{ijkl}^{AAAA} A_{ij} \bar{A}_{jk} A_{kl} \bar{A}_{li}.$$

This approximation is admissible close to the quantum phase transition where the fields T^γ vanish below some critical coupling and take some small value above.

The phase fluctuations of the A field give rise to new U(1) gauge fields [9, 14, 54]. Consider for a moment an anisotropic lattice where the coupling along bonds in direction \mathbf{a}_3 is different from the coupling along \mathbf{a}_1 and \mathbf{a}_2 . This can as well be seen as a square lattice with nearest- and next-nearest-neighbor couplings. For this model it is known that the phase fluctuations give rise to a two-component U(1) gauge field and an additional Higgs field which gaps out the U(1) gauge fluctuations [54, 55]. In the isotropic case, all directions have to be treated equally, and therefore the U(1) gauge symmetry is replaced by $U_1(1) \times U_2(1) \times U_3(1)$. However, all the $U_\gamma(1)$ gauge groups come with an additional Higgs field and therefore all gauge fluctuations are gapped, so that we can safely neglect the phase fluctuations in our derivations of an effective theory for the triplet fields, T^γ .

Lattice gauge theories of U(1) and \mathbb{Z}_2 gauge fields coupled to a Higgs field and matter were studied by Fradkin and Shenker [56]. Using their results it can be argued that the spinon excitations remain unconfined [14].

C

Appendix C

Fourth Order Contribution to the Effective Action

We define the four-point vertex function,

$$\begin{aligned} \Gamma_{\alpha\beta\gamma\delta}^{(4)}(q_1, q_2, q_3) &:= -\frac{J_2^4}{2N\beta} \sum_k'' G_{0,k}^{(n)} G_{0,-k+q_1}^{(n)} G_{0,k+q_3}^{(n)} G_{0,-k+q_2-q_3}^{(n)} \\ &\quad \text{tr}_2 \left[\sigma^{\tau(\alpha)} \sigma^{\tau(\beta)} \sigma^{\tau(\gamma)} \sigma^{\tau(\delta)} \right] \text{sgn}(\alpha) \text{sgn}^*(\beta) \text{sgn}(\gamma) \text{sgn}^*(\delta) \\ &\quad \cos(a(k_\alpha - q_{1,\alpha})) \cos(a(k_\beta + q_{3,\beta})) \cos(a(k_\gamma - q_{2,\gamma} + q_{3,\gamma})) \cos(ak_\delta), \end{aligned}$$

evaluate the Matsubara summation for vanishing external frequencies and momenta, and get

$$\begin{aligned} \Gamma_{\alpha\beta\gamma\delta}^{(4)}(0, 0, 0) &= -\frac{J_2^4}{8\lambda^3 N} \sum_{\mathbf{k}, k_\gamma \geq 0} \text{tr}_2 \left[\sigma^{\tau(\alpha)} \sigma^{\tau(\beta)} \sigma^{\tau(\gamma)} \sigma^{\tau(\delta)} \right] \text{sgn}(\alpha) \text{sgn}^*(\beta) \text{sgn}(\gamma) \text{sgn}^*(\delta) \\ &\quad \cos(ak_\alpha) \cos(ak_\beta) \cos(ak_\gamma) \cos(ak_\delta). \end{aligned}$$

Using Pauli matrix identities, we can rewrite this expression as

$$\begin{aligned} &\Gamma_{\alpha\beta\gamma\delta}^{(4)}(0, 0, 0) \\ &= -\frac{J_2^4}{4\lambda^3 N} \sum_{\mathbf{k}, k_\gamma \geq 0} \text{sgn}(\alpha) \text{sgn}^*(\beta) \text{sgn}(\gamma) \text{sgn}^*(\delta) \cos(ak_\alpha) \cos(ak_\beta) \cos(ak_\gamma) \cos(ak_\delta) \\ &\quad \{ \delta_{\alpha\beta} \delta_{\gamma\delta} + \delta_{\alpha\delta} \delta_{\beta\gamma} + \delta_{\alpha\gamma} \delta_{\beta\delta} (-1 + 2(\delta_{\alpha,2} + \delta_{\beta,2}) - 4\delta_{\alpha,2} \delta_{\alpha\beta}) \} \\ &= -\frac{J_2^4}{4\lambda^3 N} \sum_{\mathbf{k}, k_\gamma \geq 0} \{ \delta_{\alpha\beta} \delta_{\gamma\delta} \cos^2(ak_\alpha) \cos^2(ak_\gamma) + \delta_{\alpha\delta} \delta_{\beta\gamma} \cos^2(ak_\alpha) \cos^2(ak_\beta) \\ &\quad + \delta_{\alpha\gamma} \delta_{\beta\delta} \text{sgn}(\alpha)^2 \text{sgn}^*(\beta)^2 \cos^2(ak_\alpha) \cos^2(ak_\beta) (-1 + 2(\delta_{\alpha,2} + \delta_{\beta,2}) - 4\delta_{\alpha,2} \delta_{\alpha\beta}) \}. \end{aligned}$$

We evaluate the momentum sum similar to the ones for the Gaussian fluctuations and get

$$\frac{1}{N} \sum_{\mathbf{k}, k_\gamma \geq 0} \cos^2(ak_\mu) \cos^2(ak_\nu) = \frac{1}{16} (2 + \delta_{\mu\nu}).$$

Inserting this into $\Gamma_{\alpha\beta\gamma\delta}^{(4)}(0, 0, 0)$, we get

$$\begin{aligned}
\Gamma_{\alpha\beta\gamma\delta}^{(4)}(0, 0, 0) &= -\frac{J_2^4}{64\lambda^3} (\delta_{\alpha\beta}\delta_{\gamma\delta} (2 + \delta_{\alpha\gamma}) + \delta_{\alpha\delta}\delta_{\beta\gamma} (2 + \delta_{\alpha\beta}) \\
&\quad -\delta_{\alpha\gamma}\delta_{\beta\delta} \operatorname{sgn}(\alpha)^2 \operatorname{sgn}^*(\beta)^2 (2 + \delta_{\alpha\beta}) \\
&\quad +2\delta_{\alpha\gamma}\delta_{\beta\delta} \operatorname{sgn}(\alpha)^2 \operatorname{sgn}^*(\beta)^2 (2 + \delta_{\alpha\beta}) (\delta_{\alpha,2} + \delta_{\beta,2} - 2\delta_{\alpha,2}\delta_{\alpha\beta})) \\
&= -\frac{J_2^4}{64\lambda^3} [2\delta_{\alpha\beta}\delta_{\gamma\delta} + 2\delta_{\alpha\delta}\delta_{\beta\gamma} + \delta_{\alpha\beta}\delta_{\beta\gamma}\delta_{\gamma\delta} \\
&\quad -2\delta_{\alpha\gamma}\delta_{\beta\delta} \operatorname{sgn}(\alpha)^2 \operatorname{sgn}^*(\beta)^2 \\
&\quad +4\delta_{\alpha\gamma}\delta_{\beta\delta} \operatorname{sgn}(\alpha)^2 \operatorname{sgn}^*(\beta)^2 (\delta_{\alpha,2} + \delta_{\beta,2} - 2\delta_{\alpha,2}\delta_{\alpha\beta})].
\end{aligned}$$

Using this result, we can now write the fourth order contribution as

$$\begin{aligned}
\tilde{\mathcal{S}}^{(4)} \approx &-\frac{J_2^4}{64\lambda^3} \frac{1}{(N\beta)^3} \sum_{q_1, q_2, q_3} \left\{ 2 \sum_{\gamma, \gamma'} T^\gamma(q_1) \bar{T}^\gamma(q_1 + q_3) T^{\gamma'}(q_2) \bar{T}^{\gamma'}(q_2 - q_3) \right. \\
&\quad +2 \sum_{\gamma, \gamma'} T^\gamma(q_1) \bar{T}^{\gamma'}(q_1 + q_3) T^{\gamma'}(q_2) \bar{T}^\gamma(q_2 - q_3) \\
&\quad + \sum_{\gamma} T^\gamma(q_1) \bar{T}^\gamma(q_1 + q_3) T^\gamma(q_2) \bar{T}^\gamma(q_2 - q_3) \\
&\quad \left. -2 \sum_{\gamma, \gamma'} T^\gamma(q_1) \bar{T}^{\gamma'}(q_1 + q_3) T^\gamma(q_2) \bar{T}^{\gamma'}(q_2 - q_3) \right\},
\end{aligned}$$

or, more compactly,

$$\begin{aligned}
\tilde{\mathcal{S}}^{(4)} &= -\frac{4u}{(N\beta)^3} \sum_{q_1, q_2, q_3} \sum_{\gamma, \gamma'} T^\gamma(q_1) \bar{T}^\gamma(q_1 + q_3) T^{\gamma'}(q_2) \bar{T}^{\gamma'}(q_2 - q_3) \\
&\quad + \frac{2u}{(N\beta)^3} \sum_{q_1, q_2, q_3} \sum_{\gamma, \gamma'} T^\gamma(q_1) \bar{T}^{\gamma'}(q_1 + q_3) T^\gamma(q_2) \bar{T}^{\gamma'}(q_2 - q_3) \\
&\quad - \frac{u}{(N\beta)^3} \sum_{q_1, q_2, q_3} \sum_{\gamma} T^\gamma(q_1) \bar{T}^\gamma(q_1 + q_3) T^\gamma(q_2) \bar{T}^\gamma(q_2 - q_3),
\end{aligned}$$

where we defined

$$u := \frac{J_2^4}{64\lambda^3}.$$

D Appendix D

Technical Results for fRG Calculations

D.1. Expressions Used in fRG Calculations

The second functional derivatives of Γ_Λ are given by

$$\begin{aligned} \frac{\delta^2 \Gamma_\Lambda}{\delta \bar{T}^\alpha(p) \delta \bar{T}^\beta(q)} &= 2 \int_k \left\{ u_\Lambda^{(n)} T^\alpha(k) T^\beta(p+q-k) + \delta_{\alpha\beta} \sum_\gamma (u_\Lambda^{(a)} + v_\Lambda \delta_{\alpha\gamma}) T^\gamma(k) T^\gamma(p+q-k) \right\} \\ \frac{\delta^2 \Gamma_\Lambda}{\delta T^\alpha(p) \delta T^\beta(q)} &= 2 \int_k \left\{ u_\Lambda^{(n)} \bar{T}^\alpha(k) \bar{T}^\beta(p+q-k) + \delta_{\alpha\beta} \sum_\gamma (u_\Lambda^{(a)} + v_\Lambda \delta_{\alpha\gamma}) \bar{T}^\gamma(k) \bar{T}^\gamma(p+q-k) \right\} \\ \frac{\delta^2 \Gamma_\Lambda}{\delta \bar{T}^\alpha(p) \delta T^\beta(q)} &= -G_{\Lambda,p,\alpha}^{-1} \delta_{\alpha\beta} (2\pi)^{d+1} \delta(p-q) + 2 \int_k \left\{ u_\Lambda^{(n)} \left(\delta_{\alpha\beta} \sum_\gamma \bar{T}^\gamma(k) T^\gamma(k+p-q) \right. \right. \\ &\quad \left. \left. + \bar{T}^\beta(k) T^\alpha(k+p-q) \right) \right. \\ &\quad \left. + 2(u_\Lambda^{(a)} + v_\Lambda \delta_{\alpha\beta}) \bar{T}^\alpha(k) T^\beta(k+p-q) \right\} \\ \frac{\delta^2 \Gamma_\Lambda}{\delta T^\alpha(p) \delta \bar{T}^\beta(q)} &= -G_{\Lambda,p,\alpha}^{-1} \delta_{\alpha\beta} (2\pi)^{d+1} \delta(p-q) + 2 \int_k \left\{ u_\Lambda^{(n)} \left(\delta_{\alpha\beta} \sum_\gamma \bar{T}^\gamma(k) T^\gamma(k-p+q) \right. \right. \\ &\quad \left. \left. + \bar{T}^\alpha(k) T^\beta(k-p+q) \right) \right. \\ &\quad \left. + 2(u_\Lambda^{(a)} + v_\Lambda \delta_{\alpha\beta}) \bar{T}^\beta(k) T^\alpha(k-p+q) \right\}. \end{aligned}$$

Using $M = \Gamma_\Lambda^{(2)} + R_\Lambda$, we get

$$(M|_{T=0})_{p,q;\alpha,\beta} = -\delta_{\alpha\beta} (2\pi)^{d+1} \delta(p-q) G_{R,p,\alpha}^{-1} \begin{pmatrix} 0 & 1 \\ 1 & 0 \end{pmatrix},$$

where we used

$$G_{R,p,\alpha}^{-1} := G_{\Lambda,p,\alpha}^{-1} - R_{\Lambda,p,\alpha}$$

and

$$(R_\Lambda)_{p,q;\alpha,\beta} = \delta_{\alpha\beta} (2\pi)^{d+1} \delta(p-q) R_{\Lambda,p,\alpha} \begin{pmatrix} 0 & 1 \\ 1 & 0 \end{pmatrix}.$$

The matrix M can be inverted with inverse

$$(M^{-1}|_{T=0})_{p,q;\alpha,\beta} = -\delta_{\alpha\beta}(2\pi)^{d+1}\delta(p-q)G_{R,p,\alpha} \begin{pmatrix} 0 & 1 \\ 1 & 0 \end{pmatrix}.$$

Thus, we can evaluate the matrix product

$$(M^{-1}|_{T=0} \partial_\Lambda R_\Lambda M^{-1}|_{T=0})_{p,q;\alpha,\beta} = \delta_{\alpha\beta}(2\pi)^{d+1}\delta(p-q)G_{R,p,\alpha}^2 \partial_\Lambda R_{\Lambda,p,\alpha} \begin{pmatrix} 0 & 1 \\ 1 & 0 \end{pmatrix}. \quad (\text{D.1})$$

Other expressions which we will need are the second functional derivatives of M :

$$\begin{aligned} \left(\frac{\delta^2 M}{\delta \bar{T}^\gamma(k) \delta \bar{T}^{\gamma'}(k')} \right)_{p,q;\alpha,\beta} &= \begin{pmatrix} 0 & 0 \\ 0 & 1 \end{pmatrix} \left[u_\Lambda^{(n)} (\delta_{\alpha\gamma} \delta_{\beta\gamma'} + \delta_{\alpha\gamma'} \delta_{\beta\gamma}) + 2 \left(u_\Lambda^{(a)} + v_\Lambda \delta_{\alpha\gamma} \right) \delta_{\alpha\beta} \delta_{\gamma\gamma'} \right] \\ &\quad 2(2\pi)^{d+1} \delta(k+k'-p-q) \end{aligned} \quad (\text{D.2})$$

$$\begin{aligned} \left(\frac{\delta^2 M}{\delta T^\gamma(k) \delta T^{\gamma'}(k')} \right)_{p,q;\alpha,\beta} &= \begin{pmatrix} 1 & 0 \\ 0 & 0 \end{pmatrix} \left[u_\Lambda^{(n)} (\delta_{\alpha\gamma} \delta_{\beta\gamma'} + \delta_{\alpha\gamma'} \delta_{\beta\gamma}) + 2 \left(u_\Lambda^{(a)} + v_\Lambda \delta_{\alpha\gamma} \right) \delta_{\alpha\beta} \delta_{\gamma\gamma'} \right] \\ &\quad 2(2\pi)^{d+1} \delta(k+k'-p-q) \end{aligned} \quad (\text{D.3})$$

$$\begin{aligned} &\left(\frac{\delta^2 M}{\delta \bar{T}^\gamma(k) \delta T^{\gamma'}(k')} \right)_{p,q;\alpha,\beta} \\ &= \begin{pmatrix} 0 & 1 \\ 0 & 0 \end{pmatrix} \left[u_\Lambda^{(n)} (\delta_{\alpha\gamma'} \delta_{\beta\gamma} + \delta_{\alpha\beta} \delta_{\gamma\gamma'}) + 2 \left(u_\Lambda^{(a)} + v_\Lambda \delta_{\alpha\beta} \right) \delta_{\alpha\gamma} \delta_{\beta\gamma'} \right] 2(2\pi)^{d+1} \delta(k-k'+p-q) \\ &\quad + \begin{pmatrix} 0 & 0 \\ 1 & 0 \end{pmatrix} \left[u_\Lambda^{(n)} (\delta_{\alpha\gamma} \delta_{\beta\gamma'} + \delta_{\alpha\beta} \delta_{\gamma\gamma'}) + 2 \left(u_\Lambda^{(a)} + v_\Lambda \delta_{\alpha\beta} \right) \delta_{\alpha\gamma'} \delta_{\beta\gamma} \right] 2(2\pi)^{d+1} \delta(k-k'-p+q) \end{aligned} \quad (\text{D.4})$$

D.2. Evaluation of Integrals

D.2.1. $I_{\gamma,\gamma'}^{(1)}$, $\gamma \neq \gamma'$

When deriving the flow equations for the quartic couplings, we have to evaluate the integral

$$I_{\gamma,\gamma'}^{(1)} = \int_p \frac{\partial_\Lambda R_{\Lambda,p,\gamma}}{G_{R,p,\gamma}^{-2} G_{R,-p,\gamma'}^{-1}},$$

where $\gamma \neq \gamma'$. Using $\Theta(0) = 1/2$ and performing the frequency integral via the residue theorem, we get

$$\begin{aligned} I_{\gamma,\gamma'}^{(1)} &= -2\Lambda \int_p \frac{\Theta(\Lambda^2 - \mathbf{p}^2) + \Lambda^2 \delta(\Lambda^2 - \mathbf{p}^2)}{(iZ_\Lambda p_0 + r_\Lambda + p_\gamma^2 + \Lambda^2 \Theta(\Lambda^2 - \mathbf{p}^2))^2 \left(-iZ_\Lambda p_0 + r_\Lambda + p_{\gamma'}^2 + \Lambda^2 \Theta(\Lambda^2 - \mathbf{p}^2) \right)} \\ &= -2\Lambda \int_{|\mathbf{p}| \leq \Lambda} \int_{-\infty}^{\infty} \frac{dp_0}{2\pi} \frac{1}{(iZ_\Lambda p_0 + r_\Lambda + p_\gamma^2 + \Lambda^2)^2 \left(-iZ_\Lambda p_0 + r_\Lambda + p_{\gamma'}^2 + \Lambda^2 \right)} \\ &\quad - 2\Lambda^3 \int_{\mathbf{p}} \int_{-\infty}^{\infty} \frac{dp_0}{2\pi} \frac{\delta(\Lambda^2 - \mathbf{p}^2)}{(iZ_\Lambda p_0 + r_\Lambda + p_\gamma^2 + \frac{1}{2}\Lambda^2)^2 \left(-iZ_\Lambda p_0 + r_\Lambda + p_{\gamma'}^2 + \frac{1}{2}\Lambda^2 \right)} \\ &= -2\Lambda \int_{|\mathbf{p}| \leq \Lambda} \frac{1}{Z_\Lambda \left(p_\gamma^2 + p_{\gamma'}^2 + 2(r_\Lambda + \Lambda^2) \right)^2} - 2\Lambda^3 \int_{\mathbf{p}} \frac{\delta(\Lambda^2 - \mathbf{p}^2)}{Z_\Lambda \left(p_\gamma^2 + p_{\gamma'}^2 + 2r_\Lambda + \Lambda^2 \right)^2}. \end{aligned}$$

Using

$$\sum_{\alpha} p_{\alpha}^2 = \frac{3}{2} \mathbf{p}^2,$$

we get for $\gamma \neq \gamma'$

$$p_{\gamma}^2 + p_{\gamma'}^2 = \sum_{\alpha} p_{\alpha}^2 - p_{\beta}^2 = \frac{3}{2} \mathbf{p}^2 - p_{\beta}^2,$$

where β is the unique index distinct from γ and γ' . Thus, we get

$$I_{\gamma, \gamma'}^{(2)} = -\frac{2\Lambda}{Z_{\Lambda}} \left(\int_{|\mathbf{p}| \leq \Lambda} \frac{dp_{\beta} dp_{\beta, \perp}}{(2\pi)^2} \frac{1}{\left(2(r_{\Lambda} + \Lambda^2) + \frac{1}{2}p_{\beta}^2 + \frac{3}{2}p_{\beta, \perp}^2\right)^2} + \int \frac{dp_{\beta} dp_{\beta, \perp}}{(2\pi)^2} \frac{\Lambda^2 \delta(\Lambda^2 - \mathbf{p}^2)}{\left(2r_{\Lambda} + \Lambda^2 + \frac{1}{2}p_{\beta}^2 + \frac{3}{2}p_{\beta, \perp}^2\right)^2} \right),$$

where $p_{\beta, \perp}$ denotes the momentum perpendicular to p_{β} . Rescaling the momenta,

$$\tilde{p}_{\beta} = p_{\beta}/\Lambda, \quad \tilde{p}_{\beta, \perp} = p_{\beta, \perp}/\Lambda,$$

and defining $\tilde{r}_{\Lambda} = r_{\Lambda}\Lambda^{-2}$ we get for the first integral

$$I_a := \frac{1}{\Lambda^2(2\pi)^2} \int_{|\tilde{\mathbf{p}}| \leq 1} d\tilde{p}_{\beta} d\tilde{p}_{\beta, \perp} \frac{1}{\left(2(\tilde{r}_{\Lambda} + 1) + \frac{1}{2}\tilde{p}_{\beta}^2 + \frac{3}{2}\tilde{p}_{\beta, \perp}^2\right)^2}.$$

We use elliptic polar coordinates

$$\tilde{p}_{\beta} = \sqrt{2}\rho \cos \phi, \quad \tilde{p}_{\beta, \perp} = \sqrt{\frac{2}{3}}\rho \sin \phi$$

and rewrite the integral as

$$\begin{aligned} I_a &= \frac{2}{\sqrt{3}\Lambda^2(2\pi)^2} \int_0^{2\pi} d\phi \int_0^{\left(\frac{2}{3}(1+2\cos^2\phi)\right)^{-1/2}} d\rho \frac{\rho}{\left(2(\tilde{r}_{\Lambda} + 1) + \rho^2\right)^2} \\ &= \frac{1}{\sqrt{3}\Lambda^2(2\pi)^2} \int_0^{2\pi} d\phi \int_0^{\left(\frac{2}{3}(1+2\cos^2\phi)\right)^{-1}} du \frac{1}{\left(2(\tilde{r}_{\Lambda} + 1) + u\right)^2} \\ &= \frac{3}{2\sqrt{3}\Lambda^2(2\pi)^2(\tilde{r}_{\Lambda} + 1)} \int_0^{2\pi} d\phi \frac{1}{\left(3 + 8(\tilde{r}_{\Lambda} + 1) + 4(\tilde{r}_{\Lambda} + 1)\cos(2\phi)\right)} \\ &= \frac{\sqrt{3}}{\Lambda^2 4\pi(\tilde{r}_{\Lambda} + 1)} \frac{1}{\sqrt{9 + 48(\tilde{r}_{\Lambda} + 1)(\tilde{r}_{\Lambda} + 2)}} \\ &= \frac{\Lambda^2}{4\pi(r_{\Lambda} + \Lambda^2)\sqrt{3\Lambda^4 + 16(r_{\Lambda} + \Lambda^2)(r_{\Lambda} + 2\Lambda^2)}}. \end{aligned}$$

For the second integral we use (circular) polar coordinates and get

$$\begin{aligned}
I_b &:= \frac{1}{\Lambda^2(2\pi)^2} \int d\tilde{p}_\beta d\tilde{p}_{\beta,\perp} \frac{\delta(1 - \tilde{\mathbf{p}}^2)}{\left(2\tilde{r}_\Lambda + 1 + \frac{1}{2}\tilde{p}_\beta^2 + \frac{3}{2}\tilde{p}_{\beta,\perp}^2\right)^2} \\
&= \frac{1}{\Lambda^2(2\pi)^2} \int_0^{2\pi} d\phi \int_0^\infty d\rho \frac{\delta(1 - \rho^2)}{\left(2\tilde{r}_\Lambda + 1 + \frac{\rho^2}{2} + \frac{\rho^2}{2}\sin^2(\phi)\right)^2} \\
&= \frac{1}{\Lambda^2(2\pi)^2} \int_0^{2\pi} d\phi \frac{1}{2} \frac{1}{\left(2\tilde{r}_\Lambda + 1 + \frac{1}{2} + \frac{1}{2}\sin^2(\phi)\right)^2} \\
&= \frac{1}{2\Lambda^2(2\pi)^2} \frac{32\pi(\tilde{r}_\Lambda + 1)}{(3 + 4(2\tilde{r}_\Lambda + 1)(2\tilde{r}_\Lambda + 3))^{3/2}} \\
&= \frac{8}{\Lambda^2\pi} \frac{(\tilde{r}_\Lambda + 1)}{(3 + 4(2\tilde{r}_\Lambda + 1)(2\tilde{r}_\Lambda + 3))^{3/2}} \\
&= \frac{8\Lambda^2}{\pi} \frac{(r_\Lambda + \Lambda^2)}{(3\Lambda^4 + 4(2r_\Lambda + \Lambda^2)(2r_\Lambda + 3\Lambda^2))^{3/2}},
\end{aligned}$$

where we assumed $r > -\Lambda^2/2$, an assumption which - similar to the one discussed in the main text - will be satisfied in our case.

Combining the contributions , we get

$$\begin{aligned}
I_{\gamma,\gamma'}^{(1)} &= -\frac{\Lambda^3}{\pi Z_\Lambda} \left(\frac{1}{2(r_\Lambda + \Lambda^2)\sqrt{3\Lambda^4 + 16(r_\Lambda + \Lambda^2)(r_\Lambda + 2\Lambda^2)}} \right. \\
&\quad \left. + \frac{16(r_\Lambda + \Lambda^2)}{(3\Lambda^4 + 4(2r_\Lambda + \Lambda^2)(2r_\Lambda + 3\Lambda^2))^{3/2}} \right).
\end{aligned}$$

Note in particular, that this expression does not depend on the indices γ, γ' but only used the fact, that they are different.

D.2.2. $I_{\gamma,\gamma}^{(1)}$

In this appendix we evaluate the integral

$$I_{\gamma,\gamma}^{(1)} = \int_p \frac{\partial_\Lambda R_{\Lambda,p,\alpha}}{G_{R,p,\gamma}^{-2} G_{R,-p,\gamma}^{-1}}.$$

Using $\Theta(0) = 1/2$ and performing the frequency integral, we get

$$I_{\gamma,\gamma}^{(1)} = -\frac{\Lambda}{2Z_\Lambda} \int_{|\mathbf{p}| \leq \Lambda} \frac{1}{(p_\alpha^2 + r_\Lambda + \Lambda^2)^2} - \frac{2\Lambda^3}{Z_\Lambda} \int_{\mathbf{p}} \frac{\delta(\Lambda^2 - \mathbf{p}^2)}{(2p_\alpha^2 + 2r_\Lambda + \Lambda^2)^2}.$$

Rescaling momenta,

$$\tilde{p}_\alpha = p_\alpha/\Lambda, \quad \tilde{p}_{\alpha,\perp} = k_{\alpha,\perp}/\Lambda,$$

and using polar coordinates, we get for the first summand

$$\begin{aligned}
I_c &:= \frac{1}{\Lambda^2(2\pi)^2} \int_{\tilde{\mathbf{p}} \leq 1} d\tilde{p}_\alpha d\tilde{p}_{\alpha,\perp} \frac{1}{(\tilde{p}_\alpha^2 + \tilde{r}_\Lambda + 1)^2} \\
&= \frac{1}{\Lambda^2(2\pi)^2} \int_0^{2\pi} d\phi \int_0^1 d\rho \frac{\rho}{(\tilde{r}_\Lambda + 1 + \rho^2 \cos^2 \phi)^2} \\
&= \frac{1}{\Lambda^2(2\pi)^2} \frac{1}{\tilde{r}_\Lambda + 1} \int_0^{2\pi} d\phi \frac{1}{1 + 2(\tilde{r}_\Lambda + 1) + \cos(2\phi)} \\
&= \frac{1}{4\pi\Lambda^2} \frac{1}{(\tilde{r}_\Lambda + 1)\sqrt{(\tilde{r}_\Lambda + 1)(\tilde{r}_\Lambda + 2)}} \\
&= \frac{\Lambda^2}{4\pi} \frac{1}{(r_\Lambda + \Lambda^2)\sqrt{(r_\Lambda + \Lambda^2)(r_\Lambda + 2\Lambda^2)}}
\end{aligned}$$

and for the second summand we get

$$\begin{aligned}
I_d &:= \frac{1}{\Lambda^2(2\pi)^2} \int d\tilde{p}_\alpha d\tilde{p}_{\alpha,\perp} \frac{\delta(1 - \tilde{\mathbf{p}}^2)}{(2\tilde{p}_x^2 + 2\tilde{r}_\Lambda + 1)^2} \\
&= \frac{1}{\Lambda^2(2\pi)^2} \int_0^\infty d\rho \int_0^{2\pi} d\phi \frac{\delta(1 - \rho^2)}{(1 + 2\tilde{r}_\Lambda + 2\rho^2 \sin^2 \phi)^2} \\
&= \frac{1}{\Lambda^2(2\pi)^2} \int_0^{2\pi} d\phi \frac{1}{2(1 + 2\tilde{r}_\Lambda + 2\sin^2 \phi)^2} \\
&= \frac{1}{2\Lambda^2(2\pi)^2} \frac{4\pi(\tilde{r}_\Lambda + 1)}{(3 + 4\tilde{r}_\Lambda(\tilde{r}_\Lambda + 2))^{3/2}} \\
&= \frac{1}{2\Lambda^2\pi} \frac{(\tilde{r}_\Lambda + 1)}{(3 + 4\tilde{r}_\Lambda(\tilde{r}_\Lambda + 2))^{3/2}} \\
&= \frac{\Lambda^2}{2\pi} \frac{(r_\Lambda + \Lambda^2)}{(3\Lambda^4 + 4r_\Lambda(r_\Lambda + 2\Lambda^2))^{3/2}}.
\end{aligned}$$

Here, we assumed again, that $r_\Lambda/\Lambda^2 > -1/2$. Combining these contributions, we get

$$I_{\gamma,\gamma}^{(1)} = -\frac{\Lambda^3}{4\pi Z_\Lambda} \left(\frac{1}{2(r_\Lambda + \Lambda^2)\sqrt{(r_\Lambda + \Lambda^2)(r_\Lambda + 2\Lambda^2)}} + \frac{4(r_\Lambda + \Lambda^2)}{(3\Lambda^4 + 4r_\Lambda(r_\Lambda + 2\Lambda^2))^{3/2}} \right).$$

In particular, this does not depend on the direction γ .

References

- [1] X.-G. Wen. Quantum orders and symmetric spin liquids. *Phys. Rev. B*, **65**, 165113, Apr 2002.
- [2] P. Kos and M. Punk. Quantum spin liquid ground states of the Heisenberg-Kitaev model on the triangular lattice. *Phys. Rev. B*, **95**, 024421, Jan 2017.
- [3] A. Auerbach. *Interacting Electrons and Quantum Magnetism*. Springer-Verlag, 1994.
- [4] A. H. MacDonald, S. M. Girvin, and D. Yoshioka. $\frac{t}{U}$ expansion for the Hubbard model. *Phys. Rev. B*, **37**, 9753–9756, Jun 1988.
- [5] J. D. Reger and A. P. Young. Monte Carlo simulations of the spin- $\frac{1}{2}$ Heisenberg antiferromagnet on a square lattice. *Phys. Rev. B*, **37**, 5978–5981, Apr 1988.
- [6] S. R. White and D. A. Huse. Numerical renormalization-group study of low-lying eigenstates of the antiferromagnetic S=1 Heisenberg chain. *Phys. Rev. B*, **48**, 3844–3852, Aug 1993.
- [7] B. Bruognolo, A. Weichselbaum, J. von Delft, and M. Garst. Dynamic structure factor of the spin- $\frac{1}{2}$ XXZ chain in a transverse field. *Physical Review B*, **94**(8), Aug. 2016.
- [8] J. Chaloupka, G. Jackeli, and G. Khaliullin. Zigzag Magnetic Order in the Iridium Oxide Na₂IrO₃. *Phys. Rev. Lett.*, **110**, 097204, Feb 2013.
- [9] S. Sachdev and N. Read. LARGE N EXPANSION FOR FRUSTRATED AND DOPED QUANTUM ANTIFERROMAGNETS. *Int. J. Mod. Phys. B*, **5**, 219–249, 1991.
- [10] F. Wang and A. Vishwanath. Spin-liquid states on the triangular and Kagomé lattices: A projective-symmetry-group analysis of Schwinger boson states. *Phys. Rev. B*, **74**, 174423, Nov 2006.
- [11] L. Tarruell and L. Sanchez-Palencia. Quantum simulation of the hubbard model with ultracold fermions in optical lattices. *Comptes Rendus Physique*, **19**(6), 365 – 393, 2018.
- [12] X.-G. Wen. *Quantum Field Theory of Many-Body Systems: From the Origin of Sound to an Origin of Light and Electrons*. Oxford University Press, 2007.

-
- [13] X.-G. Wen. Colloquium: Zoo of quantum-topological phases of matter. *Rev. Mod. Phys.*, **89**, 041004, Dec 2017.
- [14] S. Sachdev. Kagomé- and triangular-lattice Heisenberg antiferromagnets: Ordering from quantum fluctuations and quantum-disordered ground states with unconfined bosonic spinons. *Phys. Rev. B*, **45**, 12377–12396, Jun 1992.
- [15] A. Mesaros and Y. Ran. Classification of symmetry enriched topological phases with exactly solvable models. *Phys. Rev. B*, **87**, 155115, Apr 2013.
- [16] S. Sachdev. *Quantum Phase Transitions*. Cambridge University Press, 2nd edition, 2011.
- [17] P. W. Anderson. Resonating valence bonds: A new kind of insulator? *Materials Research Bulletin*, **8**(2), 153–160, Feb 1973.
- [18] P. W. Anderson. The Resonating Valence Bond State in La_2CuO_4 and Superconductivity. *Science*, **235**(4793), 1196–1198, Mar 1987.
- [19] G. Misguich. Quantum spin liquids. *preprint*, [arXiv:0809.2257](https://arxiv.org/abs/0809.2257), 2008.
- [20] L. Balents. Spin liquids in frustrated magnets. *Nature*, **464**(7286), 199–208, Mar 2010.
- [21] M. Punk. Condensed Matter Field Theory. Lecture Notes, 2016. https://www.physik.uni-muenchen.de/lehre/vorlesungen/wise_16_17/TVI_TMP-TA4/lecture-notes/index.html. Last visited on 09/03/2020.
- [22] L. Messio, B. Bernu, and C. Lhuillier. Kagome Antiferromagnet: A Chiral Topological Spin Liquid? *Phys. Rev. Lett.*, **108**, 207204, May 2012.
- [23] J. Thönnißen. Multiloop Functional Renormalization Group Studies of Heisenberg Models on the Kagome Lattice. Master Thesis, Ludwig-Maximilians-Universität München, 2019.
- [24] A. Kitaev. Anyons in an exactly solved model and beyond. *Annals of Physics*, **321**(1), 2–111, 2006.
- [25] M. Becker, M. Hermanns, B. Bauer, M. Garst, and S. Trebst. Spin-orbit physics of $j = \frac{1}{2}$ Mott insulators on the triangular lattice. *Phys. Rev. B*, **91**, 155135, Apr 2015.
- [26] P. Kos. Quantum Spin Liquid Ground States of the Heisenberg-Kitaev Model on the Triangular Lattice. Master Thesis, Ludwig-Maximilians-Universität München, 2016.
- [27] J. Knolle and R. Moessner. A Field Guide to Spin Liquids. *Annual Review of Condensed Matter Physics*, **10**(1), 451–472, 2019.
- [28] Y. Shimizu, K. Miyagawa, K. Kanoda, M. Maesato, and G. Saito. Spin Liquid State in an Organic Mott Insulator with a Triangular Lattice. *Physical Review Letters*, **91**(10), Sept 2003.
- [29] R. Coldea, D. A. Tennant, A. M. Tsvelik, and Z. Tylczynski. Experimental Realization of a 2D Fractional Quantum Spin Liquid. *Phys. Rev. Lett.*, **86**, 1335–1338, Feb 2001.
-

-
- [30] K. M. Ranjith, P. Schlender, T. Doert, and M. Baenitz. Magnetic Properties of an Effective Spin- $\frac{1}{2}$ Triangular-Lattice Compound LiYbS₂. *preprint*, **arXiv:2003.00566**, 2020.
- [31] J. Chaloupka, G. Jackeli, and G. Khaliullin. Kitaev-Heisenberg Model on a Honeycomb Lattice: Possible Exotic Phases in Iridium Oxides A₂IrO₃. *Phys. Rev. Lett.*, **105**, 027204, Jul 2010.
- [32] Y. Singh, S. Manni, J. Reuther, T. Berlijn, R. Thomale, W. Ku, S. Trebst, and P. Gegenwart. Relevance of the Heisenberg-Kitaev Model for the Honeycomb Lattice Iridates A₂IrO₃. *Phys. Rev. Lett.*, **108**, 127203, Mar 2012.
- [33] T. Dey, A. V. Mahajan, P. Khuntia, M. Baenitz, B. Koteswararao, and F. C. Chou. Spin-liquid behavior in $J_{\text{eff}} = \frac{1}{2}$ triangular lattice compound Ba₃IrTi₂O₉. *Phys. Rev. B*, **86**, 140405, Oct 2012.
- [34] A. A. Abrikosov, L. P. Gorkov, and I. Dzyaloshinski. *Methods of Quantum Field Theory in Statistical Physics*. Dover Publications, 1976.
- [35] A. Fetter and J. Walecka. *Quantum Theory of Many-Particle Systems*. McGraw-Hill, 1971.
- [36] A. Altland and B. D. Simons. *Condensed Matter Field Theory*. Cambridge University Press, 2nd edition, 2010.
- [37] K. G. Wilson. The renormalization group: Critical phenomena and the Kondo problem. *Rev. Mod. Phys.*, **47**, 773–840, Oct 1975.
- [38] R. Shankar. Renormalization-group approach to interacting fermions. *Rev. Mod. Phys.*, **66**, 129–192, Jan 1994.
- [39] M. E. Fisher. Renormalization group theory: Its basis and formulation in statistical physics. *Rev. Mod. Phys.*, **70**, 653–681, Apr 1998.
- [40] J. Cardy. *Scaling and Renormalization in Statistical Physics*. Cambridge Lecture Notes in Physics. Cambridge University Press, 1996.
- [41] P. Kopietz, L. Bartosch, and F. Schütz. *Introduction to the Functional Renormalization Group*. Springer-Verlag, 2010.
- [42] R. Flint and P. Coleman. Symplectic N and time reversal in frustrated magnetism. *Phys. Rev. B*, **79**, 014424, Jan 2009.
- [43] M. L. Baez and J. Reuther. Numerical treatment of spin systems with unrestricted spin length S : A functional renormalization group study. *Phys. Rev. B*, **96**, 045144, Jul 2017.
- [44] C. A. R. Sá de Melo, M. Randeria, and J. R. Engelbrecht. Crossover from BCS to Bose superconductivity: Transition temperature and time-dependent Ginzburg-Landau theory. *Phys. Rev. Lett.*, **71**, 3202–3205, Nov 1993.
- [45] A. M. J. Schakel. Time-Dependent Ginzburg-Landau Theory and Duality. *preprint*, **arXiv:cond-mat/9904092**, 1999.
- [46] D. I. Uzunov. On the zero temperature critical behaviour of the nonideal Bose gas. *Physics Letters A*, **87**(1-2), 11–14, Dec 1981.
-

- [47] C. Wetterich. Functional renormalization for quantum phase transitions with nonrelativistic bosons. *Phys. Rev. B*, **77**, 064504, Feb 2008.
- [48] A. Aharony. Dependence of Universal Critical Behaviour on Symmetry and Range of Interaction. In C. Domb and M. Green, editors, *Phase Transitions and Critical Phenomena*, volume 6, pages 357–424. Academic Press, 1976.
- [49] D. I. Uzunov. *Introduction to the Theory of Critical Phenomena: Mean Field, Fluctuations and Renormalization*. World Scientific, 2nd edition, 2010.
- [50] K. G. Wilson and M. E. Fisher. Critical Exponents in 3.99 Dimensions. *Phys. Rev. Lett.*, **28**, 240–243, Jan 1972.
- [51] F. B. Kugler and J. von Delft. Multiloop functional renormalization group for general models. *Phys. Rev. B*, **97**, 035162, Jan 2018.
- [52] A. M. Essin and M. Hermele. Classifying fractionalization: Symmetry classification of gapped \mathbb{Z}_2 spin liquids in two dimensions. *Phys. Rev. B*, **87**, 104406, Mar 2013.
- [53] X. Chen, Z.-C. Gu, Z.-X. Liu, and X.-G. Wen. Symmetry protected topological orders and the group cohomology of their symmetry group. *Phys. Rev. B*, **87**, 155114, Apr 2013.
- [54] S. Sachdev. Schwinger boson theory of Z_2 spin liquids. Lecture Notes, 2018. http://qpt.physics.harvard.edu/phys268b/Lec11_Schwinger_boson_theory_of_Z2_spin_liquids.pdf. Last visited on 09/03/2020.
- [55] M. Punk. Topology in Condensed Matter Physics. Lecture Notes, 2017. https://www.physik.uni-muenchen.de/lehre/vorlesungen/sose_17/topology_cmp/lecture-notes/index.html. Last visited on 09/03/2020.
- [56] E. Fradkin and S. H. Shenker. Phase diagrams of lattice gauge theories with Higgs fields. *Phys. Rev. D*, **19**, 3682–3697, Jun 1979.
- [57] L. Messio, C. Lhuillier, and G. Misguich. Time reversal symmetry breaking chiral spin liquids: Projective symmetry group approach of bosonic mean-field theories. *Phys. Rev. B*, **87**, 125127, Mar 2013.
- [58] G. Misguich. Schwinger boson mean-field theory: Numerics for the energy landscape and gauge excitations in two-dimensional antiferromagnets. *Phys. Rev. B*, **86**, 245132, Dec 2012.
- [59] G. Misguich and F. Mila. Quantum dimer model on the triangular lattice: Semiclassical and variational approaches to vison dispersion and condensation. *Phys. Rev. B*, **77**, 134421, Apr 2008.
- [60] N. Read and S. Sachdev. Valence-Bond and Spin-Peierls Ground States of Low-Dimensional Quantum Antiferromagnets. *Phys. Rev. Lett.*, **62**, 1694–1697, Apr 1989.
- [61] A. E. Trumper, L. O. Manuel, C. J. Gazza, and H. A. Ceccatto. Schwinger-Boson Approach to Quantum Spin Systems: Gaussian Fluctuations in the “Natural” Gauge. *Phys. Rev. Lett.*, **78**, 2216–2219, Mar 1997.
- [62] A. M. Tsvelik. *Quantum Field Theory in Condensed Matter Physics*. Cambridge University Press, 2nd edition, 2003.

- [63] F. Wang. Schwinger boson mean field theories of spin liquid states on a honeycomb lattice: Projective symmetry group analysis and critical field theory. *Phys. Rev. B*, **82**, 024419, Jul 2010.
- [64] F. J. Wegner. Duality in Generalized Ising Models and Phase Transitions without Local Order Parameters. *Journal of Mathematical Physics*, **12**(10), 2259–2272, 1971.
- [65] M. P. A. Fisher, P. B. Weichman, G. Grinstein, and D. S. Fisher. Boson localization and the superfluid-insulator transition. *Phys. Rev. B*, **40**, 546–570, Jul 1989.
- [66] M. Hermanns, I. Kimchi, and J. Knolle. Physics of the Kitaev Model: Fractionalization, Dynamic Correlations, and Material Connections. *Annual Review of Condensed Matter Physics*, **9**(1), 17–33, 2018.

Erklärung:

Hiermit erkläre ich, die vorliegende Arbeit selbständig verfasst zu haben und keine anderen als die in der Arbeit angegebenen Quellen und Hilfsmittel benutzt zu haben.

München, den 10. März 2020

Felix Palm